

ABSTRACT

Title of Dissertation:

CHARACTERIZATION OF
CHRONIC MONOCULAR
DEPRIVATION AND ESTROGEN
ADMINISTRATION IN ADULT
RODENTS

Deepali Clare Sengupta, Doctor of
Philosophy, 2018

Dissertation directed by:

Dr. Elizabeth Quinlan, Professor,
Department of Biology,
Neuroscience and Cognitive
Science Program

Reduced synaptic plasticity and excitatory synapse density contribute to age-related cognitive decline, and constrain recovery of function from injury in adults. A parallel reduction in circulating sex hormones in both sexes, particularly estrogens, exacerbates this decline in synaptic plasticity. Conversely, estrogen therapy in aged members of many species restores synapse density, promotes synaptic plasticity, and improves learning/memory. Importantly, acute estrogen administration can promote rapid synaptogenesis, and these new synapses can be stabilized by activity.

Here I ask if estrogen treatment can promote synaptic plasticity in the primary visual cortex (V1) of aged rats. I demonstrate robust expression of estrogen receptors (ERs) in V1 of adult male and female rats, suggesting an opportunity to enhance plasticity with estrogens. I test this hypothesis following the induction of amblyopia by chronic monocular deprivation (cMD). I show that cMD reduces thalamic innervation from the deprived eye, and increases molecular markers which constrain plasticity, consistent with observations that the deficits induced by cMD are highly resistant to reversal. Surprisingly, cMD did not change markers for excitatory synapses, suggesting a homeostatic increase in synapses serving the non-deprived eye (NDE) to maintain synaptic density within an optimal range. Importantly, visually-evoked potentials (VEPs) induced by repetitive visual stimulation to the deprived eye depress more rapidly than those of the NDE, consistent with cMD inducing an increase in the probability of neurotransmitter release (Pr) at synapses in the cMD pathway.

In contrast, treatment of cMD adults with a single dose of 17α estradiol significantly increased markers for excitatory synapses, and estradiol treatment followed by visual stimulation also increased markers for excitatory synapse activity. Repetitive estradiol treatments increased excitatory synapse markers, but not synaptic activity markers. Furthermore, one dose of estradiol enhanced VEP amplitude following repetitive visual stimulation, however this was observed only in response to stimulation of the NDE. As presynaptic ERs are known to increase Pr at glutamatergic synapses, this suggests that the effects of estradiol

are specific to spared synapses where Pr has not been up-regulated by deprivation. Exploiting this selectivity may allow for receptive field remapping of spared inputs around a scotoma or cortical infarct.

CHARACTERIZATION OF CHRONIC MONOCULAR DEPRIVATION AND
ESTROGEN ADMINISTRATION IN ADULT RODENTS

By:

Deepali Clare Sengupta

Dissertation submitted to the Faculty of the Graduate School of the
University of Maryland, College Park, in partial fulfillment
of the requirements for the degree of
Doctor of Philosophy
2018

Advisory Committee:
Professor Elizabeth Quinlan, Chair
Professor Matthew Roesch, Dean's Representative
Professor Gregory Ball
Professor Catherine Carr
Professor Erica Glasper Andrews

© Copyright by
Deepali Clare Sengupta
2018

Dedication:

It truly takes a village to get a PhD. I first want to thank my advisor and mentor, Dr. Elizabeth M. Quinlan. She believed in my potential as a scientist starting with our very first meeting. Her mentorship, the resources provided by her lab, and the research group she has built have shaped me, in her image, into a determined experimentalist and truly critical thinker. I also want to thank the Quinlan lab members, including: Dr. Crystal L. Lantz for her collaboration and continuous guidance, Dr. Sachiko Murase for her constant generosity with her time and knowledge, and Andrew Borrell for his unfailing willingness to help in any way he can. I could not have completed this degree or furthered my research without the help of my committee: Dr. Gregory Ball, Dr. Catherine Carr, and Dr. Erica Glasper Andrews. They have all truly invested in my success and provided invaluable direction in shaping the path of my work. My thanks are also owed to my NACS cohort-mates and fellow grad students, which have given me a wonderful community of support throughout the years and lifelong friendships. Before graduate school or any higher learning, my amazing parents, Drs. Louise and Somnath Sengupta, set a high standard of intellectual accomplishment and sowed the seeds of scientific curiosity, starting with my first microscope set. My siblings, Sheila Becherer, Joshua Sengupta, and Jonah Sengupta, gave me all the love and encouragement I could ask for as their older sister. My husband and partner in life, Michael Deaton, has supported and loved me throughout this academic journey, from writing applications to buying snacks for my defense. Finally, my dog, Pepper Daisy, has paid her rent in full since I adopted her the day after my qualifying exam, by being the world's best emotional support animal. I dedicate this dissertation and the success that comes after it to all of them.

Table of Contents

Dedication	ii
Table of Contents	iii
List of Figures and Tables	v
Chapter 1 : Introduction	1
1.1 Neural consequences of aging	1
1.3 Interaction of loss of hormones with aging	4
1.4 Reintroduction of estrogen promotes plasticity	5
1.5 cMD as a model for loss of function and synapses	7
1.7 Significance / Aims	9
Specific Aim 1	12
Specific Aim 2	13
Chapter 2 : Further characterization of the anatomical and physiological effects of chronic monocular deprivation in the primary visual cortex of aged rats	14
2.1 Abstract	14
2.2 Introduction	15
2.3 Identification and validation of tools employed in this thesis to track synaptic density and plasticity	20
2.4 Materials and Methods	25
2.5 Results	31
2.5.1 Trans-neuronal viral tracing reveals decrease in innervation of cMD V1	31
2.5.2. Inhibitory interneuron activity and ECM expression increased with cMD	33
2.5.3 Excitatory synapse density is preserved despite cMD	35
2.5.4 Accelerated depression of deprived eye visually-evoked responses during repetitive visual stimulation	42
2.6 Discussion	44
Chapter 3 : The effects of estrogen and visual stimulation on V1 of cMD adult rats	48
3.1 Abstract	48
3.2 Introduction	49
3.3 Materials and Methods	54
3.4 Results	59
3.4.1 Robust expression of ER α and ER β in binocular region of V1 of adult male and female rats	59

3.4.2 17 α -estradiol administration does not stimulate growth of reproductive tissue of gonadally-intact animals.....	60
3.4.3 17 α E2 administration increases markers for plasticity in the amblyopic visual cortex	62
3.4.4 17 α E2 increases the size of excitatory post-synaptic densities	65
3.4.5 17 α E2 decreases expression of presynaptic markers	68
3.4.6 17 α E2 increases colocalization of pS831 and thalamic afferent markers	72
3.4.7 17 α E2 followed by visual stimulation further decreases markers for constrained plasticity in the cMD V1	74
3.4.8 17 α E2 followed by visual stimulation further increases size of excitatory synapses and synaptic signaling.....	77
3.4.9 17 α E2 followed by visual stimulation decreases expression of presynaptic markers	79
3.4.10 7 days of 17 α E2 administration increases excitatory synapse size ..	83
3.4.11 7 days of 17 α E2 administration downregulates markers for excitatory presynaptic terminals	89
3.4.12 7 days of 17 α E2 increases colocalization of synaptic markers.....	93
3.4.13 Assessing the effect of 17 α E2 administration on Stimulus-Selective Response Potentiation	98
3.4.14. Markers for constrained plasticity are differentially regulated following 17 α E2 administration and SRP stimulation protocol.....	102
3.4.15. 17 α E2 administration followed by SRP stimulation protocol increases markers for excitatory synapses.....	104
3.5 Discussion.....	113
Chapter 4 : Implications of Results & Future Directions for research.....	119
4.1 Discussion of Results.....	119
4.1.1 Novel observations regarding the anatomical consequences of cMD in aged V1	119
4.1.2 Assessing the effects of estrogen and visual stimulation on V1 of cMD adult rats.....	121
4.2 Limitations of Experimental Approach	128
4.3 Recommendations for Future Research	129
Bibliography	1

List of Figures and Tables	Pg.
Figure 1: Localization of excitatory synaptic proteins in dendritic spines	2
Figure 2: DE + Visual Experience induces spinogenesis	9
Figure 3: Estrogen will stimulate synaptogenesis and increase strength of visual response	11
Figure 4: Trans-neuronal tracing reveals reduced innervation from deprived eye to V1	32
Figure 5: cMD increases PV and WFA staining in V1b contralateral and ipsilateral to cMD	34
Table 1: PSD95 size / number following cMD	35
Figure 6: Characterization of the anatomical response of excitatory synapses to cMD	36
Table 2: pS831 size / number following cMD	38
Table 3: VGlut1 size / number following cMD	39
Table 4: VGlut2 size / number following cMD	39
Figure 7: Colocalization of excitatory synapse markers	40
Table 5: Colocalization of synaptic markers following cMD	41
Figure 8: Rapid depression of VEPs in response to stimulus of deprived eye	44
Figure 9: Non-nuclear estrogen receptors in visual cortex of male and female adult rats	60
Figure 10: 17 α estradiol does not enhance gonad weight of intact male and female adult rats	61
Figure 11: 17 α E2 reduces PV and WFA staining in V1b contralateral and ipsilateral to cMD	64
Figure 12: 17 α E2 increases size of markers for excitatory post-synaptic densities	67
Table 6: VGlut1 size / number following 17 α E2	69
Figure 13: 17 α E2 decreases markers for cortico-cortical and thalamocortical synapses	70
Table 7: VGlut2 size / number following 17 α E2	71

Table 8: Colocalization of synaptic markers following E5	72
Figure 14: Colocalization of pS831 increased at thalamocortical synapses	74
Figure 15: 17 α E2 followed by visual stimulus reduces PV and WFA staining in V1b contralateral and ipsilateral to cMD	76
Figure 16: 17 α E2 followed by visual stimulus increases markers for excitatory post-synaptic densities and synaptic activity	78
Figure 17: 17 α E2 followed by visual stimulation decreases markers for cortico-cortical and thalamocortical synapses	81
Table 9: Colocalization of synaptic markers following 17 α E2 + Vis Stim	82
Table 10: PSD95 size / number following 7d 17 α E2	85
Figure 18: 7 days of 17 α E2 increases markers for excitatory synapses independent of pS831	86
Table 11: pS831 size / number following 7d 17 α E2	88
Table 12: VGlut1 size / number following 7d 17 α E2	90
Table 13: VGlut2 size / number following 7d 17 α E2	91
Figure 19: 7 days of 17 α E2 decreases markers for cortico-cortical and thalamocortical synapses	92
Table 14: Colocalization of synaptic markers following 7d 17 α E2	94
Figure 20: Colocalization of cortico-cortical marker increased following 7 days of 17 α E2	97
Figure 21: Colocalization of thalamocortical marker increased following 7 days of 17 α E2	98
Figure 22: 17 α E2 promotes SRP specifically in non-deprived eye responses	101
Figure 23: 17 α E2 before SRP protocol reduces PV and WFA staining in cMD V1b	103
Table 15: PSD95 size / number following 17 α E2 24hrs	105
Table 16: pS831 size / number following 17 α E2 24hrs	106
Figure 24: 17 α E2 prior to SRP protocol increases markers for excitatory synapses and activity	107

Figure 25: 17 α E2 before SRP protocol increases size of thalamocortical afferent markers	109
Table 17: VGlut2 size / number following 17 α E2 24hrs	110
Table 18: Colocalization of synaptic markers following size / number following 17 α E2 24hrs	111

Chapter 1 : Introduction

1.1 Neural consequences of aging

Our world population is increasing in age (W. He et al., 2016) and age-related cognitive decline is a progressively significant issue (Gauthier et al., 2006). Cognitive decline that is independent of other disease, is strongly correlated with a global idiopathic shrinking and thinning of the cerebral cortex (Du et al., 2007; Pacheco et al., 2015; Singh et al., 2006). The decrease in brain matter and cognitive function over time is observed during normal aging in healthy individuals. For example, high resolution MRI reveals a significant reduction in total surface area, cortical thickness, and intracortical volume in both cerebral hemispheres in older participants (mean age = 76.6) relative to younger and middle-aged subjects (mean age = 22.8, mean age = 48.6, respectively)(Salat et al., 2004). Decreased brain volume and thickness have been correlated with reduced performance in a variety of cognitive tasks, including tasks that assess episodic, explicit, and working memory (Gunning-Dixon & Raz, 2003; Head et al., 2008; Raz et al., 1998). The effect of cortical atrophy with age is also observed in non-human primate studies, with a gross reduction in the thickness of cortical and subcortical areas correlated with reduced cognitive performance (Picq et al., 2012).

Counterintuitively, the gross reduction of cortical mass and cognitive task performance during normal aging does not appear to result from a loss of

neuronal density, as several reports demonstrate that neuron number is preserved with age in humans and non-human primates (Gunning-Dixon & Raz, 2003; J. H. Morrison & Hof, 1997). Instead, the reduction in cortical mass and cognition is correlated with a reduction in synaptic density, specifically excitatory synapses on dendritic spines, and a reduction of activity-dependent plasticity at these synapses (Bailey et al., 2011; J. H. J. Morrison & Baxter, 2012; Young et al., 2014).

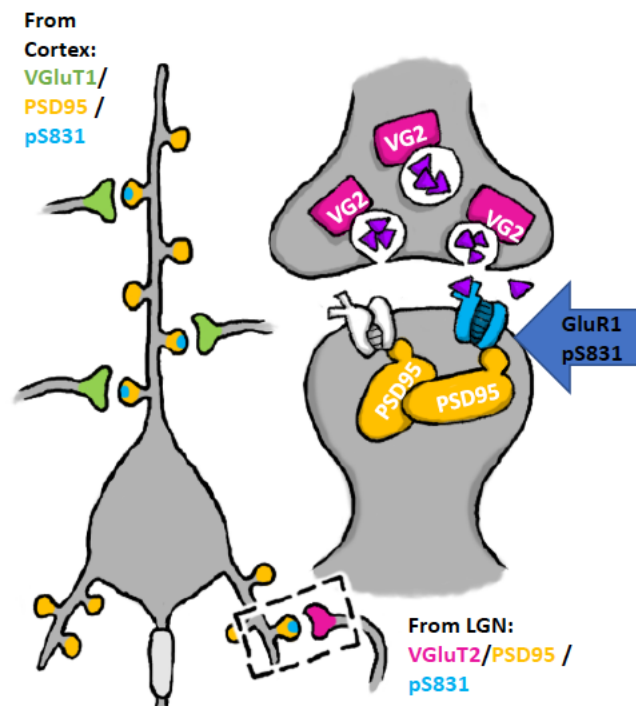


Figure 1: Localization of synaptic proteins at excitatory synapses.

Left: Spine structures distributed on the apical and basolateral dendrites of a primary cortical neuron. Cortico-cortical connections express the presynaptic protein VGlut1+ (green) and thalamocortical connections express the presynaptic protein VGlut2+ (magenta). Right: A magnified representation of the excitatory spiny synapse surrounded by the dashed box. In the post synaptic compartment, post-synaptic density scaffold protein PSD95 (yellow), is essential for synapse organization and present in most excitatory cortical synapses. Phosphorylation of Serine-831 residue on

The loss of dendritic spines with age is well-documented, and as spines are the site of the majority of excitatory synaptic connections in the CNS (Bourne

& Harris, 2008), this reduction is predicted to significantly compromise cortical function (Peters, Morrison, Rosene, & Hyman, 1998; Peters, Sethares, & Luebke, 2008) (Fig.1). In non-human primates, a significant reduction in dendritic spines was revealed in dye-filled primary neurons across the prefrontal and temporal cortices, which correlated with a reduction in performance of cognitive tasks (Duan et al., 2003; D. Dumitriu et al., 2010). Similarly, a strong negative correlation has been demonstrated in rodents between age and dendritic spine density in the prefrontal cortex (Bloss et al., 2011; Nunzi et al., 1987).

Dendritic spines are also important substrates for synaptic plasticity and learning, as changes in dendritic spine number and/or size have been repeatedly correlated with changes in synaptic strength (Cane et al., 2014; Hotulainen & Hoogenraad, 2010; Kasai et al., 2010). In addition, the size of the spine head is highly correlated with the size of the postsynaptic density (PSD), a collection of scaffolding proteins, such as PSD95 (McAllister, 2007), neurotransmitter receptors and signaling molecules that comprise the post-synaptic active zone (Harris et al., 1992). At excitatory synapses, the size of the PSD is highly correlated with the number of synaptic AMPA subtype of glutamate receptor, the primary ionotropic glutamate receptor in the mammalian CNS, and therefore highly correlated with synaptic strength (Nusser et al., 1998; Song & Huganir, 2002). Dendritic spines can receive excitatory input from thalamic or cortical axons, which can be distinguished by the expression of distinct vesicular glutamate transporters, VGlut2 in thalamic axons and VGlut1 in cortical axons

(VGlut1, VGlut2) (Liguz-Leczna & Skangiel-Kramska, 2007b). Individual spiny synapses can express long-term potentiation (LTP), an activity-dependent increase in synaptic strength resulting from coincident activity and thought to be the neural correlate of memory (Bliss & Cooke, 2011; S. F. Cooke & Bliss, 2006). Furthermore, photolysis of caged glutamate reveals that an enlargement of dendritic spine volume is associated with LTP at single spines (Matsuzaki et al., 2004). Thus, dendritic spine size and PSD size correlate with the strength of excitatory synapses, and have been used effectively to track changes in synaptic strength (Khan et al., 2013; Kim et al., 2007; Q. Sun & Turrigiano, 2011; Zhang & Lisman, 2012)

1.3 Interaction of loss of hormones with aging

The loss of spine synapses with normal aging is widely thought to be exacerbated by the developmental decline in circulating sex hormones. In humans, age-related cognitive decline has long been associated with a decrease in circulating sex hormones (Muller et al., 2005; Yaffe et al., 2000, 2002). In fact, induction of menopause through surgical methods, either by hysterectomy or oophorectomy in premenopausal women, causes accelerated cognitive decline (Bove et al., 2014). In non-human primates, aged ovariectomized (OVX) animals performed poorly in delayed match-to-sample (DNMS) tasks compared to younger cohorts (P. R. Rapp et al., 2003). In rodents, an age-related decrease in estrogen levels is correlated with a decrease in the number of glutamatergic

synapses (Hao et al., 2006). OVX aged rodents show cognitive impairment compared to sham-operated subjects (Savonenko & Markowska, 2003). Furthermore, OVX aged non-human primates have significantly reduced dendritic spine density in PFC compared to young OVX animals (Hao et al., 2006; J. H. J. Morrison & Baxter, 2012; Tang et al., 2004). Primary neurons in the aged rat hippocampus have reduced apical and basal dendritic spine density in comparison to young OVX subjects (Gould et al., 1990). Similarly, inhibition of estrogen biosynthesis, via inhibition of aromatase, acutely induces spine synapse loss (Zhou et al., 2010). Furthermore, age-related decline in cognitive tasks and dendritic spine density are reversed by estrogen treatment in OVX females (Bailey et al., 2011; Dumitriu et al., 2010; Hara et al., 2016). Taken together, the 'one-two' punch of aging combined with reduction in sex hormones induces significant decrease in synaptic density, plasticity, and cognitive performance.

1.4 Reintroduction of estrogen promotes plasticity

A large body of work demonstrates that reintroduction of sex hormones, specifically estrogen, improves cognition. Estrogen therapy (ET) in oophorectomized premenopausal women helps to prevent age-related cognitive impairment and improves verbal memory (Sherwin, 2012). In addition, ET reduces the development of all-cause dementia if initiated by age 65 (Henderson et al., 2007). Initiation of ET in early post-menopause improves global cognition, attention, and concentration (MacLennan et al., 2006), prevents cognitive decline in normally-aging adults (Bagger et al., 2005), and has been proposed to prevent

the development of Alzheimer's disease (Zandi, 2002). Furthermore, ET in postmenopausal women attenuated the progression of cognitive decline in subjects with mild cognitive decline (Yoon et al., 2018). These studies support foundational work demonstrating that cognitive task performance peaks during periods of high circulating estrogens in premenopausal women (Bailey et al., 2011).

In aged rhesus macaques, estrogen replacement following OVX improves cognitive performance (P. R. Rapp et al., 2003). Following ET, OVX subjects acquired cognitive tasks more quickly and performed tasks with more accuracy. Additionally, estrogen replacement in OVX rats improved object/place recognition and enhanced spatial working memory (Gibbs, 1999; Jacome et al., 2010). Estrogen also reduces the severity score and improves water maze performance of rodents following traumatic brain injury (Lu et al., 2018). Estrogen administered immediately before task learning and/or testing also improved performance in social learning, social recognition, object recognition and object placement in adult OVX rodents (Luine et al., 2003; Phan et al., 2012). Interestingly, estrogen administered immediately after a task improved object recognition and memory consolidation (Gresack & Frick, 2006).

These effects of estrogen are thought to be due to estrogen-dependent rejuvenation of synaptic function, structure, and excitability to levels that promote plasticity. Cyclic fluctuations of estrogen alter dendritic spine density and synaptic

potentiation in the hippocampus and cortex (Chen et al., 2009; Gould et al., 1990; Warren et al., 1995; Woolley & McEwen, 1993). ET in adult rodents has been shown to increase the probability of neurotransmitter release at excitatory synapses, enhance synaptic strength, and promote synaptic plasticity (Huang & Woolley, 2012; Khan et al., 2013; Kramár et al., 2013; Rudick et al., 2003; Smejkalova & Woolley, 2010). Inhibition of estrogen synthesis also protects against seizure and excitotoxicity (Liu et al., 2012). Importantly, estradiol administration promotes the formation of new dendritic spines rapidly and non-genomically, presumably via activation of membrane-bound estrogen receptors (ERs) associated with the PSD (Hojo et al., 2008; Srivastava et al., 2010). Newly formed dendritic spines are hypothesized to be stabilized and integrated into cortical circuits by activity-dependent, modality-dependent stimulation (Kramár et al., 2013; Srivastava et al., 2011).

1.5 cMD as a model for loss of function and synapses

Development of interventions to promote the generation of new spines in the aged brain requires an experimental system with rigorous temporal and spatial control of synaptic activity, as well as experimental tools that allow for the tracking excitatory synapses and other aspects of cortical circuitry with high resolution. An asymmetry in the visual input across the two eyes, due to cataract, strabismus, or anisometropia, causes amblyopia (Fig. 2A) and a significant reduction in vision through the weaker eye. Amblyopia affects an estimated 3% of the world's human population and is the most common form of monocular

blindness (Webber & Wood, 2005). Deprivation amblyopia, induced by a congenital cataract, can be replicated experimentally by chronic monocular deprivation (cMD). Initiated at eye opening and persisting until after adolescence (cMD from postnatal day 14 (P14) until ~P150 (He et al., 2007)), cMD reduces vision in the deprived eye, and causes multiple deficits in the deprived eye pathway, including a significant decrease in the strength and selectivity of visually-evoked responses, and a corresponding decrease in dendritic spine density in the visual cortical hemisphere dominated (contralateral) by the deprived eye (Montey & Quinlan, 2011) (Fig. 2B). The severe amblyopia induced by cMD was previously thought to be irreversible beyond an early postnatal critical period (Hubel & Wiesel, 1970). However, the Quinlan lab has shown that robust plasticity can be reactivated in adulthood by dark exposure (DE) (He, Hodos, & Quinlan, 2006; Murase et al., 2017; Bridi et al., 2018). DE followed by visual stimulation promotes the recovery from cMD, including visual acuity, synaptic strength, and dendritic spine density (Eaton et al., 2016; Montey et al., 2013; Montey & Quinlan, 2011; Murase et al., 2017)(Fig. 2C).

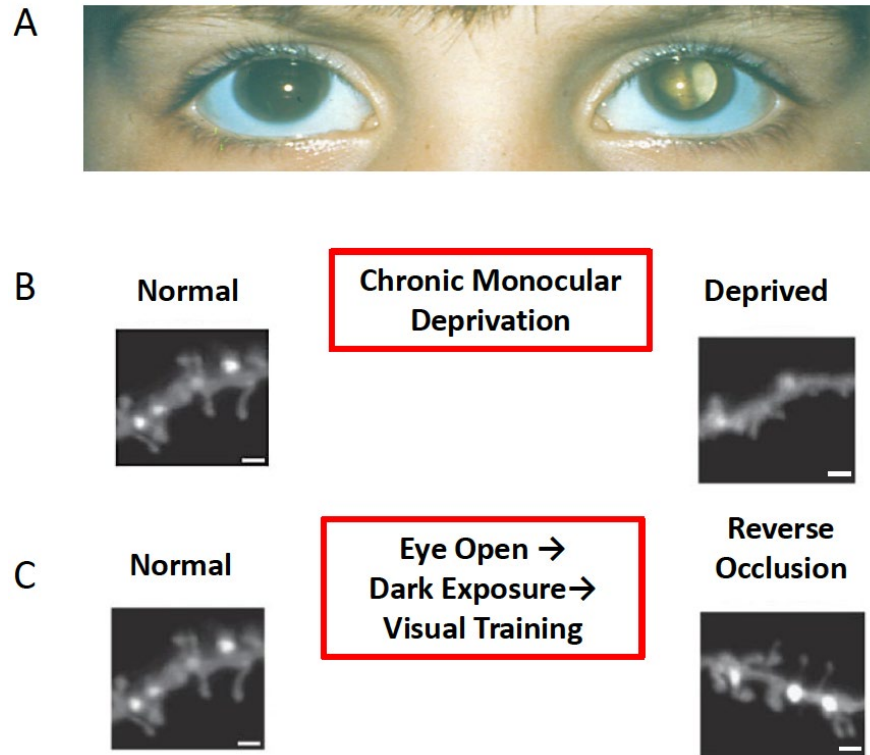


Figure 2: Dark Exposure + Visual Training induces spinogenesis
A. Human child with congenital cataract in left eye, which will induce amblyopia if left untreated. **B.** Dil-filled dendritic branches of neurons in binocular region of primary visual cortex (V1b) reveal striking difference in number and shape of dendritic spine in adult rats that were normally-reared (left) and chronically-monocularly deprived (right) from P14-P150. **C.** Following reverse deprivation (open closed eye and close open eye), subjects received 10 days of dark exposure (DE) followed by visual training. Dendritic spine density on the neurons in the deprived hemisphere (right) have recovered dendritic spine density to the level of non-deprived visual cortical neurons (left). Scale bar = 2.5 μ m; data from Montey & Quinlan, 2011.

1.7 Significance / Aims

DE is slow and may be difficult to administer, I was therefore motivated to identify potential pathways to enhance plasticity in the aged amblyopic visual cortex that can be used as a substitute for, or used in conjunction with, visual deprivation. I hypothesized that the potent neuromodulator, estrogen, which has been previously demonstrated to rejuvenate spine synapse density lost with age and/or hormone deprivation, would induce synaptogenesis at excitatory synapses in cMD visual cortex.

Furthermore, this morphological plasticity could be harnessed to drive experience-dependent incorporation of newly-formed spiny synapses into functional circuits to promote strengthening of deprived eye visual responses (Fig 3). An estrogen-based method for the recovery of active excitatory synapses in the adult V1 would be a novel strategy for the treatment of amblyopia, with the potential to be translated to other functional deficits, such as those due to stroke or scotoma. I tested this hypothesis with the following specific aims:

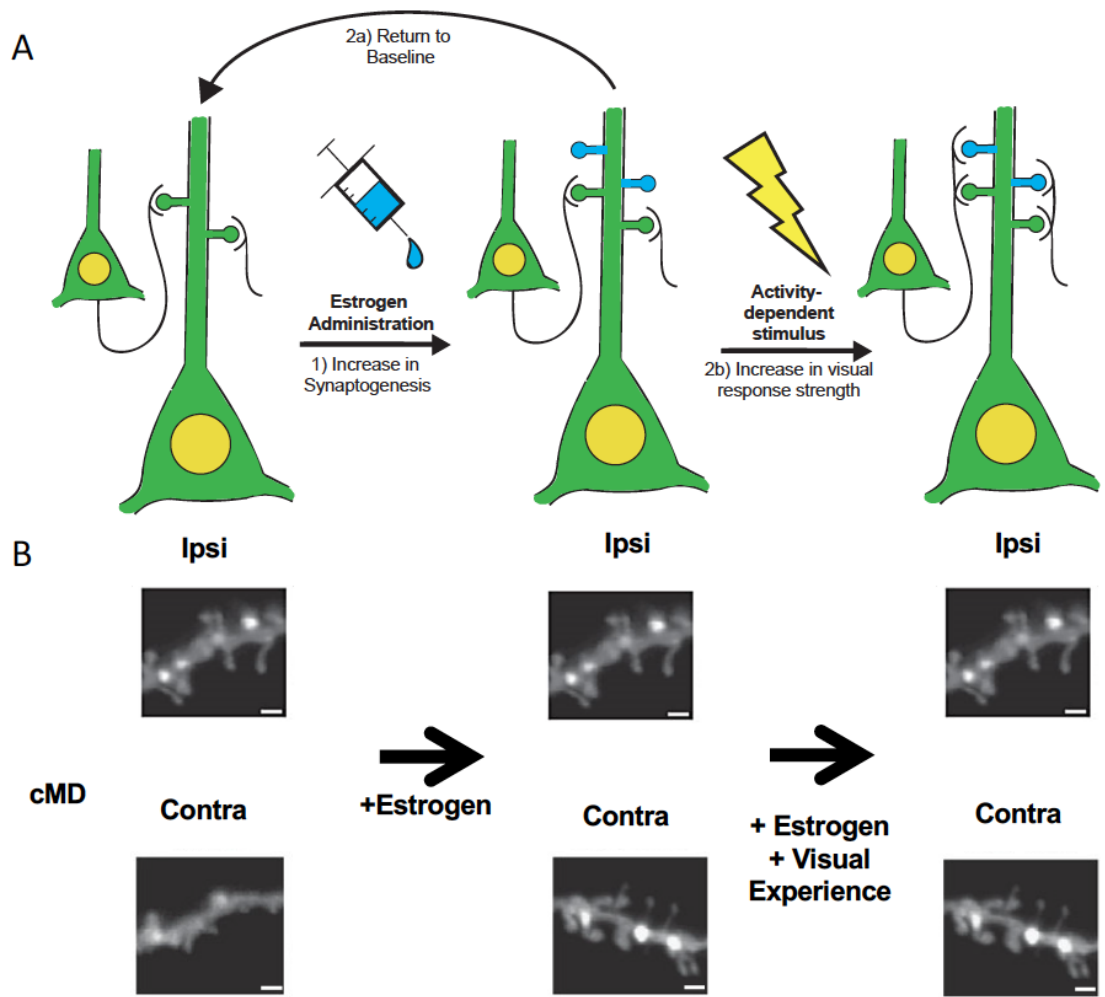


Figure 3: Estrogen will stimulate synaptogenesis and increase strength of visual responses

A. Experimental Schematic: I propose that a single administration of estrogen will stimulate spinogenesis / synaptogenesis (1) and the new spines / synapses will either be stabilized and incorporated into functional circuits with salient visual experience (2b) or eliminated (2a). **B.** Experimental Prediction: Estrogen paired with visual experience will rescue the anatomical and visual plasticity deficits inflicted by chronic monocular deprivation (cMD). Estrogen will stimulate synaptogenesis and increase strength of visual responses Scale bar: 2.5 μm .

Specific Aim 1

I characterized the anatomical and physiological effects of cMD in rodent V1 using viral tracing, immunohistochemistry, and electrophysiology. I used cMD to induce a significant asymmetry in the visual experience across the two eyes. I employed transneuronal tracers delivered intraocularly to identify the neurons in V1 that serve each eye, and examined molecular markers for the density of the extracellular matrix (ECM) and the excitability of fast-spiking interneurons (PV) to ask if cMD impacts plasticity in V1. I also asked if cMD impacted the number and/or size of excitatory synapses in the deprived and non-deprived cortex by quantifying the intensity and distribution of the scaffold protein PSD95. I examine the effect of cMD on the number and/or size of thalamic and cortical presynaptic specializations by quantifying the intensity and distribution of presynaptic excitatory neurotransmitter transporters, VGlut1 and VGlut2. I also examined if cMD impacted the activity of signaling pathways known to regulate postsynaptic glutamate receptor function by measuring the intensity and distribution of the glutamate A1 (GluA1) subunit of the α -amino-3-hydroxy-5-methyl-4-isoxazolepropionic acid receptor (AMPA), phosphorylated on residue Serine 831 (pS831). In collaboration with a physiologist in the Quinlan lab (Dr. Crystal Lantz), we examined the amplitude of visually evoked local field potentials (VEPs) in response to repetitive visual stimulation, to ask if cMD impacted the short-term depression of VEPs. This work identified novel anatomical and physiological consequences of cMD, and is presented in Chapter 2.

Specific Aim 2

I used quantitative immunohistochemistry and electrophysiology to ask if estrogen treatment impacts the anatomical and functional deficits induced by cMD. I demonstrate the presence of estrogen receptor (ER) alpha and beta, in intact male and female subjects, and confirm that $17\alpha E_2$ treatment does not induce negative peripheral effects. I ask if estrogen treatment alone, or estrogen treatment followed by repetitive visual stimulation regulates the density of the ECM, the excitability of PVs, the number and/or size of excitatory synapses, thalamic and cortical presynaptic specializations, and the activity of postsynaptic PKC/CaMKII signaling. Collaboratively, I asked if estrogen treatment impacted the long-term stimulus selective response potentiation induced by repetitive visual stimulation. This work identified a surprising specificity to the effect of estrogen in the amblyopic visual cortex, and is presented in Chapter 3. In Chapter 4, I expand on the interpretation of these results, and pose a list of interesting follow-up experiments.

Chapter 2 : Further characterization of the anatomical and physiological effects of chronic monocular deprivation in the primary visual cortex of aged rats

2.1 Abstract

Monocular deprivation is the classical model of receptive field plasticity confined to a postnatal critical period. Chronic monocular deprivation (cMD), monocular lid suture from before eye opening until adulthood, induces severe amblyopia that is highly resistant to reversal in adults, and is a model of the visual deficits caused by unilateral cataract. Here I further characterize the anatomical and physiological effects of cMD in the binocular region of primary visual (V1b) cortex of adult rats. I used trans-neuronal anterograde tracers to show that cMD reduces thalamic input from both eyes to V1b, and expands the area innervated by the non-deprived eye into the monocular region of primary visual cortex (V1m). To ask about the level of plasticity in the deprived and non-deprived cortex following cMD, I tracked the expression of two markers that have been repeatedly correlated with the state of plasticity. The expression of parvalbumin (PV) reflects activity in fast-spiking interneurons, which provide strong perisomatic inhibition to cortical pyramidal neurons. The lectin *Wisteria floribunda* agglutinin (WFA) binds to a major component of the extracellular matrix (ECM), the maturation of which imposes constraints on anatomical plasticity. Following cMD, there is an increase in PV and WFA staining in V1b of both cortical hemispheres, consistent with reduced plasticity in the aged amblyopic cortex. Quantitative immunohistochemistry revealed no difference in

the density of excitatory synaptic markers in the deprived versus non-deprived V1b, suggesting that synapses lost by cMD may be counter-balanced by an increase in synapses serving the non-deprived. Importantly, visual responses evoked by repetitive stimulation of the deprived eye depressed more rapidly than responses of the non-deprived eye, suggesting the cMD increases the probability of neurotransmitter release synapses serving the deprived eye.

2.2 Introduction

The plasticity of ocular dominance (OD) of neurons in the binocular region of primary visual cortex (V1b) is one of the best studied models of receptive field plasticity confined to a postnatal critical period (T N Wiesel & Hubel, 1965; Torsten N Wiesel & Hubel, 1963). Neurons in V1b in rodent have a strong preference for stimulation from the contralateral eye (contralateral bias), as approximately twice as many thalamic afferents to cortex serve the contralateral than ipsilateral eye (Coleman et al., 2009). When a unilateral deficit is induced by monocular deprivation of the dominant, contralateral eye, there is a shift in the ocular preference of binocular neurons away from the contralateral / deprived eye and towards the ipsilateral / non-deprived eye. The shift in ocular preference induced by monocular deprivation is due in part to a reduction in the number of thalamic afferents serving the deprived eye (Hubel et al., 1976; Shatz & Stryker, 1978). If the monocular deprivation is initiated at eye opening and maintained into adulthood (chronic monocular deprivation (cMD)), the physiological, anatomical, and acuity deficits in the deprived eye pathway are highly resistant to

reversal (He et al., 2007). These deficits are observed at the anatomical, physiological and psychophysical level and include a significant reduction in the strength and selectivity of visually responses evoked in the deprived eye, a significant reduction in the number of dendritic spines in V1b contralateral to the deprived eye, and a significant reduction in spatial acuity of the deprived eye (Montey & Quinlan, 2011) .

It is well known that the development of the visual system depends on visual experience, and can be significantly attenuated by dark rearing (Kirkwood et al., 1995; Mower et al., 1981). Dark rearing from birth prevents many aspects of visual system maturation, such as the refinement of cortical receptive fields, the neuronal selectivity for ocular preference and other aspects of visual stimuli, visual acuity and maturation of gamma-aminobutyric acid (GABA)-ergic inhibitory circuits (M Fagiolini et al., 1994; Morales et al., 2002; Mower, 1991; Regal et al., 1976). In addition, dark rearing attenuates developmental changes in the N-methyl-D-aspartate (NMDA) subtype of glutamate receptors (NMDARs), the ionotropic glutamate receptor that is central to Hebbian plasticity mechanisms due to dual activation requirements (ligand and voltage) and permeability to calcium. In V1, NMDARs at birth are comprised of NR2B and NR1 subunits, and have slow kinetics and high sensitivity to agonists (Monyer et al., 1994). Evidence suggests that these properties may promote synaptic potentiation after NMDAR activation (Paoletti et al., 2013). During the first 5 postnatal weeks of development, there is a progressive reduction in NR2b-containing NMDARs and

progressive inclusion of the NR2A-containing NMDARs, which increases kinetics and decreases calcium permeability (Vicini et al., 1998). Reports indicate that these properties may reduce synaptic potentiation after NMDAR activation. Dark-rearing from birth prevents the switch in NMDAR composition and the developmental reduction in the expression of synaptic potentiation (Quinlan et al., 1999).

Surprisingly dark exposure (DE) in adults can also enhance plasticity in the visual cortex. DE increases the number of NR2B-containing NMDARs in V1b and lowers the threshold for synaptic potentiation (Bridi et al., 2018; He et al., 2006). In addition, DE rejuvenates endocannabinoid-dependent long-term depression of inhibitory transmission, and extends the window for integration of spike-timing dependent plasticity (Guo et al., 2012; S. Huang et al., 2010, 2015). These mechanisms lead to a re-expression of critical period-like plasticity, and can promote reversal of anatomical and physiological deficits induced by cMD (He et al., 2007; Montey & Quinlan, 2011). When DE is followed by visual training, such as repetitive performance in a visual discrimination task, deprived eye acuity levels fully recover (Montey et al., 2013).

Ongoing work is beginning to reveal the mechanisms for re-expression of plasticity following DE. DE followed by light re-exposure (LRx) degrades the perisynaptic extracellular matrix (ECM), and is an obligatory step in the reactivation of structural and functional plasticity by DE (Murase et al., 2017).

Maturation of the ECM has long been known to constrain structural and functional plasticity in adult circuits. Reduction in perineuronal nets (PNNs) a dense specialization of ECM that ensconce mature parvalbumin+ (PV+) interneurons has been repeatedly correlated with enhanced plasticity (Balmer, 2016). Accordingly, proteolysis of PNNs using an exogenous enzyme (chondroitinase ABC (ChABC)) reactivates ocular dominance plasticity in adult rodents (Pizzorusso et al., 2002). In amblyopic rodents, the reactivation of plasticity by repetitive chABC treatment promotes the recovery of ocular dominance of visually-evoked potentials and visual acuity (Pizzorusso et al., 2006).

DE is not the only method being explored to enhance plasticity in the adult visual cortex. Pharmacological or genetic suppression of cortical inhibition can cause re-expression of plasticity in adults (Bochner et al., 2014; Gu et al., 2016; Morishita et al., 2010), consistent with evidence that maturation of inhibition regulates the timing of the critical period (Michela Fagiolini & Hensch, 2000; Takao K Hensch, 2005; Iwai et al., 2003). In addition, environmental enrichment, which encourages behavioral and sensorimotor exploration, enhances plasticity in adult V1b (Bartoletti et al., 2004; Greifzu et al., 2014; Kalogeraki et al., 2017). Amblyopic rats that receive reverse suture (RS, opening of the deprived eye, closure of the non-deprived eye) followed by environmental enrichment, have basal levels of inhibitory neurotransmitter GABA reduced by a factor of 3 in contralateral V1b. Electrophysiological and behavioral measures of visual acuity

in the deprived eye also improve to the level of the non-deprived eye, and contralateral bias is restored (Sale et al., 2007).

In addition, blockade of paired immunoglobulin-like receptor B (PirB), which binds major histocompatibility complex I (MHC I) in neurons and recruits phosphatases that may restrict neuronal responses to activity-dependent and Ca^{2+} signaling, (Syken et al., 2006) reinstates plasticity in adults (Bochner et al., 2014). Genetic deletion of PirB reinstates OD plasticity in mice well past the critical period (postnatal day 70-74, P70-74) promoting a significant open-eye expansion in response to brief MD. Similarly, blockade of the native PirB receptor with a soluble ectodomain in wild type adults leads to a comparable expansion of the open eye representation following MD. Receptor blockade and eye opening reversed deficits in chronically monocularly deprived animals and increased spine density in deprived V1, increased deprived-eye VEP amplitudes, and significantly improved visual acuity of the deprived eye.

Finally, enhancement of cholinergic transmission in V1 has been shown to reverse the deficits of cMD. Genetic deletion of the molecule Lynx1, which binds to nAChRs and reduces their affinity for acetylcholine, reactivates robust ocular dominance plasticity in response to brief MD (Morishita et al., 2010). In turn, Lynx1 knockouts experienced spontaneous reversal of cMD (spanning the length of the critical period) by merely opening the deprived eye. When cholinergic transmission was enhanced in WTs by a cholinesterase inhibitor, a similar

spontaneous reversal of cMD was observed (assessed as recovery of high spatial acuity). Lynx1 is localized on PV+ cells in V1, leading to the hypothesis that blockade of the Lynx1-nAChR interaction disinhibits pyramidal neurons in V1.

Thus, various MD paradigms have been used to investigate experience-dependent plasticity in a spatially and temporally-controlled manner, as well as well as the mechanisms of loss / recovery of neuronal anatomy and physiological function. Importantly, most other labs perform MD that is initiated ~P21, allowing for one week of binocular vision before MD. In contrast, the Quinlan lab initiates MD at eye opening and continuing to adulthood. However, there has been little characterization of this form of cMD at the molecular level, which I proposed was essential for understanding barriers to recovery and developing further interventions for reversal of the deficit.

2.3 Identification and validation of tools employed in this thesis to track synaptic density and plasticity

To quantify the number and size of excitatory synapses, I will track PSD95, a major component of mature excitatory post-synaptic densities. PSD95 is one of the earliest detectable proteins at the postsynaptic density in nascent synaptic connections (McAllister, 2007). PSD95 co-localizes several critical synaptic proteins, including neurotransmitter (NT) receptors, as well as cytoskeletal elements which organize and create the structure of the synapse,

and is thought to enable aspects of spine synapse maturation and LTP induction / expression (Chen et al., 2011; Sheng & Kim, 2011). The majority of dendritic spine synapses contain PSD95 (El-Husseini et al., 2000) and PSD95 accumulation has been shown to be essential for the stabilization and maintenance of spines (Cane et al., 2014). Importantly, spine enlargement is correlated with the enlargement of PSD95 immunoreactive area (Ehrlich et al., 2007). Therefore, PSD95 puncta number and can be used as a correlate for excitatory synaptic number and strength.

Thalamic axons and cortical axons both make excitatory synapses onto pyramidal neurons in V1. Vesicular glutamate transporter 1 (VGlut1) is present in cortical axons, and vesicular glutamate transporter 2 (VGlut2) is present in thalamocortical axons (Liguz-Lecznar & Skangiel-Kramska, 2007a). Consistent with known innervation patterns of cortical and thalamic projections, VGlut1 labels terminals in all layers of the cortex, while VGlut2 labeling is heavy in thalamo-recipient layers (Layers I, IV, and VI) (Lei et al., 2013). I will use VGlut1 and VGlut2 to track excitatory synapses in rodent V1 made by cortical and thalamic afferents.

In addition to markers for excitatory synapses, it would be useful to have a marker for synaptic activity. Traditionally, immunohistochemistry (IHC) for activity-dependent immediate early genes such as c-Fos has been used to track the activation of neurons within circuits (Bullitt, 1990). However, immediate early

genes label the nucleus and peri-nuclear cytoplasm of recently active neurons, and cannot resolve which synapses on these neurons were recently stimulated. The same limitations exist for recently developed methods for the activity of neurons in real time *in vivo*, such as GCaMP, which is biased toward the strong calcium increase seen in the cell body, and back-propagating action potentials in the dendrites (Chen et al., 2012; Tian et al., 2009). Alternatively, phosphorylation / dephosphorylation of synaptic proteins by signaling cascades following synaptic activation has the potential to report activity of single synapses. The α -amino-3-hydroxy-5-methyl-4-isoxazolepropionic acid subtype of glutamate receptor (AMPA), comprised of GluR1/GluR2 or GluR2/GluR3 heterodimers, mediate the majority of fast-glutamatergic transmission in the brain (Anggono & Huganir, 2012). They are highly mobile proteins that undergo constitutive and activity-dependent trafficking and increases in the number / changes subunit composition mediate LTP and LTD (Malenka & Bear, 2004) Synaptic activity and resulting calcium influx results induces Ca^{2+} /calmodulin dependent kinase II (CaMKII) / Protein Kinase C (PKC)-dependent phosphorylation of the Serine 831 residue of the GluR1 subunit (pS831), which regulates AMPAR trafficking (Barria et al., 1997). Importantly, rapid and transient phosphorylation of S831 is induced by salient stimulation, with an onset of less than 30 minutes and persistence for ~2 hours (Whitlock et al., 2006). Thus, phosphorylation of S831-GluR1 reflects recent synaptic CaMKII/PKC activity (Ferrario et al., 2011; Whitlock et al., 2006), I will therefore use antibody that recognizes the GluR1 subunit of AMPAR only if phosphorylated at S831 (Barry & Ziff, 2002; Lee et al., 2007).

The experience-dependent maturation of GABAergic inhibition has been strongly implicated in the initiation and closure of critical period plasticity (Fagiolini & Hensch, 2000; Hensch, 2005; Iwai et al., 2003). According to this model, a threshold level of inhibition is necessary to initiate the critical period, and further maturation of inhibitory circuits terminates the critical period. The Quinlan lab recently used manipulations of the neurotrophin NRG1/ erbB receptor tyrosine kinase signaling pathway, which controls the strength of excitation onto fast spiking interneurons (FS INs), to reversibly regulate ocular dominance plasticity. NRG1 increases the excitability of FS INs, but the impact of this increase depends on the initial state of excitatory input: NRG1 application during the critical period induced precocious closure, while blockade of NRG1 signaling in adults reactivated the critical period for ocular dominance plasticity (Gu et al., 2016). Similarly, pharmacological enhancement of inhibition at the initiation of MD with diazepam, a positive allosteric modulator of GABA_ARs, blocks OD plasticity during the critical period. Conversely, pharmacogenetic reduction of PV interneuron output with G_i-DREADD induces robust OD plasticity in adults (Kuhlman et al., 2013).

Importantly, inhibitory basket cells, which make up of the majority of interneurons in the cortex, express the calcium-binding protein parvalbumin (PV) (Whissell et al., 2015). PVs have fast-spiking dynamics and innervate the cell bodies of pyramidal neurons (Freund & Katona, 2007). Mature PV+ basket cells

are ensconced in thick extracellular matrix specialization known as perineuronal nets (PNNs), which may electrochemically sequester synapses around the soma, (Carstens et al., 2016) and provide binding sites for molecules that maintain the excitability of PV+ interneurons (Balmer, 2016). PNNs can be visualized with wisteria floribunda (WFA), a plant lectin that binds a N-acetyl-D-galactosamine side chain of the chondroitin sulfate proteoglycans (CSPGs), a major component of the ECM (Miyata & Kitagawa, 2016). Both the maturation of PV circuitry and the PNNs have been correlated with reduced synaptic plasticity (Balmer, 2016; Harauzov et al., 2010; Lensjø et al., 2017). Therefore, I will use PV immunoreactivity and WFA staining as two ways to assess the potential for synaptic plasticity in V1 circuits.

The shift in ocular dominance following brief MD has been shown to reduce the input from the deprived thalamus to the cortex (Fagiolini et al., 1994; Gordon & Stryker, 1996; Gu et al., 2013; Maffei et al., 2004). To quantify the effect of cMD on thalamic-innervation of the cortex, I will use intraocular injection of the H129 strain of herpes simplex virus 1 (HSV-H129), an anterograde, trans-neuronal viral neuronal tracer that can be engineered to express different fluorophores (N. Sun et al., 1996). H129 expressing either EGFP or mCherry will be injected intraocularly into each eye, trans-neuronal anterograde transport will label neurons in the primary visual cortex are innervated by each eye. I will use HSV-H129 to ask how cMD impacts of the representation of the deprived and non-deprived eye in V1b.

cMD is also known to induce significant changes in the physiological response properties of neurons in V1b. In addition to the decrease in the strength and selectivity of visual responses evoked through deprived eye stimulation, I hypothesize that cMD may regulate presynaptic function, including a compensatory increase in presynaptic release probability. Previous reports have shown that brief deprivation induces an increase in release probability of excitatory neurons onto excitatory neurons in response to deprived-eye stimulation in the visual thalamus and in response to dark rearing in the visual cortex (Krahe & Guido, 2011; Yashiro et al., 2005). These experiments were a collaboration with Dr. Crystal L. Lantz, a postdoc in the Quinlan lab with expertise in cortical electrophysiological recordings. We will examine changes in the amplitude of the VEP during repetitive visual stimulation, which reflects the initial release probability, in response to stimulation of the deprived and non-deprived eye. Together, the work described in this chapter will characterize the anatomical and functional consequences of cMD in the deprived and non-deprived V1.

2.4 Materials and Methods

Subjects

Long Evans Rats (strain 006, RRID:RGD_2308852) were purchased from Charles River Laboratories (Raleigh, NC). Equal numbers of adult (>postnatal day 180, >P180) males and females were used. Animals were raised in 12/12

hour light/dark cycle and all experiments were performed, or subjects were sacrificed, 6 hours into the light phase. All procedures conformed to the guidelines of the University of Maryland Institutional Animal Care and Use Committee and the Guide for the Care and Use of Laboratory Animals of the National Institutes of Health.

Monocular deprivation

Subjects were anesthetized with ketamine/xylazine (100 mg/10 mg/kg, intraperitoneal). The margins of the upper and lower lids of one eye were trimmed and sutured together using a 5-0 suture kit with polyglycolic acid (CP Medical). Subjects were returned to their home cage after recovery at 37°C for 1-2 hours and disqualified in the event of suture opening.

Antibodies

The following antibodies/dilutions were used: mouse anti-parvalbumin (PV; Millipore; RRID:AB_2174013, 1:1000); mouse anti-Post Synaptic Density 95kd (PSD95; ThermoFisher; RRID: AB_325399, 1:200); rabbit anti-phospho-Serine 831-GluR1 (pS831; Sigma Aldrich; RRID:AB_1977218, 1:1000), guinea pig anti-Vesicular Glutamate Transporter 1 (VGlut1; Millipore; RRID:AB_11214451, 1:1000); guinea pig anti-Vesicular Glutamate Transporter 2 (VGlut2; Millipore; RRID:AB_2665454, 1:2000); followed by appropriate secondary antibodies: goat anti-rabbit and anti-mouse IgG conjugated to Alexa-488, 546, or 647 (Life

Technologies; RRID:AB_143165, RRID:AB_AB_2534118, RRID:AB_2535805, 1:300).

Reagents

HSV-H129 EGFP (strain 772; University of Pittsburgh Center for Neuroanatomy and Neurotropic Viruses (CNNV)) and HSV-H129 mCherry (strain 373; CNNV) were diluted 1:1 with diH₂O and 3 µl was injected intraocularly (right eye: mCherry; left eye: EGFP) for anterograde delivery to primary visual cortex. Chondroitin sulfate proteoglycans (CSPGs) were visualized with fluorescein wisteria floribunda lectin (WFA, Vector Labs; 1:1000).

Immunohistochemistry

Subjects were perfused with phosphate buffered saline (PBS) followed by 4% paraformaldehyde (PFA) in PBS. The brain was post-fixed in 4% PFA for 24 hours followed by 30% sucrose for 48 hours, and cryo-protectant solution (0.58 M sucrose, 30% (v/v) ethylene glycol, 3 mM sodium azide, 0.64 M sodium phosphate, pH 7.4) for 24 hours prior to sectioning. Coronal sections (40 µm) were made on a Leica freezing microtome (Model SM 2000R). Sections were blocked with 4% normal goat serum (NGS) in PBS for 1 hour. Antibodies were presented in blocking solution for 24 hours, followed by appropriate secondary antibodies.

Confocal imaging and analysis

Images were acquired on a Zeiss LSM 710 confocal microscope. HSV anterograde viral tracer signal was visualized in single z-section images (2.8 mm² or 1.4 mm²), acquired with a 5x (Zeiss Plan-neofluar 5x/0.16, NA=0.16) or 10x lens (Zeiss Plan-neofluar 10x/0.30, NA=0.30), and a mean intensity profile was calculated using FIJI (NIH). The cortical distribution of WFA and PV immunoreactivity was determined in a z-stack (9 x 7.5 µm sections) acquired with the same 10X lens. Maximal intensity projections (MIPs; 500 µm width, 900 µm depth from cortical surface) were used to obtain mean intensity profile in FIJI. For PSD95, pS831, VGlut1, and VGlut2 staining, MIPs of z-stacks (40 slices x 0.9 µm images) were acquired at 100X (Zeiss Plan-neofluar 100x/1.3 Oil DIC, NA=1.3). PSD95, pS831, VGlut1, and VGlut2 puncta were selected (PSD95 and pS831: 0.02-0.6 µm², VGlut1 and VGlut2: 0.02-2 µm²) in MIPs (of 28.34 x 28.34 x 40 µm z-stack images, 550 µm depth from cortical surface) based on fluorescence thresholding (autothreshold) in FIJI. Co-localization of pS831, PSD95, VGlut1, and VGlut2 was analyzed in single z-section images (28.34 x 28.34 µm images, 550 µm depth from cortical surface) taken at 100X (Zeiss Plan-neofluar 100x/1.3 Oil DIC, NA=1.3), using the JACoP plugin in FIJI (NIH).

Acute In Vivo Recordings

Visually evoked potentials (VEPs) were recorded from the binocular region of primary visual cortex (V1b) of adult rats contralateral to the chronically deprived eye. Rats were anesthetized with 3% isoflurane in 100% O₂ and a 3 mm

craniotomy was produced over V1b (centered 3 mm lateral to the midline and 7 mm posterior from Bregma). A 1.8 mm 16-channel platinum-iridium linear electrode array (~112 μm site spacing, 250 k Ω , (Zold & Hussain Shuler, 2015)) was inserted perpendicular to V1b (dorsal/ventral, 1.8 mm). Recordings under 2.5% isoflurane in 100% O₂ commenced 30 minutes after electrode insertion. Local field potentials were acquired via a RZ5 amplifier (Tucker Davis Technology) with a 300 Hz low pass filter and a 60 Hz notch filter. VEPs were evoked through passive viewing of repetitive flash stimuli (full field, 28 cd/m², 100% contrast, alternating 1Hz (0.5 second white, 0.5 second black), via MATLAB (MathWorks) with Psychtoolbox extensions (Brainard, 1997; Pelli, 1997)). Average VEP waveforms were calculated for the 100 visual presentations and were assigned to layers based on waveform shape. VEP amplitude was measured from peak to trough of the evoked response in MATLAB, as in (Murase et al., 2017) . To examine the short-term plasticity of VEP amplitude, each eye was individually presented with full field flash stimulus, alternating between black and white every 0.5 seconds. Single trial VEP responses were normalized to the first evoked response.

Experimental Design and Statistical Analysis

Primary visual cortex was defined with anatomical landmarks (shape of the dorsal hippocampal commissure, deep cerebral white matter tract, and the forceps major of the corpus callosum). Modest shrinkage due to fixation and cryoprotection reduced vertical depth to 900 μm (Wehrl et al., 2015). Fluorescent

puncta were identified using size exclusion parameters defined by unbiased quantification for each marker following the construction of a cumulative distribution of puncta size, and setting a 10% lower bound and 90% upper bound (Cane et al., 2014; Lei et al., 2013). An unpaired two-tailed Student's T-test was used to determine the significance between two independent experimental groups, and a paired Student's T-test was used for two measurements within the same subject. One-way ANOVA was used to determine statistical significance between three independent groups. Repeated measures ANOVA, with between group comparisons, was used to determine the significance of more than two measures within the same subjects, followed by a Tukey-Kramer honestly significant difference *post hoc* for pairwise comparisons if $p < 0.05$ (JASP). A Kolmogorov-Smirnov test (K-S Test) was used to determine the significance between the distributions of two independent data sets. Multi-dimensional K-S Test was used for data sets with two independent measurements (MATLAB). Statistical significance ($p < 0.05$) is represented as asterisks in figures, data is described as mean \pm standard error (mean \pm SEM).

2.5 Results

2.5.1 Trans-neuronal viral tracing reveals decrease in innervation of cMD V1

To test the hypothesis that cMD (from P14 – P180) reduces deprived-eye innervation to the contralateral V1, I injected viral trans-neuronal tracer HSV-H129 EGFP into the right eye (strain 772) and HSV-H129 mCherry into the left eye (strain 373) of an adult binocular control and an adult cMD subjects, allowing 5 days for the labeling to reach V1. Eye-specific innervation from the thalamus to the cortex, revealed by dual intraocular HSV-H129, confirms > 1.5 fold innervation of layer 4 from the contralateral than the ipsilateral eye in adult binocular controls (Average Fluorescence \pm SEM; Ipsi HSV-EGFP 54.61 ± 0.22 , Contra HSV-mCherry 81.33 ± 0.85 ; Fig.4B). cMD significantly decreases the thalamic innervation from the deprived/contralateral eye, reducing the initial contralateral bias (Average Fluorescence \pm SEM; Ipsi HSV-EGFP 40.26 ± 0.25 , Contra HSV-mCherry 47.38 ± 0.22 , Fig.4B). cMD also expands the territory innervated by the non-deprived / ipsilateral eye into the monocular region of V1 (V1m), as expected from a previous report in felines (Tagawa et al., 2005).

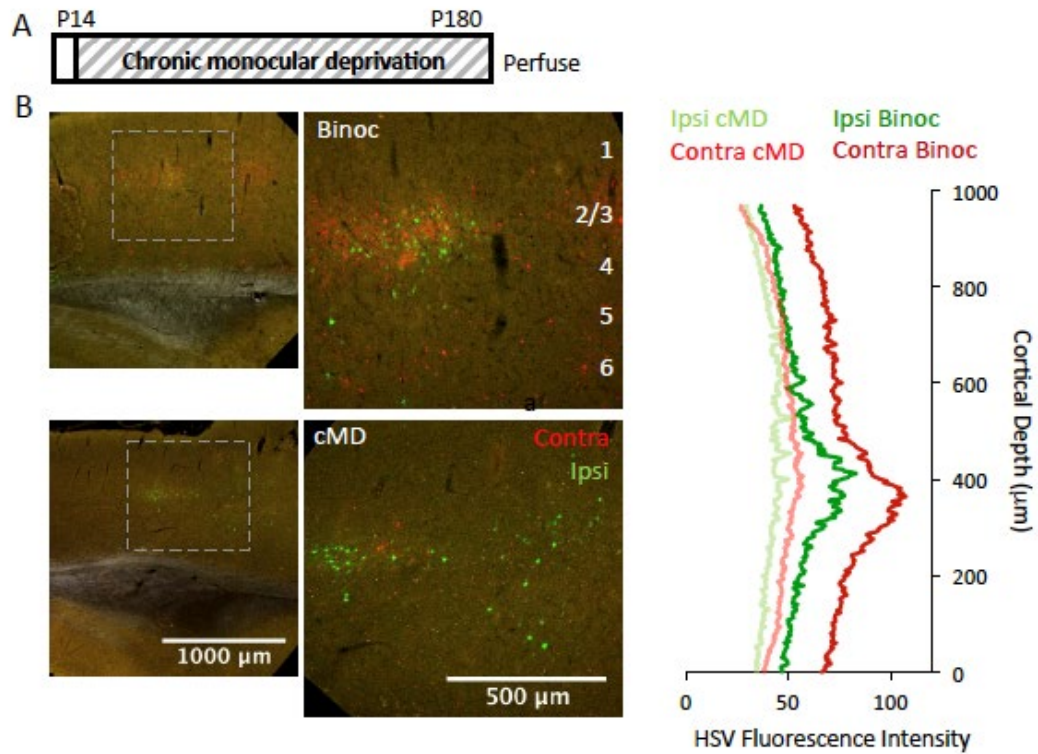


Figure 4. Trans-neuronal tracing reveals reduced innervation from deprived eye to V1
A. Experimental timeline. Subjects receive monocular deprivation from eye opening (~postnatal day 14, ~P14) to adulthood (>P180). **B.** Left: Confocal double fluorescent micrographs of V1b 5 days after delivery of H129 373, mCherry into contralateral and H129 772, EGFP into ipsilateral eye in a control binocular (top) and a cMD subject (bottom). (ML: 4mm AP:-6.72 mm DV: 1.5mm; ROI: 2000 μm x 2000 μm ; 5x mag with 0.6x digital zoom; 900 μm x 1000 μm ; 10x mag with 0.6x digital zoom). Right: Reduced H129 mCherry and EGFP in V1b following cMD.

2.5.2. Inhibitory interneuron activity and ECM expression increased with cMD

To ask if cMD altered the excitability of fast-spiking interneurons (FS INs), I examined the effect of visual deprivation on the expression of the calcium-binding protein parvalbumin (PV), known to be regulated by activity (Donato et al., 2013; Murase et al., 2017). Monocular deprivation from eye opening until P180 induced a significant increase in the expression of PV in V1b contralateral and ipsilateral to the occluded eye relative to binocular controls (AVG±SEM; Binoc 22.54±2.68 vs. Contra cMD 26.18±2.67, $p < 0.001$; Binoc 22.54±2.68 vs. Ipsi cMD 25.59±1.42, $p < 0.001$, K-S Test, $n=6$, Fig.5B). As the activity of FS INs is negatively correlated with pyramidal neuron excitability, this high ratio of inhibition / excitation, is expected to contribute to the stability of cMD cortex and resistance to reversal.

Another powerful negative regulator of synaptic plasticity is the maturation of the extracellular matrix (ECM), which is known to constrain plasticity in adult circuits (Carulli et al., 2010; Gogolla et al., 2009; Oray et al., 2004; Pfeffer et al., 2013; Pizzorusso et al., 2002, 2006). Tracking ECM density with WFA (which labels N-acetyl-D-galactosamine side chains of the CSPGs, a primary component of ECM) in cMD subjects revealed an increase WFA staining in V1b contralateral and ipsilateral to the occluded eye compared to binocular controls (AVG±SEM; Binoc 15.00±2.00 vs. Contra cMD 16.63±2.08, $p < 0.001$; Binoc 15.00±2.00 vs. Ipsi cMD 18.23±2.79, $p < 0.001$, K-S Test, $n=6$, Fig.5C). The

increase in CSPG density is also expected to contribute to the stability of cMD cortex and resistance to reversal.

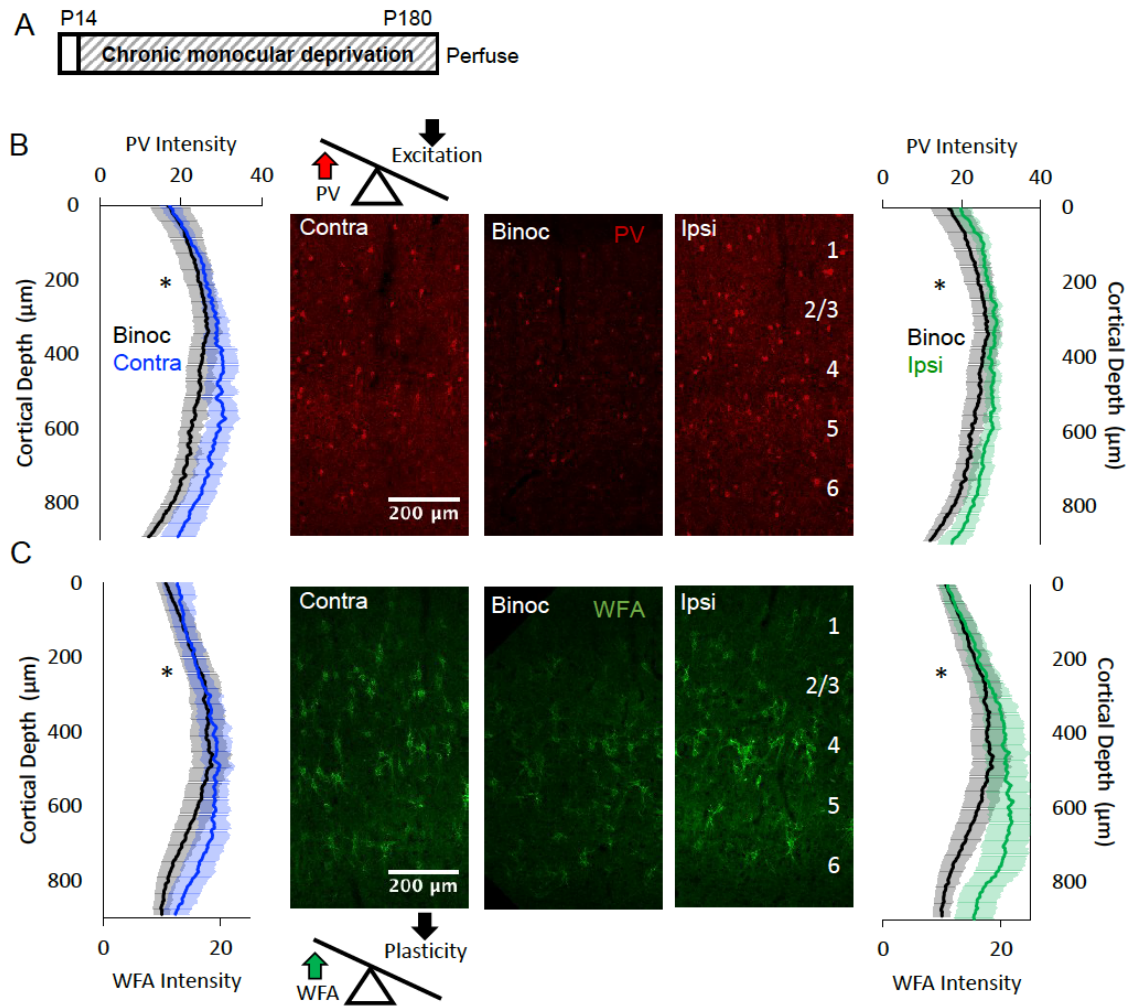


Figure 5: cMD increases PV and WFA staining in V1b contralateral and ipsilateral to cMD

A. Experimental timeline. Subjects receive monocular deprivation from eye opening (~P14) to adulthood (>P180). **B.** Above: Graphic representations of impact of PV expression on pyramidal neuron excitability. Below: Fluorescent micrographs of PV distribution in V1b (red, V1; ML: 4 mm AP: -6.72 mm DV: 1.5mm; ROI: 900 μm x 500 μm; 10x mag; MIP). cMD significantly increases PV intensity in V1b contralateral and ipsilateral to cMD, $*=p<0.01$, K-S Test, Binoc n=4, cMD n=6. **C.** Above: Fluorescent micrographs of WFA distribution in V1b (green, V1; ML: 4mm AP: -6.72 mm DV: 1.5mm; ROI: 900 μm x 500 μm; 10x mag; MIP). cMD significantly increases WFA intensity in V1b contralateral and ipsilateral to cMD, $*=p<0.001$, K-S Test, Binoc n=4, cMD n=6. Below: Graphic representations of impact of PV expression on plasticity.

2.5.3 Excitatory synapse density is preserved despite cMD

To ask if cMD impacted the number and/or size of excitatory synapses in V1b, I quantified the size and numbers of immunoreactive puncta for the scaffold protein PSD95. Despite cMD, quantitative immunofluorescence revealed no difference in PSD95 puncta number in V1b contralateral or ipsilateral to the occluded eye, however, PSD95 puncta size was significantly reduced by cMD relative to binocular controls (Table 1, Fig.6B).

Table 1: PSD95 size / number following cMD			
PSD95 Puncta Size	Average+/- SEM	n	P value
Binoc	0.081±0.01 μm^2	4	KS test
Contra cMD	0.080±0.01 μm^2	6	*=p<0.001 vs. Binoc
Ipsi cMD	0.078±0.01 μm^2	6	*=p<0.001 vs. Binoc
PSD95 Puncta #	Average+/- SEM	n	P value
Binoc	279.58±36.99	4	one-way ANOVA, F(df,15)=0.46, p=0.64
Contra cMD	250.97±29.30	6	Non-Significant (NS), p>0.05
Ipsi cMD	235.60±35.44	6	NS, p>0.05

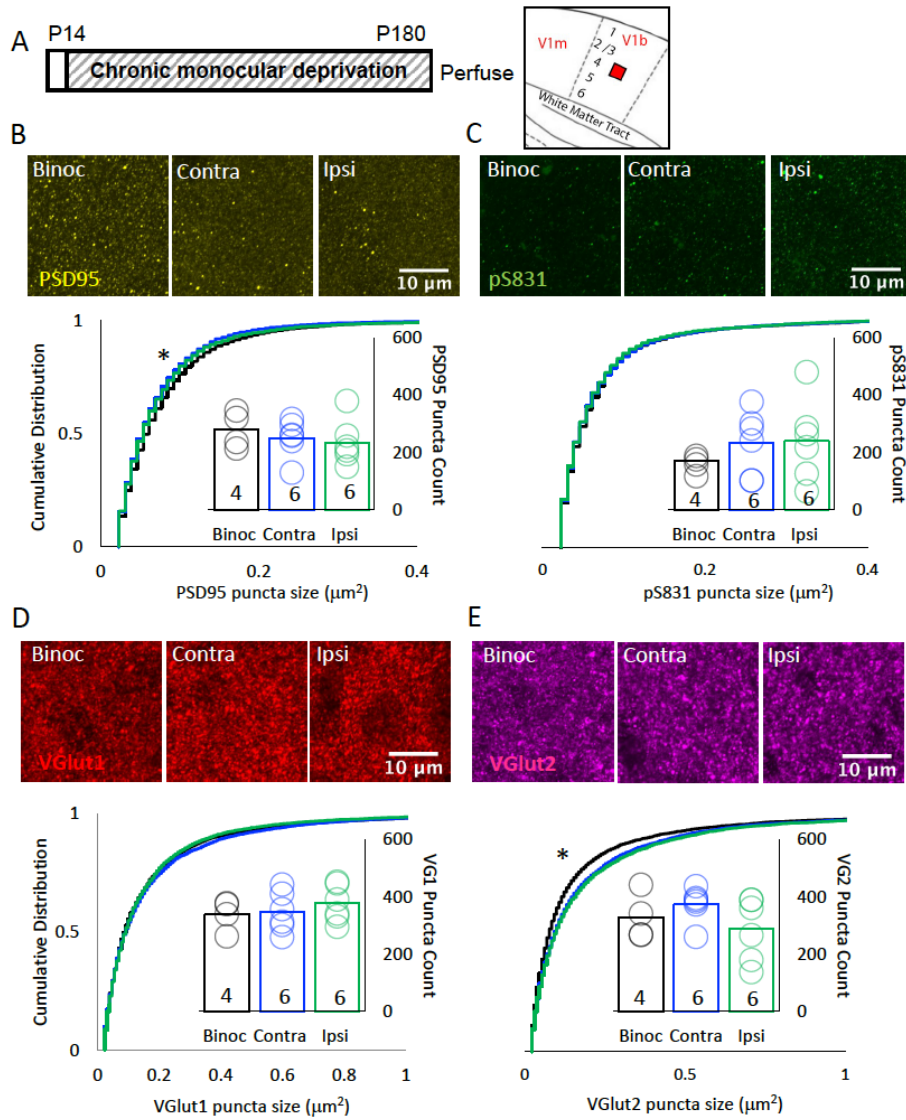


Figure 6. Characterization of the anatomical response of excitatory synapses to cMD

A. Left: Experimental timeline. Subjects receive monocular deprivation from eye opening (~P14) to adulthood (>P180). Right: Fluorescent micrograph ROI location in Layer 4 of V1b (red box). **B.** Top: Fluorescent micrographs of PSD95 (yellow) from Binocular Control (Binoc, left), Contralateral cMD (Contra cMD, middle), and Ipsilateral cMD (Ipsi cMD, right) V1b (ML: 4mm AP: -6.72 mm DV: 1.5mm; ~500 μ m from surface; ROI: 28.34 μ m x 28.34 μ m x 40 μ m, 100x mag with 3x digital zoom; maximal intensity projection (MIP)). Bottom: Significant decrease in size and no change in number of PSD95 immunoreactive puncta in V1b following cMD in contralateral and ipsilateral hemispheres, $*=p<0.001$, K-S Test, Binoc n=4, cMD n=6. **C.** Top: Fluorescent micrographs of pS831 (green) from Binocular Control (Binoc, left), Contralateral cMD (Contra cMD, middle), and Ipsilateral cMD (Ipsi cMD, right) V1b (ML: 4mm AP: -6.72 mm DV: 1.5 mm; ~500 μ m from surface; ROI: 28.34 μ m x 28.34 μ m x 40 μ m, 100x mag with 3x digital zoom; MIP). Bottom: No change in average immunoreactive puncta number or cumulative puncta size distribution of pS831, Binoc =4, cMD = 6. **D.** Top: Fluorescent micrographs of VGlut1 (Red) from Binocular Control (Binoc, left), Contralateral cMD (Contra cMD, middle), and Ipsilateral cMD (Ipsi cMD, right) V1b (ML: 4mm AP: -6.72 mm DV: 1.5mm; ~500 μ m from surface; ROI: 28.34 μ m x 28.34 μ m x 40 μ m, 100x mag with 3x digital zoom; maximal intensity projection (MIP)). Bottom: No change in average immunoreactive puncta number or cumulative puncta size distribution of pS831, Binoc =4, cMD = 6. **E.** Top: Fluorescent micrographs of VGlut2 (magenta) from Binocular Control (Binoc, left), Contralateral cMD (Contra cMD, middle), and Ipsilateral cMD (Ipsi cMD, right) V1b (ML: 4mm AP: -6.72 mm DV: 1.5 mm; ~500 μ m from surface; ROI: 28.34 μ m x 28.34 μ m x 40 μ m, 100x mag with 3x digital zoom; MIP). Bottom: Significant increase in size and no change in number of PSD95 immunoreactive puncta in V1b following cMD in contralateral and ipsilateral hemispheres, $*=p<0.001$, K-S Test, Binoc n=4, cMD n=6.

To ask if cMD impacted the activity of signaling pathways known to regulate glutamate receptor function and plasticity, I examined the size and number of immunoreactive puncta of the glutamate A1 (GluA1) subunit of the α -amino-3-hydroxy-5-methyl-4-isoxazolepropionic acid receptor (AMPA), phosphorylated on residue Serine 831 (pS831). Again, despite cMD, quantitative immunofluorescence revealed no difference number, nor in the size of pS831 puncta in V1b contralateral or ipsilateral to the occluded eye (Table 2, Fig.6C).

Table 2: pS831 size / number following cMD			
pS831 Puncta Size	Average+/- SEM	n	P value
Binoc	0.075±0.003 μm^2	4	KS test
Contra cMD	0.073±0.002 μm^2	6	NS, $p>0.05$ vs. Binoc
Ipsi cMD	0.069±0.005 μm^2	6	NS, $p>0.05$ vs. Binoc
pS831 Puncta #	Average+/- SEM	n	P value
Binoc	159.98±17.79	4	one-way ANOVA, F(df, 15)= 0.69, $p=0.51$
Contra cMD	234.74±49.94	6	NS, $p>0.05$
Ipsi cMD	240.40±64.77	6	NS, $p>0.05$

To investigate how cMD impacted the distribution of excitatory afferents, I examined the number and size distributions of markers for thalamic axons (vesicular glutamate transporter 2 (VGlut2)) and cortical axons (vesicular glutamate transporter 1 (VGlut1)). Again, I observed no significant difference in the number of VGlut2 puncta in V1b contralateral or ipsilateral to the occluded eye, although there was an increase in puncta size (Table 4, Fig.6E). Furthermore, there was no significant difference in the number or size of VGlut1 puncta number in V1b contralateral or ipsilateral to the occluded eye (Table 3, Fig.6D).

Table 3: VGlut1 size / number following cMD			
VGlut1 Puncta Size	Average+/- SEM	n	P value
Binoc	0.17±0.02 μm^2	4	KS test
Contra cMD	0.17±0.02 μm^2 vs.	6	NS, p>0.05 vs. Binoc
Ipsi cMD	0.17±0.02 μm^2	6	NS, p>0.05 vs. Binoc
VGlut1 Puncta #	Average+/- SEM	n	P value
Binoc	330.13±47.61	4	one-way ANOVA, F(df,15)=0.51, p=0.61
Contra cMD	348.00±31.03	6	NS, p>0.05
Ipsi cMD	376.89±28.74	6	NS, p>0.05

Table 4: VGlut2 size / number following cMD			
VGlut2 Puncta Size	Average+/- SEM	n	P value
Binoc	0.16±0.01 μm^2	4	KS test
Contra cMD	0.18±0.01 μm^2	6	*=p<0.001 vs. Binoc
Ipsi cMD	0.17±0.02 μm^2	6	*=p<0.001 vs. Binoc
VGlut2 Puncta #	Average+/- SEM	n	P value
Binoc	330.13±47.61	4	one-way ANOVA, F(df,15)=1.46, p=0.26
Contra cMD	373.69±26.56	6	NS, p>0.05
Ipsi cMD	287.69±49.28	6	NS, p>0.05

To ask if the excitatory synapse markers employed (PSD95, VGlut1 and VGlut2, and pS831) reveal competent excitatory synapses, I used Pearson's coefficient analysis to assess colocalization between markers. Pearson's correlation coefficient (PCC) values range from -1 (anti-correlation of two populations) to 1 (perfect correlation) and 0 meaning no overlap of two groups (Dunn et al., 2011). In binocular controls, PCC for postsynaptic marker PSD95 showed high colocalization with presynaptic markers VGlut1 (cortico-cortical synapses) and VGlut2 (thalamocortical synapses) (Table 5, Fig.7). Similarly, there was high colocalization between pS831 and PSD95 (Table 5, Fig.7) and pS831 with VGlut1 and VGlut2 (Table 5, Fig.7). The high PCC values suggest that individual markers reflect competent excitatory synapses.

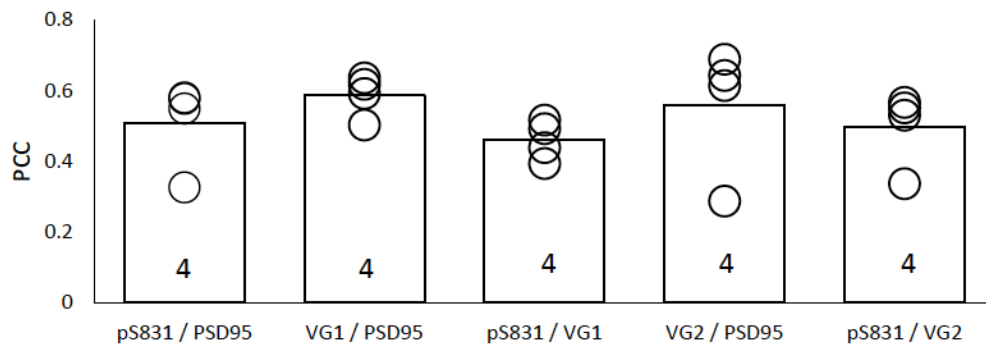


Figure 7. Colocalization of excitatory synapse markers

Left to right: Colocalization analysis using Pearson's Correlation Coefficient (PCC) of PSD95 / pS831, VGlut1 / PSD95, VGlut1 / pS831, VGlut2 / PSD95, and VGlut2 / pS831 of Binocular controls reveals high overlap of synaptic markers, n=4.

Table 5.: Colocalization of synaptic markers following cMD			
PSD95-VGlut1 Coloc.	Average+/- SEM	n	P value
Binoc	0.59±0.03	4	one-way ANOVA, F(df,15) =0.08, p=0.92
Contra cMD	0.57±0.04	6	NS, p>0.05
Ipsi cMD	0.58±0.03	6	NS, p>0.05
pS831-VGlut1 Coloc.	Average+/- SEM	n	P value
Binoc	0.46±0.03	4	one-way ANOVA, F(df,15)=0.26, p=0.77
Contra cMD	0.42±0.05	6	NS, p>0.05
Ipsi cMD	0.45±0.03	6	NS, p>0.05
PSD95-VGlut2 Coloc.	Average+/- SEM	n	P value
Binoc	0.56±0.09	4	one-way ANOVA, F(df,15)=1.69, p=0.22
Contra cMD	0.45±0.03	6	NS, p>0.05
Ipsi cMD	0.45±0.02	6	NS, p>0.05
pS831-VGlut2 Coloc.	Average+/- SEM	n	P value
Binoc	0.51±0.06	4	one-way ANOVA, F(df,15)=1.46, p=0.26
Contra cMD	0.37±0.03	6	NS, p>0.05
Ipsi cMD	0.38±0.03	6	NS, p>0.05
pS831-PSD95 Coloc.	Average+/- SEM	n	P value
Binoc	0.50±0.05	4	one-way ANOVA, F(df,15)=3.49, p=0.06

Contra cMD	0.48±0.02	6	NS, p>0.05
Ipsi cMD	0.50±0.02	6	NS, p>0.05

However, the PCC of any combination of these excitatory synapse markers did not change in either hemisphere of V1b following cMD (Table 5). Together, this suggests that although thalamic input from the deprived eye to the cortex is reduced by MD, overall excitatory synaptic density and thalamic innervation is maintained. This suggests that deprivation-induced reduction in synaptic input from deprived eye to the cortex may be counter-balanced by an increase in other excitatory synapses, including those serving the non-deprived eye.

2.5.4 Accelerated depression of deprived eye visually-evoked responses during repetitive visual stimulation

cMD significantly reduces the amplitude of the VEP from the deprived eye and reduces the stimulus selectivity of individual V1b neurons (He et al., 2007; Montey et al., 2013), however how cMD impacts the biophysical properties deprived eye relative to non-deprived eye synapse is unknown. Brief monocular deprivation (5-7 days) increase the probability of neurotransmitter release at retino-geniculate synapses serving the deprived eye (Krahe & Guido, 2011), a homeostatic change that is thought to compensate for reduced activity due to deprivation. To ask if cMD impacts the probability of neurotransmitter release, my colleague Dr. Crystal L. Lantz examined the amplitude of visually evoked potentials (VEPs) recorded from the binocular region of primary visual cortex

(V1b) contralateral to the deprived eye in response to repetitive visual stimulation. A microelectrode array was inserted perpendicular to V1b (dorsal/ventral, 1.8 mm) and recordings under 2.5% isoflurane commenced 30 minutes after electrode insertion. To examine the short-term plasticity of VEP amplitude, each eye was individually presented with full field flash stimulus (28 cd/m²) alternating between black and white every 0.5 seconds. Single trial VEP responses were normalized to the first evoked response. VEPs were isolated from layer 2/3 of V1b contralateral to the occluded eye were acquired in response to repetitive flash stimuli (full field, 0.5 second white, 0.5 second black) and amplitudes were normalized to the first VEP (Fig. 8B). The depression of VEP amplitudes during repetitive stimulation was greater in response to stimulation of the deprived / contralateral eye than non-deprived / ipsilateral eye (Second VEP response normalized to first, μV , $\text{AVG} \pm \text{SEM}$; Ipsi: 0.59 ± 0.13 , Contra: 0.29 ± 0.02 ; Repeated measures ANOVA, $p < 0.001$, $F = 47.683$, between groups, $p = 0.007$, $F = 15.773$, $n = 4$ subjects, Fig. 8B). The magnitude of synaptic depression depends on initial release probability (Regehr, 2012), therefore the enhanced depression of the deprived/contralateral eye pathway suggests that cMD increased the probability of neurotransmitter release.

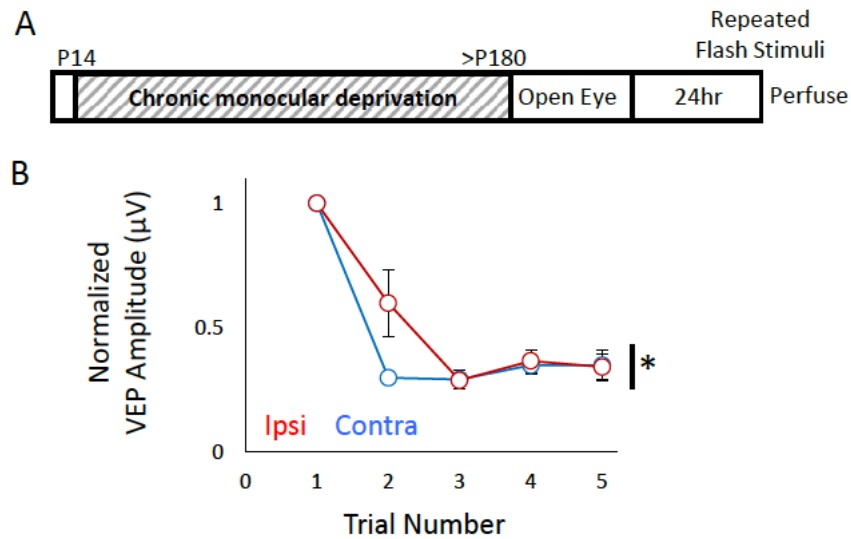


Figure 7: Rapid depression of VEPs in response to stimulus of deprived eye

A. Experimental timeline. Subjects receive monocular deprivation from eye opening (~P14) to adulthood (>P180) then undergo eye opening. VEPs in response to repeated 1 Hz flash stimuli are assessed after 24 hours. **B.** VEP amplitudes in response to flash stimuli evoked from ipsilateral (non-deprived, red) and contralateral eye (deprived, blue) normalized to amplitude of first response. Contralateral eye VEPs depress more rapidly than ipsilateral eye VEPs. * $p < 0.05$, between groups repeated measures ANOVA, $n = 4$ subjects.

2.6 Discussion

The chronic MD employed here differs from other animal models of MD, in that the cMD is initiated at eye opening, prior to the onset of vision. Therefore, this cMD prevents early binocular vision and replicates the absence of binocular vision in children born with a unilateral congenital cataract. Following cMD there is a reduction in thalamic input to the cortex serving the deprived eye. However, excitatory synaptic density remains unchanged, suggesting a homeostatic plasticity to maintain synaptic activity and density following MD. In addition, molecular markers that reflect the state of plasticity in the circuit suggest that

plasticity is low in the cMD adult cortex, which is likely to contribute to extreme resistance to spontaneous reversal from cMD.

My trans-neuronal tracing with HSV-H129 supports previous observations that cMD significantly decreases the thalamic innervation to the cortex from the deprived/contralateral eye, which is a strong contributor to the reduction in contralateral bias (Montey & Quinlan, 2011; Tagawa et al., 2005). These experiments also reveal a maintenance of connectivity between the deprived eye and the visual cortex, despite very prolonged monocular deprivation. This is consistent with the observation the visually-evoked potentials and single unit activity can be evoked the deprived eye following cMD, however these visual responses are weak and un-tuned. The maintenance of anatomical and functional connectivity is also likely to be necessary to enable recovery from cMD.

Two fundamental characteristics of circuits that impact plasticity include the level of excitability of pyramidal neurons and the density of ECM. In both cases, an intermediate level is thought to be permissive, to allow spike-timing-dependent changes in synaptic strength for the former, and to allow synaptic expansion / retraction for the latter. cMD resulted in an increase in PV expression and an increase in WFA staining, two changes that are predicted to constrain plasticity in the adult cortex. It is unlikely that these increases are an initial response to MD, as MD induces a rapid decrease in the excitability of FS INs and

disinhibition of pyramidal neurons (Kuhlman et al., 2013). It is more likely that the changes represent homeostatic responses to prolonged MD. Importantly, change in PV expression and WFA staining are co-regulated. The maturation of PV+ interneurons coincides with the development of stable extracellular matrix (ECM) and PNNs have binding sites for molecules that regulate AMPAR content at excitatory synapses onto PV neurons, like NARP and NRG1 (Gu et al., 2013; Gu et al., 2016).

The observation that PSD95 and pS831 immunoreactive puncta are unchanged following cMD appears at first to conflict with previous reports that cMD induced a significant reduction (50%) in dendritic spine density in deprived cortex (Montey & Quinlan, 2011). One possibility is that following cMD, dendritic spines collapse, but PSD structure is maintained. Work performed in pyramidal neurons in culture demonstrates a retraction of dendritic spines that is independent of a loss of PSD95, and in some cases, spine retraction was associated with an increase in PSD95 fluorescence on the dendritic shaft (Woods et al., 2011).

The observation that cMD appears to increase the initial probability of release at synapses serving the deprived-eye has interesting implications for the potential expression of further plasticity at these synapses. The increase in release probability would occlude pre-synaptic forms of Hebbian potentiation, which may also contribute to the lack of plasticity in cMD adults. This may offer

an additional explanation as to why simply opening the deprived eye or giving visual experience alone does not induce a recovery of visual acuity. These findings provide a foundation for the development of potential interventions to reverse the deficits induced by cMD, as well as inform the interpretation of the subsequent experiments employing hormone administration to the deprived visual system.

Chapter 3 : The effects of estrogen and visual stimulation on V1 of cMD adult rats

3.1 Abstract

Estrogen delivery has been shown to enhance synaptic density and plasticity in the hippocampus and prefrontal cortex. Here I test the hypothesis that estrogen promotes plasticity in V1 of adult amblyopes, a possibility that is supported by the presence of both major estrogen receptor subtypes in V1 of adult male and female rodents. Markers for molecular changes that are known correlates of cortical plasticity levels, PV expression and WFA staining, are decreased following $17\alpha\text{E}2$ administration. Quantitative immunohistochemistry reveals $17\alpha\text{E}2$ increases the size of PSD95 puncta, a marker for excitatory postsynaptic densities in cMD V1, suggesting enhanced anatomical plasticity. $17\alpha\text{E}2$ followed by visual stimulation amplifies each of these changes, and increases markers for synaptic CaMKII/PKC activity. Importantly, $17\alpha\text{E}2$ administration prior to a subthreshold visual stimulation protocol significantly enhanced visually-evoked potentials evoked from the non-deprived, but not deprived, eye. An increase in release probability of deprived eye synapses is predicted following cMD, suggesting that estrogen-induced enhancement of plasticity may be limited to synapses with an initial low release probability. Thus, the sensitivity to estrogen in adult V1 is determined autonomously by synaptic characteristics that reflect the history of synaptic activity.

3.2 Introduction

Estrogen is commonly referred to as a female steroid sex hormone, but has been demonstrated to play an important role in the both male and female physiology across species (Mechoulam et al., 1984; Micevych & Christensen, 2012; Ozon, 1972; Schulster et al., 2016). Estradiol, the most potent and ubiquitous member of the estrogen class, is produced and circulates at high levels in mammals, invertebrates, amphibians, fish, and birds (Mechoulam et al., 1984; Ozon, 1972). In the periphery, 17β estradiol is the predominant form of circulating estradiol and is tightly conserved across species (Thornton, 2001). 17β estradiol is implicated in the regulation of female reproductive cycles, development of secondary sex characteristics, development / maintenance of reproductive tissues, and mediation of effects in other organs, such as the heart, liver, skin and bones (Melmed, 2016). Though 17β estradiol levels in males are lower than to females, estradiol is implicated in the regulation of spermatogenesis, masculinization of specific brain areas, immune function, and cardiovascular health (Carreau et al., 2003; Lombardi et al., 2001; Schulster et al., 2016). Importantly, estradiol can be synthesized in the brain and local actions of estradiol on neurons has been reported in both males and females (Hara et al., 2015; Saldanha et al., 2011).

Estrogen signaling in the brain is mediated by two major receptor subtypes: Estrogen Receptor alpha ($ER\alpha$) and Estrogen Receptor beta ($ER\beta$). $ER\alpha$ is present in multiple tissue types, including neuronal, and has high

homology across species (Cui et al., 2013; Kumar et al., 2011; Thornton, 2001). ER α and ER β are of similar size (530 versus 495 amino acids), possess similar DNA-binding domains (96% homology), ligand-binding domains (56% homology), and bind to the same hormone response element on DNA (Weiser et al., 2008). ER α and ER β are expressed throughout the brain and spinal cord and can be activated by distinctive, subtype-specific agonists. The mechanistic pathways activated by each receptor subtype are varied but overlap (Cui et al., 2013). Historically, estrogen-induced effects were thought to be primarily mediated through receptors that act on the cell nucleus and mediate transcriptional effects. In this case, estradiol crossing the cell membrane binds to cytoplasmic ER α or ER β , induces homo- or heterodimerization and transport of the receptor complex into the nucleus, which binds to estrogen response elements (ERE) on DNA to regulate transcription (Levin, 2005). However, cell membrane-bound receptors also exist, and have been shown to mediate diverse and rapid effects in the brain that are independent of transcription. At excitatory synapses, activation of presynaptic ER α / ER β increases glutamatergic transmission and increases mESPC frequency and amplitude, which is thought to promote synaptic potentiation (Oberlander & Woolley, 2016; Smejkalova & Woolley, 2010). Importantly, an estrogen-induced increase mEPSC frequency has been shown to be specific for synapses with low initial probability of release (Smejkalova & Woolley, 2010). Postsynaptic ER β activation can stimulate the formation of dendritic spines by activation of cofilin / actin polymerization (Kramár et al., 2013) and increase in synapse size via PSD95 translation (Akama & McEwen,

2003). At inhibitory synapses, 24 hours of estrogen administration to hippocampal neurons in culture activates presynaptic ER α reduces the strength of inhibitory transmission (decreases mIPSCs) and increases mEPSCs, and dendritic spine density (Murphy et al., 1998). Acute estrogen rapidly reduces mIPSC frequency in pyramidal neurons of layer 2/3 V1 in older mice, and an ER α antagonist occludes the decrease in mIPSC amplitude observed following dark exposure (Gao et al., 2017). Post-synaptic ER α activation in inhibitory neurons can suppress GABAergic transmission via retrograde endocannabinoids (G. Z. Huang & Woolley, 2012). Furthermore, ER α / ER β signaling in the inhibitory post-synaptic compartment can cause destabilization of the scaffold protein gephyrin and GABA $_A$ Rs and reduce inhibitory synaptic currents, demonstrated by reduced mIPSC amplitudes (Mukherjee et al., 2017).

Each of the above mentioned effects on synaptic function occur rapidly, and independently of the regulation of transcription. Estrogen application to rodent hippocampal slices increases the magnitude and lowers the threshold for LTP in CA3 neurons within 30 minutes in response to theta burst stimulation delivered to CA1 (Kramár et al., 2013). This effect is equally robust in hippocampal slices from males and females, and is accompanied by an increase in the size of PSD95 puncta, suggesting that estrogen induces plasticity in both sexes through similar mechanisms. Acute estrogen administered to OVX rats induces a rapid (within 30 minutes) and dose-dependent increase in the dendritic spines on CA1 neurons in the hippocampus (MacLusky et al., 2005). Estrogen

increases NMDAR conductance at excitatory TA-CA1 synapses in hippocampus and upregulates the density of immature dendritic spines, which is attenuated by blockade of GluN2B-containing NMDAR (Smith et al., 2016). In mature, mushroom-type spines, estrogen increases the colocalization of PSD95 and the GluR2 subunit of the AMPAR (Avila et al., 2017). However, administration of estrogen to the dorsal hippocampus increases the density of immature-type spines, while temporarily attenuating AMPAR-mediated mEPSCs (Phan et al., 2015).

Conversely, the decrease in circulating estrogen with age is strongly correlated with a decrease in cognitive function and concurrent loss of neuronal dendritic spines in humans and animal models (expanded discussion of this work was presented in Chapter 1, (Bailey et al., 2011; Dumitriu et al., 2010; P. R. Rapp et al., 2003)). Importantly, reintroduction of estrogen through hormone replacement therapy improves cognition and increases dendritic spine density to the level of younger and non-hormone deprived cohorts in humans, non-human primates, and rodents (Bagger et al., 2005; Gibbs, 1999; Hao et al., 2006; Hara et al., 2016; Rapp et al., 2003; Savonenko & Markowska, 2003). However, estrogen can also have off-target negative impacts, depending on dosage and time course of therapy (Manson et al., 2014). It is therefore imperative that potential therapeutic use of estrogen to improve plasticity minimize risk while maximizing the benefit to brain function and neuronal anatomy.

Here, I will test the hypothesis that a low concentration of 17 α E2 enhances plasticity in primary visual cortex of adult amblyopic rodents. For these experiments I chose to use 17 α -Estradiol (17 α E2), a stereoisomer of the main circulating estradiol (17 β) that is inactive in the reproductive systems of adult animals, but induces rapid and potent synaptogenesis in the hippocampus that is ~2 fold higher in magnitude than an equivalent doses of 17 β estradiol (MacLusky et al., 2005; Toran-Allerand et al., 2005). 17 α has 100-fold lower efficacy for nuclear ERs of both subtypes, and a preferential affinity for ER α (Kuiper et al., 1997). I will administer a single dose of 17 α E2 and examine the expression of markers for synaptic plasticity and excitatory synaptic density and activity, predicting that 17 α E2 creates a more permissive environment for anatomical plasticity and increases synaptic density. Activity-dependent stimulation has been predicted to be essential for the stabilization and incorporation of newly-formed, estrogen-induced synapses (Srivastava, 2012; Srivastava et al., 2008). Therefore, I will also test the hypothesis that 17 α E2 followed by visual stimulus will result in a greater increase in synaptic density and activity than 17 α E2 alone. Collaboratively with Dr. Crystal Lantz, I will examine the effect of 17 α E2 administration to cMD subjects on the expression of activity-dependent plasticity of visual responses in the visual cortex, and ask if 17 α E2 has similar effect on plasticity of synapses serving the deprived and non-deprived eye. Together, these results will be the first anatomical and physiological assessment of estrogen-induced plasticity in amblyopic rodent visual cortex and will potentially inform estrogen-based therapy for sensory deficits.

3.3 Materials and Methods

Subjects

Long Evans Rats (strain 006, RRID:RGD_2308852) were purchased from Charles River Laboratories (Raleigh, NC). Equal numbers of adult (>postnatal day 180, >P180) males and females were used. Animals were raised in 12/12 hour light/dark cycle and experiments were performed, or subjects were sacrificed, 6 hours into the light phase. All procedures conformed to the guidelines of the University of Maryland Institutional Animal Care and Use Committee and the Guide for the Care and Use of Laboratory Animals of the National Institutes of Health.

Monocular deprivation

Subjects were anesthetized with ketamine/xylazine (100 mg/10 mg/kg, intraperitoneal). The margins of the upper and lower lids of one eye were trimmed and sutured together using a 5-0 suture kit with polyglycolic acid (CP Medical). Subjects were returned to their home cage after recovery at 37°C for 1-2 hours and disqualified in the event of suture opening.

Antibodies

The following antibodies/dilutions were used: rabbit anti-estrogen receptor α (ER α ; ThermoFisher, RRID: AB_325813, 1:1000); mouse anti-estrogen receptor β (ER β ; ThermoFisher; RRID:AB_930765, 1:1000); mouse anti-parvalbumin (PV; Millipore; RRID:AB_2174013, 1:1000); mouse anti-Post Synaptic Density 95kd

(PSD95; ThermoFisher; RRID: AB_325399, 1:200); rabbit anti-phospho-Serine 831-GluR1 (pS831; Sigma Aldrich; RRID:AB_1977218, 1:1000), guinea pig anti-Vesicular Glutamate Transporter 1 (VGlut1; Millipore; RRID:AB_11214451, 1:1000); guinea pig anti-Vesicular Glutamate Transporter 2 (VGlut2; Millipore; RRID:AB_2665454, 1:2000); followed by appropriate secondary antibodies: goat anti-rabbit and anti-mouse IgG conjugated to Alexa-488, 546, or 647 (Life Technologies; RRID:AB_143165, RRID:AB_AB_2534118, RRID:AB_2535805, 1:300).

Reagents

4',6-Diamidino-2'-phenylindole dihydrochloride (DAPI, Sigma; 1:10000) was used to visualize cell nuclei. Chondroitin sulfate proteoglycans (CSPGs) were visualized with fluorescein wisteria floribunda lectin (WFA, Vector Labs; 1:1000). 17 α Estradiol (17 α E2; Sigma Aldrich) was diluted to 15 μ g/kg in sesame oil (Sigma Aldrich) and administered subcutaneously (s.c.).

Visual Stimulus

A subset of subjects was anesthetized with 2.5% isoflurane in 100% O₂ 30 minutes after 17 α E2 administration and received visual stimulation by passive viewing of 200 x 1 second trials of square-wave gratings (0.05 cycles per degree (cpd), 100% contrast, 28 cd/m², reversing at 1 Hz, via MATLAB (MathWorks) with Psychtoolbox extensions (Brainard, 1997; Pelli, 1997).

Immunohistochemistry

Subjects were perfused with phosphate buffered saline (PBS) followed by 4% paraformaldehyde (PFA) in PBS. The brain was post-fixed in 4% PFA for 24 hours followed by 30% sucrose for 48 hours, and cryo-protectant solution (0.58 M sucrose, 30% (v/v) ethylene glycol, 3 mM sodium azide, 0.64 M sodium phosphate, pH 7.4) for 24 hours prior to sectioning. Coronal sections (40 μm) were made on a Leica freezing microtome (Model SM 2000R). Sections were blocked with 4% normal goat serum (NGS) in PBS for 1 hour. Antibodies were presented in blocking solution for 24 hours, followed by appropriate secondary antibodies.

Confocal imaging and analysis

Images were acquired on a Zeiss LSM 710 confocal microscope. Co-localization of ER α and ER β with DAPI was analyzed in single z-sections (70.86 x 70.86 μm images, 550 μm depth from cortical surface) taken at 40X (Zeiss Plan-neofluar 40x/1.3 Oil DIC, NA=1.3), using the JACoP plugin in FIJI (NIH). The cortical distribution of WFA and PV immunoreactivity was determined in a z-stack (9 x 7.5 μm sections) acquired with the same 10X lens. Maximal intensity projections (MIPs; 500 μm width, 900 μm depth from cortical surface) were used to obtain mean intensity profile in FIJI. For PSD95, pS831, VGlut1, and VGlut2 staining, MIPs of z-stacks (40 slices x 0.9 μm images) were acquired at 100X (Zeiss Plan-neofluar 100x/1.3 Oil DIC, NA=1.3). PSD95, pS831, VGlut1, and VGlut2 puncta were selected (PSD95 and pS831: 0.02-0.6 μm^2 , VGlut1 and VGlut2: 0.02-2

μm^2) in MIPs (of $28.34 \times 28.34 \times 40 \mu\text{m}$ z-stack images, $550 \mu\text{m}$ depth from cortical surface) based on fluorescence thresholding (autothreshold) in FIJI. Co-localization of pS831, PSD95, VGlut1, and VGlut2 was analyzed in single z-sections ($28.34 \times 28.34 \mu\text{m}$ images, $550 \mu\text{m}$ depth from cortical surface) taken at 100X (Zeiss Plan-neofluar 100x/1.3 Oil DIC, NA=1.3), using the JACoP plugin in FIJI (NIH).

Acute In Vivo Recordings

Visually evoked potentials (VEPs) were recorded from the binocular region of primary visual cortex (V1b) of cMD adult rats contralateral to the chronically deprived eye. Rats were anesthetized with 3% isoflurane in 100% O_2 and a 3 mm craniotomy was produced over V1b (centered 3 mm lateral to the midline and 7 mm posterior from Bregma). A 1.8 mm 16-channel platinum-iridium linear electrode array ($\sim 112 \mu\text{m}$ site spacing, 250 k Ω , (Zold & Hussain Shuler, 2015)) was inserted perpendicular to V1b (dorsal/ventral, 1.8 mm). Recordings under 2.5% isoflurane in 100% O_2 commenced 30 minutes after electrode insertion. Local field potentials were acquired via a RZ5 amplifier (Tucker Davis Technology) with a 3000 Hz low pass filter and a 60 Hz notch filter. VEPs were evoked through passive viewing of 100 x 1 second trials of square-wave gratings (0.05 cycles per degree (cpd), 100% contrast, reversing at 1 Hz, 28 cd/m^2 , via MATLAB (MathWorks) with Psychtoolbox extensions (Brainard, 1997; Pelli, 1997). Average VEP waveforms (100 stimuli) were assigned to layers based on waveform shape. VEP amplitude was measured from peak to trough of the

evoked response in MATLAB, as in (Murase et al., 2017). To examine the short-term plasticity of VEP amplitude, each eye was individually presented with full field flash stimulus, alternating between black and white every 0.5 seconds. Single trial VEP responses were normalized to the first evoked response.

Experimental Design and Statistical Analysis

Primary visual cortex was defined with anatomical landmarks (shape of the dorsal hippocampal commissure, deep cerebral white matter tract, and the forceps major of the corpus callosum). Modest shrinkage due to fixation and cryoprotection reduced vertical depth to 900 μm (Montey & Quinlan, 2011; Wehrl et al., 2015). Fluorescent puncta were identified using size exclusion parameters defined by unbiased quantification for each marker following the construction of a cumulative distribution of puncta size, and setting a 10% lower bound and 90% upper bound (Cane et al., 2014; Lei et al., 2013). An unpaired two-tailed Student's T-test was used to determine the significance between two independent experimental groups, and a paired Student's T-test was used for two measurements within the same subject. One-way ANOVA was used to determine statistical significance between three independent groups. Repeated measures ANOVA, with between group comparisons, was used to determine the significance of more than two measures within the same subjects, followed by a Tukey-Kramer honestly significant difference *post hoc* for pairwise comparisons if $p < 0.05$ (JASP). A Kolmogorov-Smirnov test (K-S Test) was used to determine the significance between the distributions of two independent data sets. Multi-

dimensional K-S Test was used for data sets with two independent measurements (MATLAB). Statistical significance ($p < 0.05$) is represented as asterisks in figures, data is described as mean \pm standard error (mean \pm SEM).

3.4 Results

3.4.1 Robust expression of ER α and ER β in binocular region of V1 of adult male and female rats

To ask if ERs exist in the adult visual cortex, I performed immunohistochemistry with well-validated antibodies. Rabbit anti-ER α (ThermoFisher, epitope: residues 1-21 of the Activation Function (AF-1) domain of the N-terminus (Kumar et al., 2011)) and mouse anti-ER β (ThermoFisher; epitope: residues 467-485 of the Ligand-Binding Domain (LBD) (Kumar et al., 2011)) reveal robust expression of ER α and ER β in the adult primary visual cortex of male and female Long Evans rats (>P180; Fig.1A). To ask if ERs are present outside the nucleus in adult V1, I compared the distribution of ER α and ER β to the distribution of DAPI (4',6-Diamidino-2'-phenylindole dihydrochloride), a fluorescent stain that binds to AT-rich sequences of DNA. Pearson's correlation coefficient reveals very low co-localization between DAPI / ER α and DAPI / ER β in adult V1 (AVG \pm SEM; DAPI-ER α : Males 0.16 \pm 0.005, Females 0.17 \pm 0.02; DAPI-ER β : Males 0.12 \pm 0.015, Females: 0.14 \pm 0.017, n=4; Fig.9B). Staining for each of the ER antibodies was lost by pre-absorption with antigen (not shown). Thus, robust expression of non-nuclear ERs persists in the aged rodent V1.

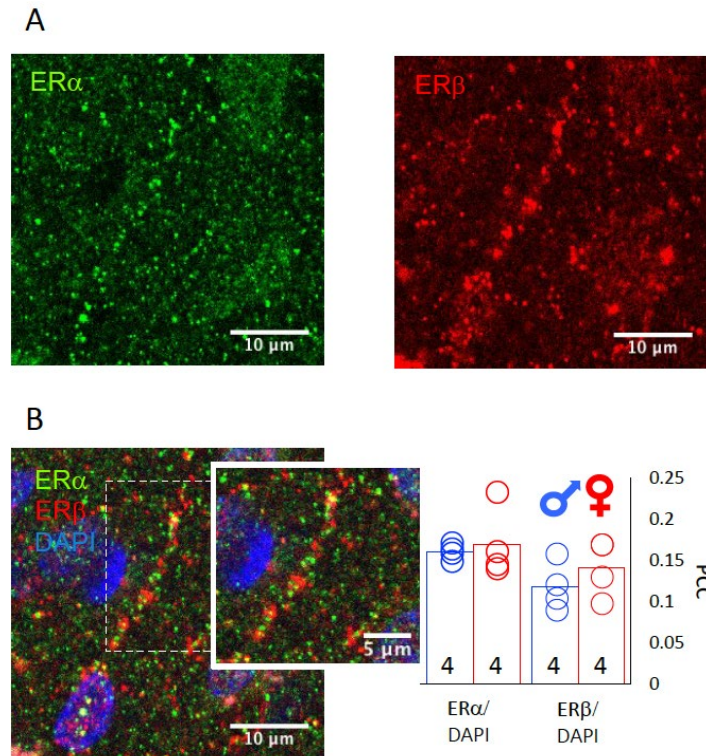


Figure 9. Non-nuclear estrogen receptors in visual cortex of male and female adult rats

A. Single z-section fluorescent micrograph of ER α (top left; green) and ER β (top right; red) immunoreactive puncta in the binocular region of primary visual cortex (V1b; ML: 4mm AP :-6.72 mm DV: 1.5mm; ~500 μ m from surface; ROI: 129.17 μ m x 129.17 μ m; 40x mag) in an adult male rat (P189). **B.** Left: Single z-section fluorescent micrographs of triple labeled ER α /ER β / DAPI (blue) in V1b (ML: 4mm AP :-6.72 mm DV: 1.5mm; ~500 μ m from surface; ROI: 129.17 μ m x 129.17 μ m; 40x mag, inset: 72 μ m x 82 μ m; 40x mag plus 3x digital zoom). Right: Pearson's correlation coefficient (PCC) reveals equally low correlation between DAPI and ER α and ER β in adult (>P180) males and females, n=4.

3.4.2 17 α -estradiol administration does not stimulate growth of reproductive tissue of gonadally-intact animals

My goal is to examine the effects of estrogen treatment in the aged amblyopic V1 using 17 α -estradiol (17 α E2), an estrogen isomer which induces ~2 fold greater synaptogenesis than an equal concentration of 17 β -estradiol, is

genomically inactive, and reported to not interact with adult reproductive tissue (MacLusky et al., 2005; Perusquía & Navarrete, 2005). To confirm the latter, I compared gonadal wet weight (normalized to body mass) in treated and untreated subjects following repetitive 17 α E2 delivery (15 μ g/kg, s.c., 1x/day for 7 days). I observed no significant difference in gonad:body weight ratio after 17 α E2 treatment in female or male subjects (>P180), suggesting that this 17 α E2 treatment did not stimulate gonadal growth (AVG \pm SEM; female vehicle (veh): 4.10 \pm 0.38 vs. female 17 α E2: 5.134 \pm 1.09; male veh: 6.01 \pm 0.90 vs. male 17 α E2: 5.59 \pm 0.34, males n=3, females n=3, Fig 10B). All subsequent experiments utilized either a single dose of 17 α E2, or the repetitive dose described above (15 μ g/kg, s.c., 1x/day for 7 days).

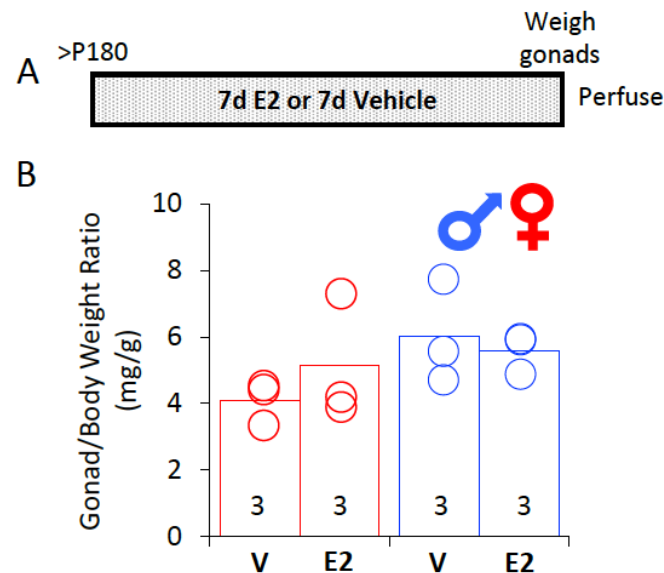


Figure 10. 17 α estradiol does not enhance gonad weight of intact male and female adult rats
A. Experimental timeline. Adult subjects (>P180) receive once-daily 17 α -estradiol for 7 days (15 μ g/kg, s.c., 1x/day for 7 days). Subjects are sacrificed and gonads dissected / weighed. **B.** No significant difference between in gonad / body weight ratio (mg/g) in intact male and female subjects which received either 7 days of vehicle (V) or 7 days of 17 α -estradiol (E2), n=3 for each group.

3.4.3 17 α E2 administration increases markers for plasticity in the amblyopic visual cortex

To ask if estrogen treatment induces changes in the cortex that correlate with enhanced plasticity, we examined the response to a single dose of 17 α E2 following cMD. We examined the effect of 17 α E2 on the expression of the activity-dependent calcium-binding protein parvalbumin (PV), a proxy for the activity of fast-spiking interneurons (FS INs) (Donato et al., 2013; Murase et al., 2017). A single dose of 17 α E2 to cMD subjects (15 μ g/kg, s.c.) induced a rapid (2.5 hour) decrease in the expression of PV in V1b contralateral and ipsilateral to the occluded eye (AVG \pm SEM; Contra cMD 26.18 \pm 2.67 vs. Contralateral cMD+17 α E2 (Contra 17 α E2) 24.68 \pm 3.61, p <0.001; Ipsi cMD 25.59 \pm 1.42 vs. Ipsilateral cMD+17 α E2 (Ipsi 17 α E2) 18.97 \pm 3.17, p <0.001, K-S Test, n =6, Fig.11B). As the activity of FS INs is negatively correlated with pyramidal neuron excitability, this complements previous reports that 17 α E2 treatment can enhance principal neuron excitability (Córdoba Montoya & Carrer, 1997; Kumar & Foster, 2002). Next, I examined the effect of 17 α E2 on the density of the extracellular matrix (ECM), the maturation of which is known to constrain plasticity in adult circuits (Carulli et al., 2010; Gogolla et al., 2009; Oray et al., 2004; Pfeffer et al., 2013; Pizzorusso et al., 2002, 2006). The ECM is primarily composed of chondroitin sulfate proteoglycans (CSPGs), which can be tracked by the binding of the lectin Wisteria-floribunda agglutinin (WFA) binding to N-acetyl-D-galactosamine in chondroitin sulfate sidechains. 17 α E2 treatment of cMD subjects (15 μ g/kg, s.c.) induced a rapid (2.5 hour) decrease in WFA

staining in V1b contralateral and ipsilateral to the occluded eye (AVG±SEM; Contra cMD 16.63±2.08 vs. Contra 17αE2 14.85±1.82, p<0.001; Ipsi cMD 18.23±2.79 vs. Ipsi 17αE2 12.62±1.56, p<0.001, K-S Test, n=6, Fig.11C). This suggests that a single administration of 17αE2 triggers changes in the adult V1 that are predicted to promote synaptic plasticity.

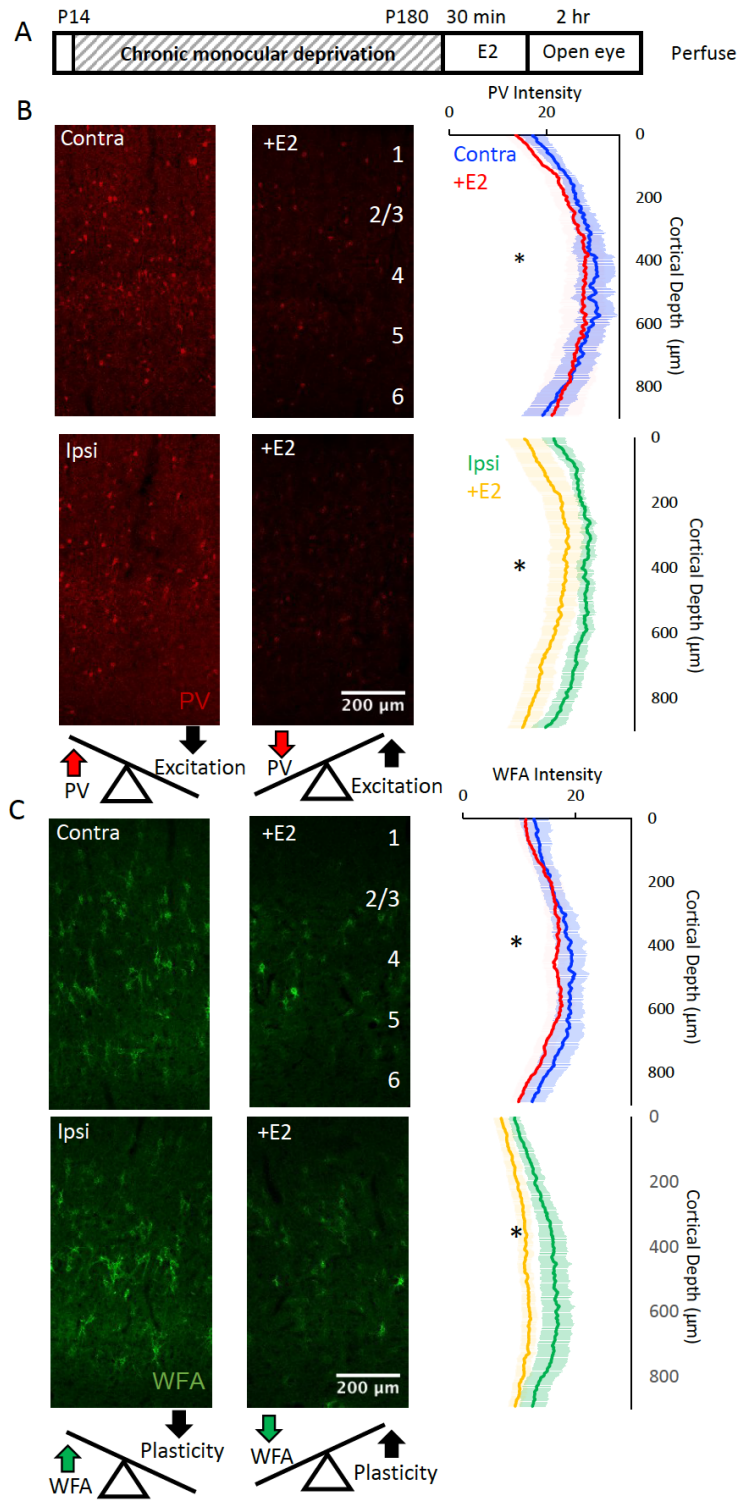


Figure 11: 17 α E2 reduces PV and WFA staining in V1b contralateral and ipsilateral to cMD

A. Experimental timeline. Subjects receive monocular deprivation from eye opening (~P14) to adulthood (>P180) and receive 17 α E2 (15 μ g/kg, s.c.) 30 minutes prior to eye opening. **B.** Top Left- Fluorescent micrographs of PV distribution in V1b (red, V1; ML: 4 mm AP: -6.72 mm DV: 1.5mm; ROI: 900 μ m x 500 μ m; 10x mag; MIP). Bottom Left: Graphic representations of impact of PV expression on pyramidal neuron excitability. Right: 17 α E2 significantly decreases PV intensity in V1b contralateral and ipsilateral to cMD, $*=p<0.01$, K-S Test, n=6. **C.** Top Left: Fluorescent micrographs of WFA distribution in V1b (green, V1; ML: 4mm AP: -6.72 mm DV: 1.5mm; ROI: 900 μ m x 500 μ m; 10x mag; MIP). Bottom Left: Graphic representations of impact of WFA expression on plasticity. Right: 17 α E2 significantly decreases WFA intensity in V1b contralateral and ipsilateral to cMD, $*=p<0.001$, K-S Test, n=6.

3.4.4 17 α E2 increases the size of excitatory post-synaptic densities

To ask if 17 α E2 treatment impacts the density of excitatory synapses, we examined the size and number of PSD95 immunoreactive puncta. 17 α E2 treatment of cMD subjects (15 μ g/kg, s.c.) induced a rapid (2.5 hour) and significant increase in the size of PSD95 immunoreactive puncta in V1b contralateral, but not ipsilateral, to the occluded eye (Contra cMD 0.080 ± 0.01 μ m² vs. Contra 17 α E2 0.082 ± 0.003 μ m², $p<0.001$; Ipsi cMD 0.078 ± 0.01 μ m² vs. Ipsi 17 α E2 0.081 ± 0.006 μ m², $p=0.55$, K-S Test, n=6, Fig.12B), but no change in PSD95 number (AVG \pm SEM; Contra cMD 250.97 ± 29.30 vs. Contra 17 α E2 324.71 ± 47.54 ; Ipsi cMD 235.60 ± 35.44 vs. Ipsi 17 α E2 303.01 ± 25.52 , n= 6, Fig.12B).

To ask if 17 α E2 impacted the activity of signaling pathways known to regulate GluA1-AMPA function and plasticity, I examined the intensity and distribution of pS831 (Barria et al., 1997; Mammen et al., 1997; Roche et al., 1996). However, we observed no increase in pS831 puncta size (AVG \pm SEM;

Contra cMD $0.073 \pm 0.002 \mu\text{m}^2$ vs. Contra 17 α E2 $0.067 \pm 0.001 \mu\text{m}^2$; Ipsi cMD $0.069 \pm 0.005 \mu\text{m}^2$ vs. Ipsi 17 α E2 $0.071 \pm 0.005 \mu\text{m}^2$, n=6, Fig.12C) or puncta number (Contra cMD 234.74 ± 49.94 vs. Contra 17 α E2 273.97 ± 47.53 ; Ipsi cMD 240.40 ± 64.77 vs. Ipsi 17 α E2 267.99 ± 40.04 ; n = 6, Fig.12C). This suggests that 17 α E2 may increase the size of pre-existing excitatory synapses consistent via a pathway that is independent of CaMKII/PKC phosphorylation of the GluA1-AMPAR.

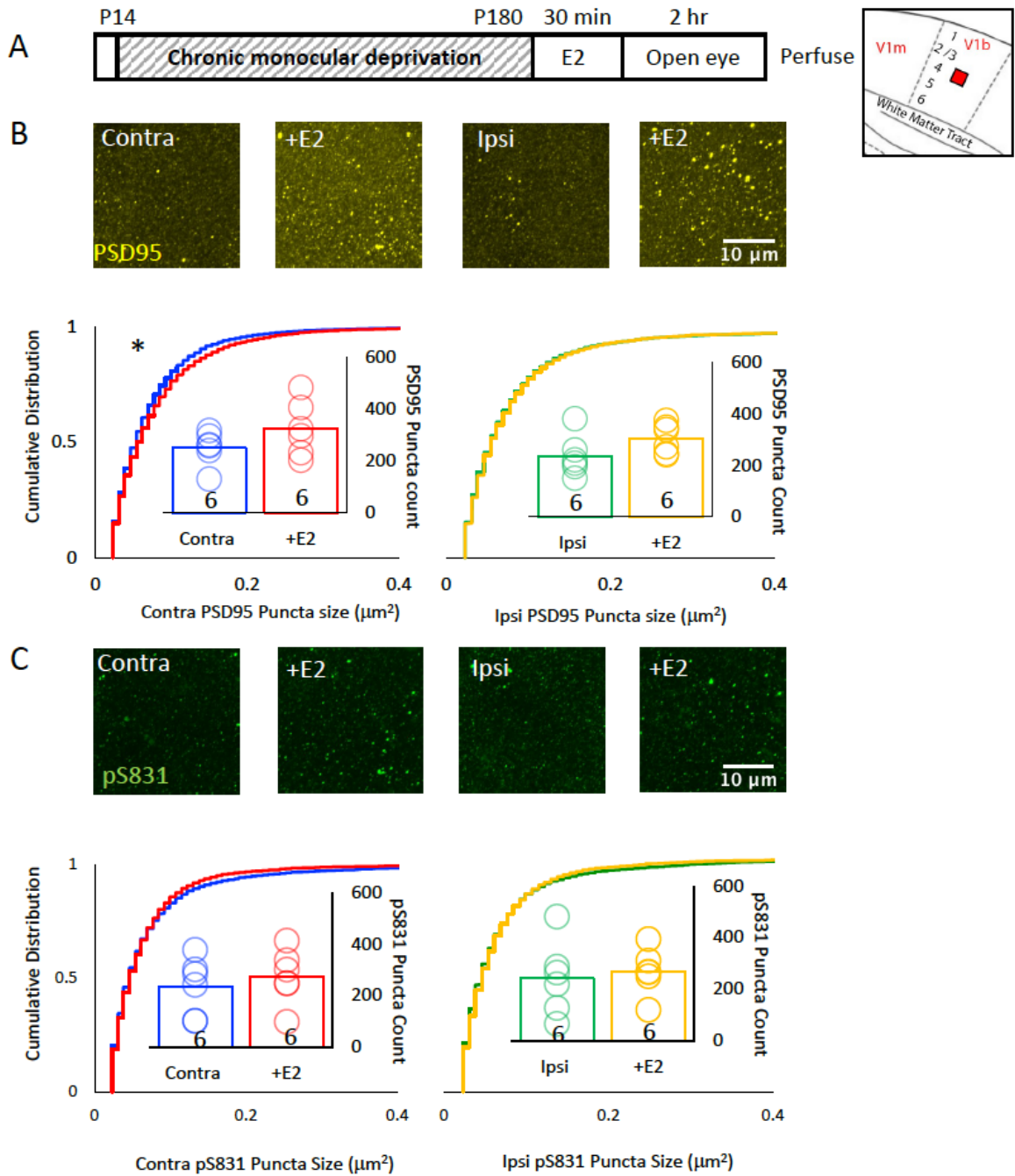


Figure 12. 17 α E2 increases size marker for excitatory post-synaptic densities

A. Experimental timeline. Subjects receive monocular deprivation from eye opening (~P14) to adulthood (>P180) and receive 17 α E2 (15 μ g/kg, s.c.) 30 minutes prior to eye opening. **B.** Top: Fluorescent micrographs of PSD95 immunoreactivity (yellow) in V1b contralateral (left) and ipsilateral (right) to cMD, (ML: 4mm AP: -6.72 mm DV: 1.5mm; ~500 μ m from surface; ROI: 28.34 μ m x 28.34 μ m x 40 μ m, 100x mag with 3x digital zoom; MIP). Bottom: Cumulative distribution of PSD95 immunoreactive puncta size (yellow) reveals significant increase in V1b contralateral (left) to the occluded eye, $*=p<0.001$, K-S Test, n=6. **C.** Top: Fluorescent micrographs of pS831 immunoreactivity (green) in V1b contralateral (left) and ipsilateral (right) to cMD, (V1; ML: 4mm AP: -6.72 mm DV: 1.5mm; ~500 μ m from surface; ROI: 28.34 μ m x 28.34 μ m x 40 μ m, 100x mag with 3x digital zoom; MIP). Bottom: Cumulative distribution of pS831 immunoreactive puncta reveals significant decrease in V1b ipsilateral (right) to cMD, K-S Test, n=6.

3.4.5 17 α E2 decreases expression of presynaptic markers

To ask if 17 α E2 treatment impacts the innervation of V1b after cMD, I examined the size and number of puncta that were immunoreactive for the cortico-cortical afferent marker VGlut1 and thalamocortical afferent marker VGlut2. 17 α E2 treatment of cMD subjects induced a significant decrease in the size of VGlut1 and VGlut2 immunoreactive puncta in V1b contralateral and ipsilateral to the occluded eye (Tables 6-7, Fig.13C). VGlut2 number did not change in either hemisphere following 17 α E2 (Table 7, Fig.13C), however there was a decrease in VGlut1 number in V1b ipsilateral to the occluded eye (Table 6, Fig.13B). The decrease in VGlut1 and VGlut2 size following 17 α E2 was not predicted, as changes in presynaptic size are thought to mirror changes in postsynaptic densities (Futai et al., 2007). However, the decrease in the size of the presynaptic markers following 17 α E2 could be indicative of decreased glutamate re-uptake in response to the administration of the hormone, as previously reported (Sato et al., 2003).

Table 6: VGlut1 size / number following 17αE2			
VGlut1 Puncta Size	Average+/- SEM	n	P value
Contra cMD	0.17±0.02μm ² vs.	6	KS Test
Contra 17αE2	0.14±0.01μm ²	6	*p=<,0.001 vs. Contra cMD
Ipsi cMD	0.17±0.02μm ²	6	KS Test
Ipsi 17αE2	0.15±0.02 μm ²	6	*p=<,0.01 vs. Ipsi cMD
VGlut1 Puncta #	Average+/- SEM	n	P value
Contra cMD	348.00±31.03	6	Student's T-test
Contra 17αE2	295.36±45.04	6	NS, p>0.05
Ipsi cMD	376.89±28.74	6	Student's T-test
Ipsi 17αE2	283.06±26.74,	6	*=p<0.05

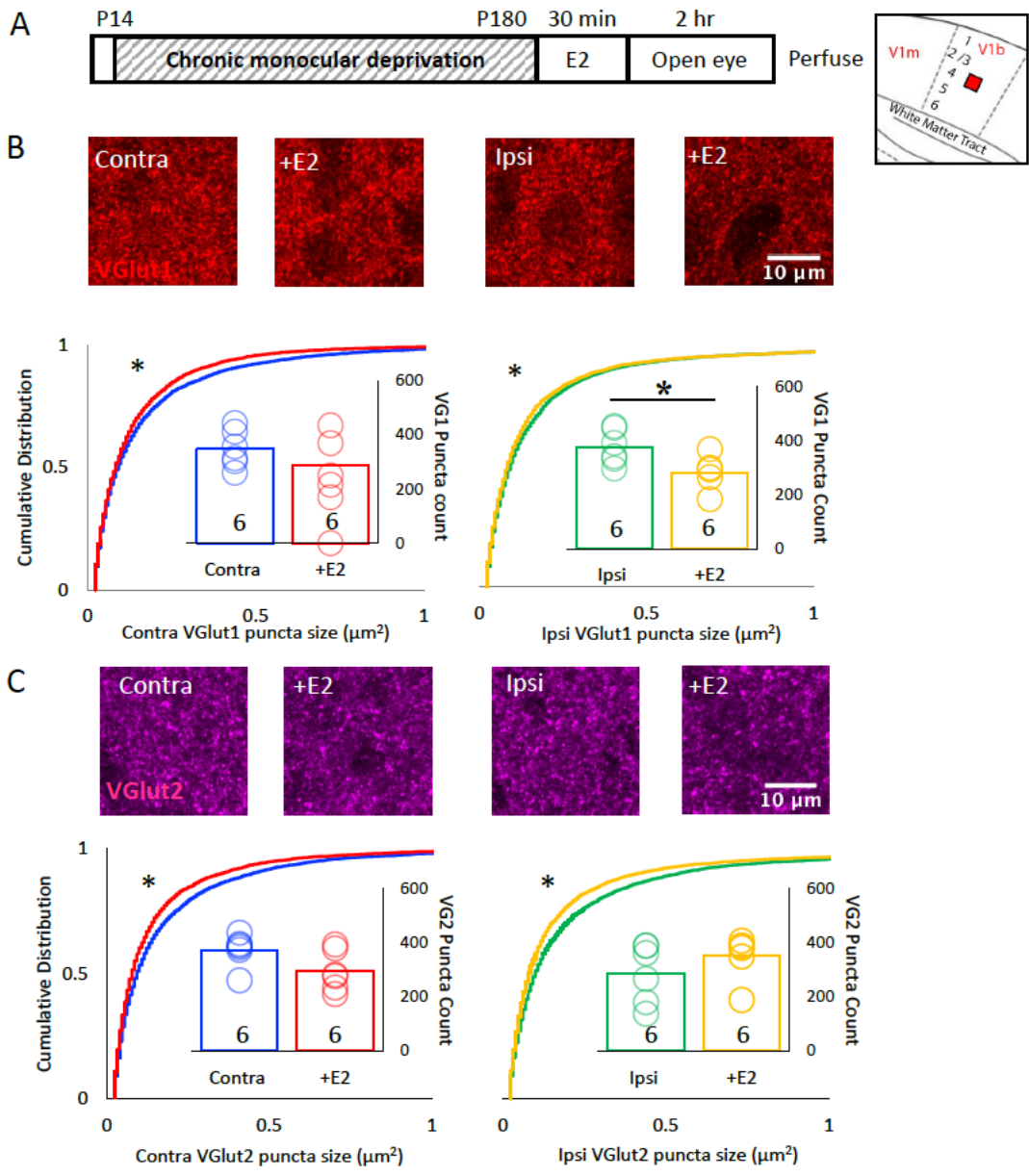


Figure 13. 17 α E2 decreases markers for cortico-cortical and thalamocortical synapses
A. Left: Experimental timeline. Subjects receive monocular deprivation from eye opening (~P14) to adulthood (>P180) and receive 17 α E2 (15 μ g/kg, s.c.) 30 minutes prior to eye opening. Right: Fluorescent micrograph ROI in Layer 4 of V1b (red box). **B.** Top: Fluorescent micrographs of VGlut1 immunoreactivity (red) in V1b contralateral (left) and ipsilateral (right) to cMD, (ML: 4mm AP: -6.72 mm DV: 1.5mm; ~500 μ m from surface; ROI: 28.34 μ m x 28.34 μ m x 40 μ m, 100x mag with 3x digital zoom; MIP). Bottom: Cumulative distribution of VGlut1 immunoreactive puncta size (red) reveals significant increase in V1b contralateral (left) and ipsilateral (right) to the occluded eye, * p <0.01, K-S Test, n=6. VGlut1 puncta count is significantly reduced following 17 α E2 in V1b ipsilateral (right) to the occluded eye, * p <0.05, Student's T-test, n=6. **C.** Top: Fluorescent micrographs of VGlut2 immunoreactivity (magenta) in V1b contralateral (left) and ipsilateral (right) to cMD, (V1; ML: 4mm AP: -6.72 mm DV: 1.5mm; ~500 μ m from surface; ROI: 28.34 μ m x 28.34 μ m x 40 μ m, 100x mag with 3x digital zoom; MIP). Bottom: Cumulative distribution of VGlut2 immunoreactive puncta reveals significant decrease in V1b contralateral (left) and ipsilateral (right) to cMD, * p <0.001, K-S Test, n=6.

Table 7: VGlut2 size / number following 17 α E2

VGlut2 Puncta Size	Average+/- SEM	n	P value
Contra cMD	0.18 \pm 0.01 μ m ²	6	*KS Test
Contra 17 α E2	0.13 \pm 0.01 μ m ²	6	* p =<,0.001 vs. Contra cMD
Ipsi cMD	0.17 \pm 0.02 μ m ²	6	KS Test
Ipsi 17 α E2	0.15 \pm 0.01 μ m ²	6	* p =<,0.01 vs. Contra cMD
VGlut2 Puncta #	Average+/- SEM	n	P value
Contra cMD	373.69 \pm 26.56	6	Student's T-test
Contra 17 α E2	296.22 \pm 33.63	6	NS, p >0.05
Ipsi cMD	287.69 \pm 49.28	6	Student's T-test
Ipsi 17 α E2	351.00 \pm 36.49	6	NS, p >0.05

3.4.6 17 α E2 increases colocalization of pS831 and thalamic afferent markers

To ask if 17 α E2 treatment changes the co-localization of the markers I use to track pre- and postsynaptic compartments, I quantified colocalization of postsynaptic marker PSD95, pS831 of GluA1-AMPA, and presynaptic markers VGlut1 and VGlut2. The PCC analysis revealed a significant increase of pS831 colocalization with VGlut2 in V1b contralateral to the deprived eye (Table 8, Fig.14A), and no change in pS831 colocalization with VGlut1 (Table 8, Fig.14B). There was also no change in either colocalization of PSD95 with VGlut1 or VGlut2, or with pS831 with PSD95 after 17 α E2 administration (Table 8). Together, this suggests the 17 α E2 may increase activity at thalamocortical synapses, but does not change the co-localization between markers for pre- and postsynaptic contributions to excitatory synapses.

Table 8: Colocalization of synaptic markers following 17αE2			
PSD95-VGlut1 Coloc.	Average+/- SEM	n	P value
Contra cMD	0.57 \pm 0.04	6	Student's T-test
Contra 17 α E2	0.55 \pm 0.03	6	p>0.05 vs. Contra cMD
Ipsi cMD	0.58 \pm 0.03	6	Student's T-test
Ipsi 17 α E2	0.54 \pm 0.05	6	p>0.05 vs. Ipsi cMD
pS831-VGlut1 Coloc.	Average+/- SEM	n	P value
Contra cMD	0.42 \pm 0.05	6	Student's T-test
Contra 17 α E2	0.45 \pm 0.02	6	p>0.05 vs. Contra cMD

Ipsi cMD	0.45±0.03	6	Student's T-test
Ipsi 17αE2	0.41±0.06	6	p>0.05 vs. Ipsi cMD
PSD95-VGlut2 Coloc.	Average+/- SEM	n	P value
Contra cMD	0.45±0.03	6	Student's T-test
Contra 17αE2	0.46±0.04	6	p>0.05 vs. Contra cMD
Ipsi cMD	0.45±0.02	6	Student's T-test
Ipsi 17αE2	0.44±0.03	6	p>0.05 vs. Ipsi cMD
pS831-VGlut2 Coloc.	Average+/- SEM	n	P value
Contra cMD	0.37±0.03	6	Student's T-test
Contra 17αE2	0.45±0.02	6	*=p<0.05 vs. Contra cMD
Ipsi cMD	0.38±0.03	6	Student's T-test
Ipsi 17αE2	0.42±0.03	6	p>0.05 vs. Ipsi cMD
pS831-PSD95 Coloc.	Average+/- SEM	n	P value
Contra cMD	0.48±0.02	6	Student's T-test
Contra 17αE2	0.52±0.03	6	p>0.05 vs. Contra cMD
Ipsi cMD	0.50±0.02	6	Student's T-test
Ipsi 17αE2	0.48±0.03	6	p>0.05 vs. Ipsi cMD

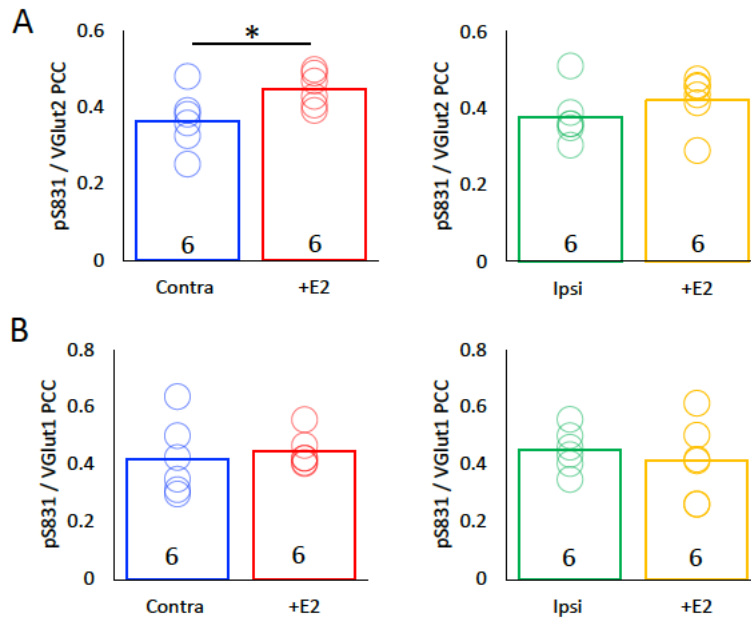


Figure 14. Colocalization of pS831 increased at thalamocortical synapses

A. VGlut2-pS831 PCC increased in cMD V1b contralateral to the occluded eye following E2, $*=p<0.05$, Student's T-test, $n=6$. **B.** No change in VGlut1-pS831 PCC in cMD V1b following E2 in contralateral and ipsilateral hemispheres, $n=6$.

3.4.7 17 α E2 followed by visual stimulation further decreases markers for constrained plasticity in the cMD V1

The response to 17 α E2 treatment alone was modest. This was not unexpected, as my hypothesis is that newly formed synapses require salient stimulation to be incorporated into functional circuits. Therefore, I next examined the response to a single dose of 17 α E2 followed by visual stimulation in cMD subjects. A single dose of 17 α E2 to cMD subjects (15 μ g/kg, s.c.) was followed 30 minutes later by a simple visual stimulus known to be sufficient to evoke responses from cMD V1 (200 x 1 second trials of square-wave gratings, 0.05 cycles per degree, 100% contrast, reversing at 1 Hz, at 45 degrees, (Montey &

Quinlan, 2011)). 17 α E2 followed by visual stimulation induced a rapid (2.5 hour) decrease in the expression of PV in V1b contralateral and ipsilateral to the occluded eye (AVG \pm SEM; Contra cMD 26.18 \pm 2.67 vs. Contralateral cMD+17 α E2+ Visual Stimulus (Contra 17 α E2 Stim) 21.83 \pm 2.63, p<0.001; Ipsi cMD 25.59 \pm 1.42 vs. Ipsilateral cMD+17 α E2+Visual Stimulus (Ipsi 17 α E2 Stim) 23.25 \pm 2.56, p<0.001, K-S Test, n=6, Fig.15B), which was lower than 17 α E2 alone (AVG \pm SEM; Contra 17 α E2 24.68 \pm 3.61 vs. Contra 17 α E2 Stim 21.83 \pm 2.63, p<0.001, K-S Test, n=6). Similarly, 17 α E2 followed by visual stimulation induced a decrease in WFA expression in V1b contralateral and ipsilateral to the occluded eye (AVG \pm SEM; Contra cMD 16.63 \pm 2.08 vs. Contra 17 α E2 Stim 11.77 \pm 1.06, p<0.001; Ipsi cMD 18.23 \pm 2.79 vs. Ipsi 17 α E2 Stim 13.25 \pm 1.32, p<0.001, K-S Test, n=6, Fig.15C), which was lower than 17 α E2 alone (AVG \pm SEM; Contra 17 α E2 14.85 \pm 1.82 vs. Contra 17 α E2 Stim 11.77 \pm 1.06, p<0.001, K-S Test, n=6). This suggests 17 α E2 followed by visual stimulation may promote robust synaptic plasticity.

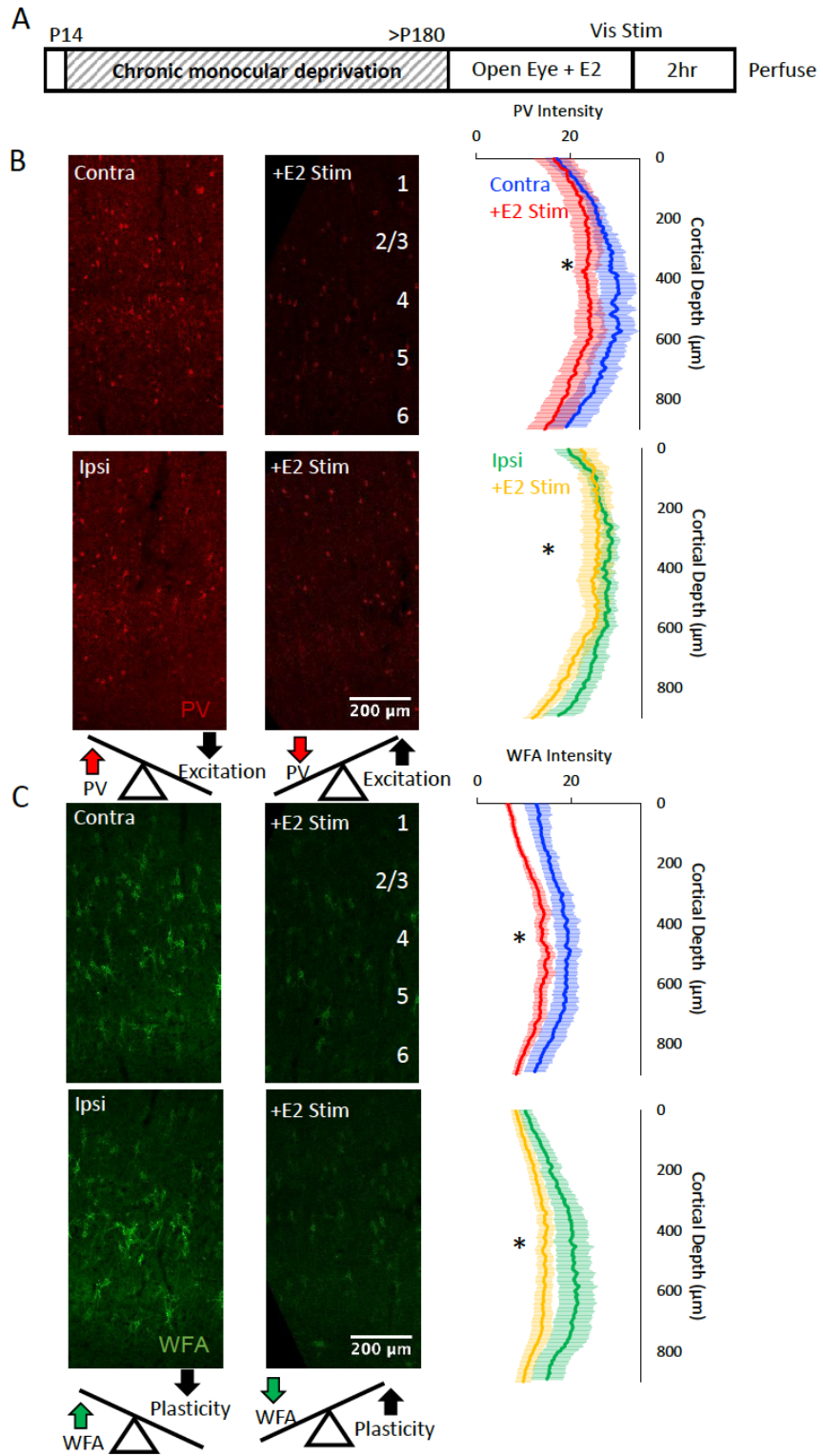


Figure 15: 17 α E2 followed by visual stimulus reduces PV and WFA staining in V1b contralateral and ipsilateral to cMD

A. Experimental timeline. Subjects receive monocular deprivation from eye opening (~P14) to adulthood (>P180) and receive 17 α E2 (15 μ g/kg, s.c.) 30 minutes prior to visual stimulus (200 phase reversal of high contrast grating at a single orientation). **B.** Top Left: Fluorescent micrographs of PV distribution in V1b (red, V1; ML: 4 mm AP: -6.72 mm DV: 1.5mm; ROI: 900 μ m x 500 μ m; 10x mag; MIP). Bottom Left: Graphic representations of impact of PV expression on pyramidal neuron excitability. Right: 17 α E2 followed by visual stimulus significantly decreases PV intensity in V1b contralateral and ipsilateral to cMD, $*=p<0.01$, K-S Test, n=6. **C.** Top Left: Fluorescent micrographs of WFA distribution in V1b (green, V1; ML: 4mm AP: -6.72 mm DV: 1.5mm; ROI: 900 μ m x 500 μ m; 10x mag; MIP). Bottom Left: Graphic representations of impact of WFA expression on plasticity. Right: 17 α E2 significantly followed by visual stimulus decreases WFA intensity in V1b contralateral and ipsilateral to cMD, $*=p<0.001$, K-S Test, n=6.

3.4.8 17 α E2 followed by visual stimulation further increases size of excitatory synapses and synaptic signaling

To ask if 17 α E2 followed by visual stimulation treatment impacts the density of excitatory synapses, I revisited markers for the postsynaptic specialization. 17 α E2 followed by visual stimulation induced a significant increase in the size of PSD95 immunoreactive puncta in V1b contralateral and ipsilateral to the occluded eye (Contra cMD $0.080\pm 0.01 \mu\text{m}^2$ vs. Contra 17 α E2 Stim $0.081\pm 0.003 \mu\text{m}^2$, $p<0.001$; Ipsi cMD $0.078\pm 0.01 \mu\text{m}^2$ vs. Ipsi 17 α E2 $0.079\pm 0.003 \mu\text{m}^2$, $p<0.05$, K-S Test, n=6, Fig.16B), but no change in PSD95 number (AVG \pm SEM; Contra cMD 250.97 ± 29.30 vs. Contra 17 α E2 306.55 ± 28.97 ; Ipsi cMD 235.60 ± 35.44 vs. Ipsi 17 α E2 306.24 ± 31.25 , n= 6, Fig.16B). In addition, I observed an increase in pS831 puncta size in V1b contralateral, but not ipsilateral, to the occluded eye (AVG \pm SEM; Contra cMD $0.073\pm 0.002 \mu\text{m}^2$ vs. Contra 17 α E2 Stim $0.071\pm 0.003 \mu\text{m}^2$, $p<0.001$; Ipsi cMD $0.069\pm 0.005 \mu\text{m}^2$ vs. Ipsi 17 α E2 Stim $0.070\pm 0.003 \mu\text{m}^2$, $p=0.07$, K-S Test, n=6, Fig.16C), yet no change in puncta number (Contra cMD 234.74 ± 49.94 vs. Contra 17 α E2 Stim

274.44±36.20; Ipsi cMD 240.40±64.77 vs. Ipsi 17αE2 Stim 282.15±39.29; n = 6, Fig.16C). This indicates that 17αE2 followed by visual stimulation may induce a non-specific increase in the size of excitatory synapses in the aged amblyopic V1, but increased activity is only observed in the hemisphere contralateral to the occluded eye.

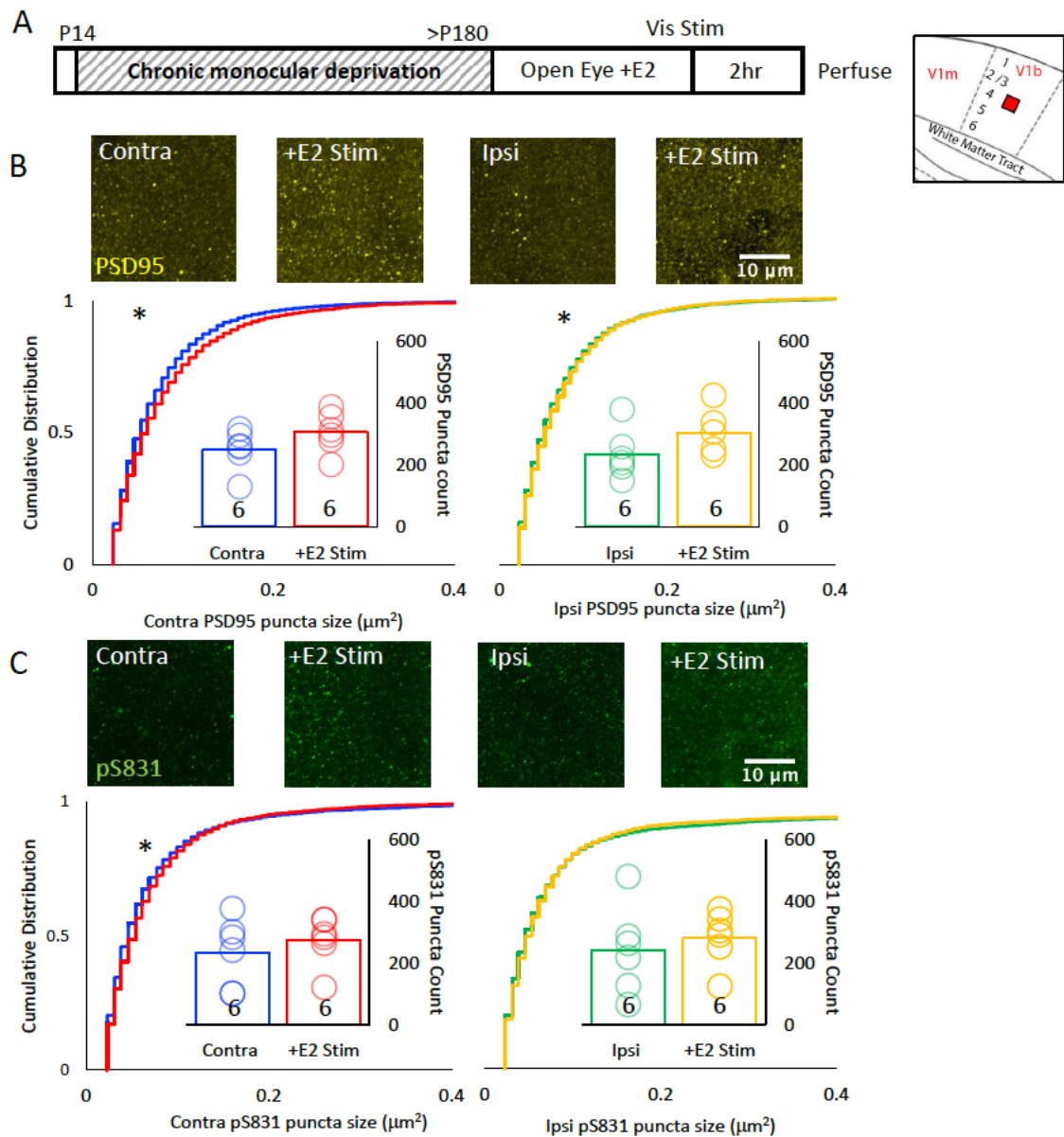


Figure 16. 17 α E2 followed by visual stimulus increases markers for excitatory post-synaptic densities and synaptic activity

A. Experimental timeline. Subjects receive monocular deprivation from eye opening (~P14) to adulthood (>P180) and receive 17 α E2 (15 μ g/kg, s.c.) 30 minutes prior to visual stimulus (200 phase reversal of high contrast grating at a single orientation). **B.** Top: Fluorescent micrographs of PSD95 immunoreactivity (yellow) in V1b contralateral (left) and ipsilateral (right) to cMD, (ML: 4mm AP: -6.72 mm DV: 1.5mm; ~500 μ m from surface; ROI: 28.34 μ m x 28.34 μ m x 40 μ m, 100x mag with 3x digital zoom; MIP). Bottom: Cumulative distribution of PSD95 immunoreactive puncta size (yellow) reveals significant increase in V1b contralateral (left) and ipsilateral (right) to the occluded eye, $*=p<0.05$, K-S Test, n=6. **C.** Top: Fluorescent micrographs of pS831 immunoreactivity (green) in V1b contralateral (left) and ipsilateral (right) to cMD, (V1; ML: 4mm AP: -6.72 mm DV: 1.5mm; ~500 μ m from surface; ROI: 28.34 μ m x 28.34 μ m x 40 μ m, 100x mag with 3x digital zoom; MIP). Bottom: Cumulative distribution of pS831 immunoreactive puncta reveals significant decrease in V1b contralateral (left) to the cMD eye, $*=p<0.001$, K-S Test, n=6.

3.4.9 17 α E2 followed by visual stimulation decreases expression of presynaptic markers

To ask if 17 α E2 treatment followed by visual stimulus impacts the number or size of presynaptic afferents in cMD V1b, I examined the cortico-cortical afferent marker VGlut1 and thalamocortical afferent marker VGlut2. Surprisingly, 17 α E2 treatment of cMD subjects followed by visual stimulus induced a significant decrease in the size of VGlut2 immunoreactive puncta in V1b contralateral and ipsilateral to the occluded eye (AVG \pm SEM: Contra cMD 0.18 \pm 0.01 μ m² vs. Contra 17 α E2 Stim 0.13 \pm 0.01 μ m², $p<0.001$; Ipsi cMD 0.17 \pm 0.02 μ m² vs. Ipsi 17 α E2 Stim 0.13 \pm 0.02 μ m², $p<0.001$; K-S Test, n=6, Fig.17C) and VGlut1 in V1b contralateral to the occluded eye (AVG \pm SEM: Contra cMD 0.17 \pm 0.02 μ m² vs. Contra 17 α E2 Stim 0.14 \pm 0.01 μ m², $p<0.001$; Ipsi cMD 0.17 \pm 0.02 μ m² vs. Ipsi 17 α E2 Stim 0.16 \pm 0.02 μ m², $p=.55$; K-S Test, n=6, Fig.17B). VGlut2 number was not changed in either hemisphere following 17 α E2 and visual stimulus (AVG \pm SEM; Contra cMD 373.69 \pm 26.56 vs. Contra 17 α E2

Stim 375.29 ± 72.36 ; Ipsi cMD 287.69 ± 49.28 vs. Ipsi $17\alpha E2$ Stim 338.18 ± 56.24 , $n = 6$, Fig.17C), however there was a decrease in the number of VGlut1 immunoreactive puncta in V1b contralateral to the occluded eye (AVG \pm SEM; Contra cMD 348.00 ± 31.03 vs. Contra $17\alpha E2$ Stim 237.69 ± 25.81 ; Ipsi cMD 376.89 ± 28.74 vs. Ipsi $17\alpha E2$ Stim 326.69 ± 50.63 , $p < 0.01$, Student's T-test, $n = 6$, Fig.17B). Again, this result was surprising, but consistent with the disconnection in PSD95 and VGlut size reported above. As with $17\alpha E2$ alone, the observed decrease in the size of the presynaptic markers following $17\alpha E2$ could be indicative of decreased glutamate re-uptake in response to the administration of the hormone, as previously reported (Sato et al., 2003).

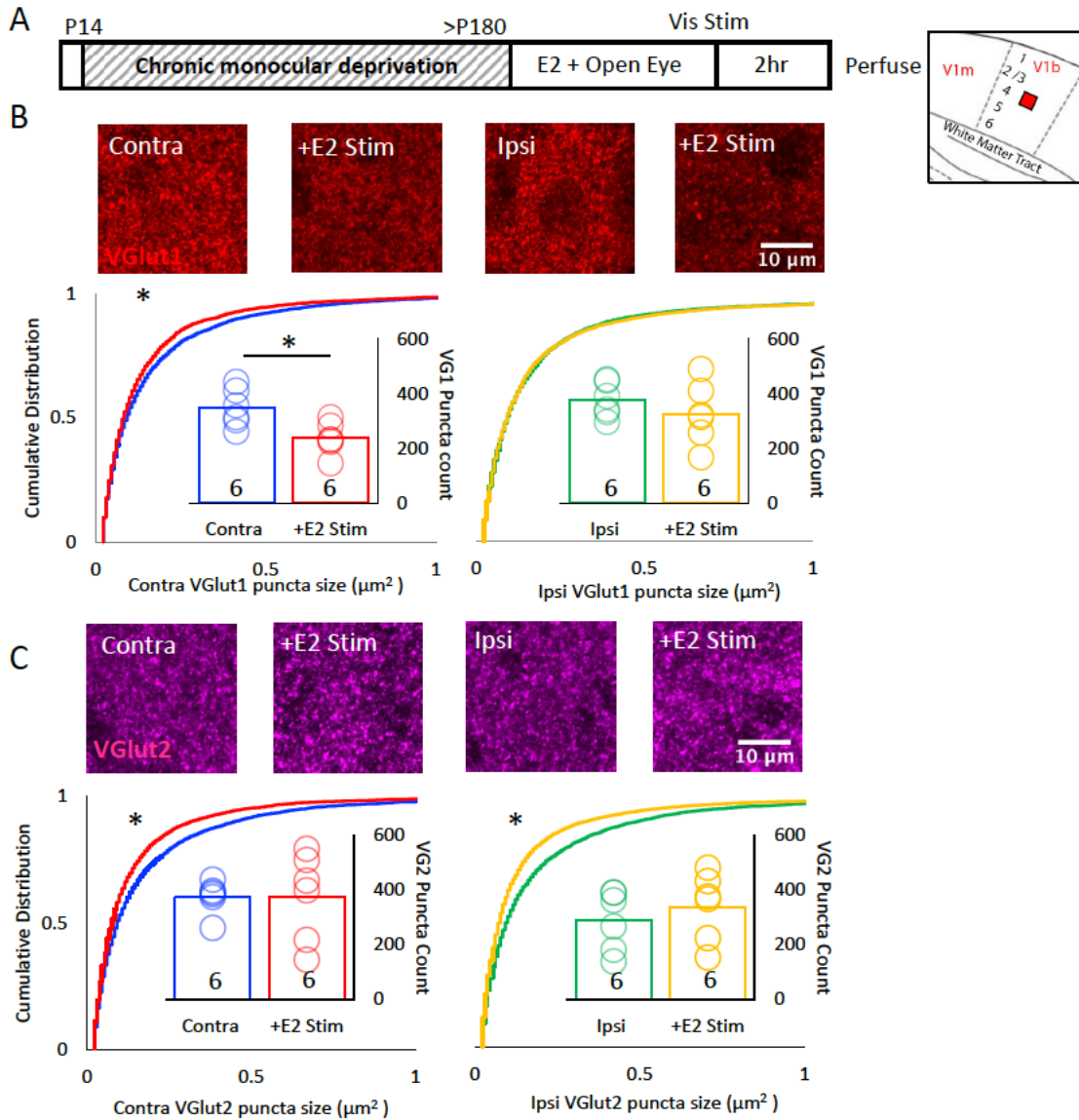


Figure 17. 17 α E2 followed by visual stimulation decreases markers for cortico-cortical and thalamocortical afferents

A. Experimental timeline. Subjects receive monocular deprivation from eye opening (~P14) to adulthood (>P180) and receive 17 α E2 (15 μ g/kg, s.c.) 30 minutes prior to visual stimulus (200 phase reversal of high contrast grating at a single orientation). **B.** Top: Fluorescent micrographs of VGlut1 immunoreactivity (red) in V1b contralateral (left) and ipsilateral (right) to cMD, (ML: 4mm AP: -6.72 mm DV: 1.5mm; ~500 μ m from surface; ROI: 28.34 μ m x 28.34 μ m x 40 μ m, 100x mag with 3x digital zoom; MIP). Bottom: Cumulative distribution of VGlut1 immunoreactive puncta size (red) reveals significant increase in V1b contralateral (left) and ipsilateral (right) to the occluded eye, *=p<0.01, K-S Test, n=6. VGlut1 puncta count is significantly reduced following 17 α E2 and visual stimulus in V1b contralateral (left) to the occluded eye, *=p<0.05, Student's T-test, n=6. **C.** Top: Fluorescent micrographs of VGlut2 immunoreactivity (magenta) in V1b contralateral (left) and ipsilateral (right) to cMD, (V1; ML: 4mm AP: -6.72 mm DV: 1.5mm; ~500 μ m from surface; ROI: 28.34 μ m x 28.34 μ m x 40 μ m, 100x mag with 3x digital zoom; MIP). Bottom: Cumulative distribution of VGlut2 immunoreactive puncta reveals significant decrease in V1b contralateral (left) and ipsilateral (right) to cMD eye, *=p<0.001, K-S Test, n=6.

PCC analysis revealed that 17 α E2 plus visual stimulation does not change the colocalization of the various markers for excitatory synapses (Table 9).

Table 9: Colocalization of synaptic markers following 17αE2 + Vis Stim			
PSD95-VGlut1 Coloc.	Average+/- SEM	n	P value
Contra cMD	0.57 \pm 0.04	6	Student's T-test
Contra 17 α E2 Stim	0.61 \pm 0.02	6	p>0.05 vs. Contra cMD
Ipsi cMD	0.58 \pm 0.03	6	Student's T-test
Ipsi 17 α E2 Stim	0.57 \pm 0.03	6	p>0.05 vs. Ipsi cMD
pS831-VGlut1 Coloc.	Average+/- SEM	n	P value
Contra cMD	0.42 \pm 0.05	6	Student's T-test
Contra 17 α E2 Stim	0.47 \pm 0.03	6	p>0.05 vs. Contra cMD
Ipsi cMD	0.45 \pm 0.03	6	Student's T-test
Ipsi 17 α E2 Stim	0.44 \pm 0.06	6	p>0.05 vs. Ipsi cMD

PSD95-VGlut2 Coloc.	Average+/- SEM	n	P value
Contra cMD	0.45±0.03	6	Student's T-test
Contra 17αE2 Stim	0.44±0.03	6	p>0.05 vs. Contra cMD
Ipsi cMD	0.45±0.02	6	Student's T-test
Ipsi 17αE2 Stim	0.48±0.03	6	p>0.05 vs. Ipsi cMD
pS831-VGlut2 Coloc.	Average+/- SEM	n	P value
Contra cMD	0.37±0.03	6	Student's T-test
Contra 17αE2 Stim	0.42±0.02	6	p>0.05 vs. Contra cMD
Ipsi cMD	0.38±0.03	6	Student's T-test
Ipsi 17αE2 Stim	0.45±0.01	6	p>0.05 vs. Ipsi cMD
pS831-PSD95 Coloc.	Average+/- SEM	n	P value
Contra cMD	0.48±0.02	6	Student's T-test
Contra 17αE2	0.47±0.03	6	p>0.05 vs. Contra cMD
Ipsi cMD	0.50±0.02	6	Student's T-test
Ipsi 17αE2 Stim	0.45±0.03,	6	p>0.05 vs. Ipsi cMD

3.4.10 7 days of 17αE2 administration increases excitatory synapse size

Encouraged by the results with a single dose of 17αE2, I next tested the hypothesis that multiple doses of 17αE2 would further promote changes in the visual cortex that were permissive for plasticity. Once daily 17αE2 treatment to cMD subjects for 7 days (15 μg/kg, s.c., 1x/day), was followed in by visual stimulation (as before, 200 x 1 second trials of square-wave gratings (0.05 cycles

per degree (cpd), 100% contrast, reversing at 1 Hz) at 45 degrees) 30 minutes after the last 17 α E2 administration. To ask if 17 α E2 followed by visual stimulation treatment impacts the density of excitatory synapses, I once more utilized PSD95 as a marker and examined the number and size of immunoreactive puncta. In cMD subjects, both 7 days of 17 α E2 treatment and 7 days of 17 α E2 treatment followed by visual stimulation induced a significant increase in the size of PSD95 immunoreactive puncta in V1b contralateral and ipsilateral to the occluded eye, but no change in PSD95 number (Table 10, Fig.18B). I observed a large increase in pS831 puncta size in V1b contralateral and ipsilateral to the occluded eye, but a significant decrease in number (Table 11, Fig.18C). This indicates that 7 days of 17 α E2 with or without visual stimulation induces an increase in the size, but not the number, of excitatory synapses in the aged V1 similar to a single dose of 17 α E2 +/- visual stimulation. The reduction in the number of pS831+ puncta, but increase in size suggests preferential activation of large excitatory synapses.

Table 10: PSD95 size / number following 7d 17αE2			
PSD95 Puncta Size	Average+/- SEM	n	P value
Contra cMD	0.080±0.01 μm ²	6	KS test
Contra 7d 17αE2	0.080±0.002 μm ² ,	8	*=p<0.001 v. Contra MD
Contra 7d 17αE2 Stim	0.075±0.003 μm ²	8	*=p<0.001 v. Contra MD
Ipsi cMD	0.078±0.01 μm ²	6	KS test
Ipsi 7d 17αE2	0.080±0.003 μm ²	8	*p<0.05 v. Ipsi MD
Ipsi 7d 17αE2 Stim	Stim 0.080±0.003 μm ²	8	*p<0.05 v. Ipsi MD
PSD95 Puncta #	Average+/- SEM	n	P value
Contra cMD	250.97±29.30	6	one-way ANOVA, F(df,21)=1.03, p=0.37
Contra 7d 17αE2	187.97±33.31	8	NS, p>0.05
Contra 7d 17αE2 Stim	275.23±46.01	8	NS, p>0.05
Ipsi cMD	235.60±35.44	6	one-way ANOVA, F(df,21)=1.99, p=0.16
Ipsi 7d 17αE2	195.88±36.83	8	NS, p>0.05
Ipsi 7d 17αE2 Stim	283.48±31	8	NS, p>0.05

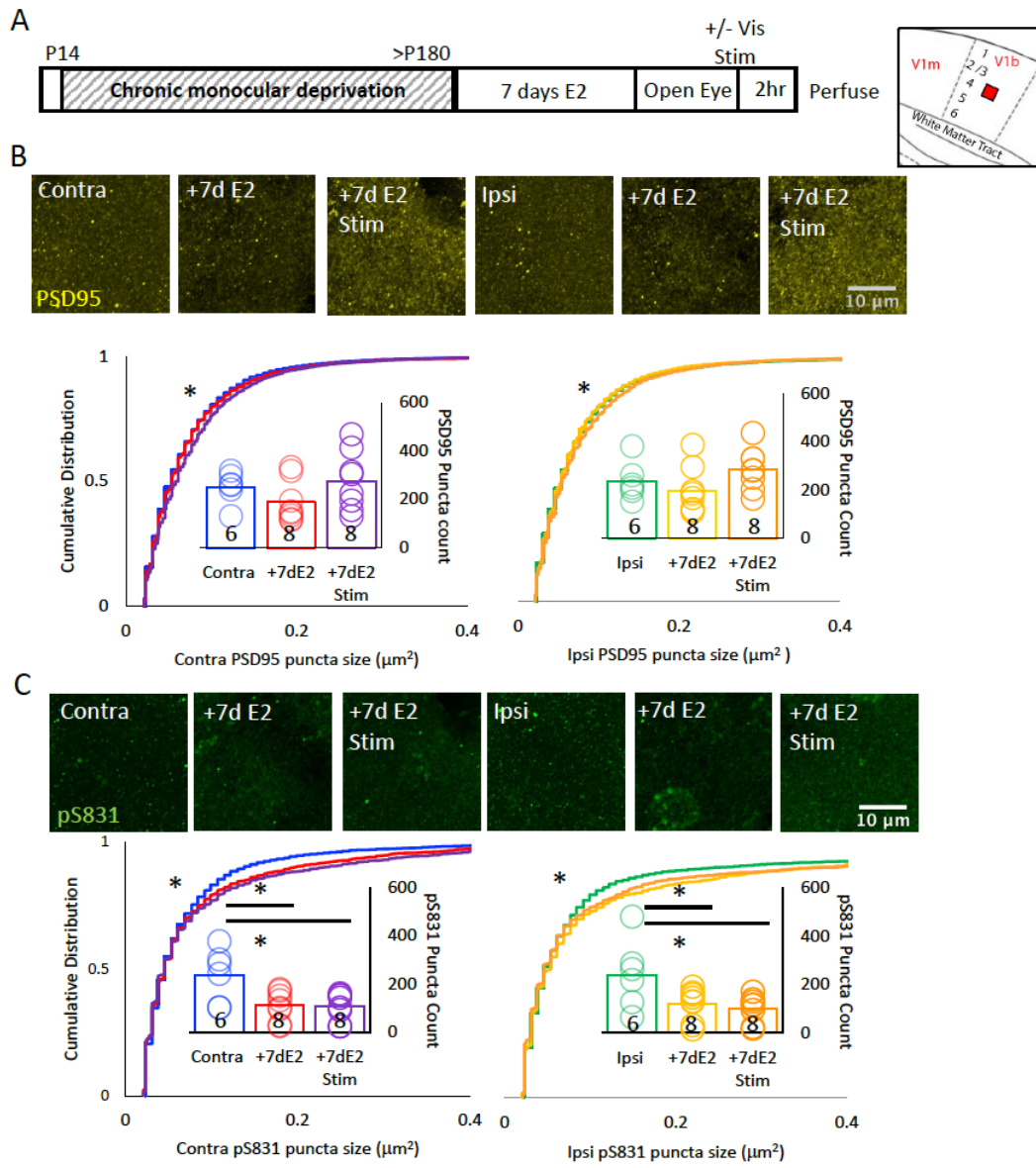


Figure 18. 7 days of 17 α E2 increases markers for excitatory synapses independent of pS831

A. Experimental timeline. Subjects receive monocular deprivation from eye opening (~P14) to adulthood (>P180) and 7 days receive 17 α E2 (15 μ g/kg, s.c., 1x/day for 7 days) and visual stimulus (200 phase reversal of high contrast grating at a single orientation) following last day of 17 α E2 treatment. **B.** Top: Fluorescent micrographs of PSD95 immunoreactivity (yellow) in V1b contralateral (left) and ipsilateral (right) to cMD and following 7 days of 17 α E2 and 7 days of 17 α E2 followed by visual stimulation, (ML: 4mm AP: -6.72 mm DV: 1.5mm; ~500 μ m from surface; ROI: 28.34 μ m x 28.34 μ m x 40 μ m, 100x mag with 3x digital zoom; MIP). Bottom: Cumulative distribution of PSD95 immunoreactive puncta size (yellow) reveals significant increase in V1b contralateral (left) and ipsilateral (right) to the occluded eye following both 7 days of 17 α E2 and 7 days of 17 α E2 with visual stimulus, $^*p < 0.05$, K-S Test, n=6, 8, 8, respectively. **C.** Top: Fluorescent micrographs of pS831 immunoreactivity (green) in V1b contralateral (left) and ipsilateral (right) to cMD and after 7 days of 17 α E2 and 7 days of 17 α E2 followed by visual stimulation, (V1; ML: 4mm AP: -6.72 mm DV: 1.5mm; ~500 μ m from surface; ROI: 28.34 μ m x 28.34 μ m x 40 μ m, 100x mag with 3x digital zoom; MIP). Bottom: Cumulative distribution of pS831 immunoreactive puncta reveals significant increase in size V1b contralateral (left) and ipsilateral (right) to the cMD eye following both 7 days of 17 α E2 and 7 days of 17 α E2 with visual stimulus, $^*p < 0.001$, K-S Test. pS831 puncta count is significantly reduced following both 7 days 17 α E2 paradigms in V1b contralateral (left) and ipsilateral (right) to the occluded eye. Contralateral V1b one-way ANOVA, $F(df,21)=6.04$, $p=0.009$, $^*p < 0.05$, Tukey-Kramer post hoc; Ipsilateral V1b: one-way ANOVA, $F(df,21)=4.62$, $p=0.02$, $^*p < 0.05$, Tukey-Kramer post hoc, n=6, 8, 8, respectively.

Table 11: pS831 size / number following 7d 17αE2			
pS831 Puncta Size	Average+/- SEM	n	P value
Contra cMD	0.073±0.002 μm ²	6	KS test
Contra 7d 17αE2	0.097±0.01μm ²	8	*=p<0.001 v. Contra MD
Contra 7d 17αE2 Stim	0.074±0.002μm ²	8	*=p<0.001 v. Contra MD
Ipsi cMD	0.069±0.005 μm ²	6	KS test
Ipsi 7d 17αE2	0.097±0.01μm ²	8	*p<0.001 v. Ipsi MD
Ipsi 7d 17αE2 Stim	0.072±0.003μm ²	8	*p<0.001 v. Ipsi MD
pS831 Puncta #	Average+/- SEM	n	P value
Contra cMD	234.74±49.94	6	one-way ANOVA, F(df,21)=6.04, p=0.009
Contra 7d 17αE2	110.53±22.39	8	*=p<0.05 TK post hoc
Contra 7d 17αE2 Stim	106.60±21.36	8	*=p<0.05 TK post hoc
Ipsi cMD	240.40±64.77	6	one-way ANOVA, F(df,21)=4.62, p=0.02
Ipsi 7d 17αE2	120.89±24.13	8	*=p<0.05 TK post hoc
Ipsi 7d 17αE2 Stim	100.66±20.59	8	*=p<0.05TK post hoc

3.4.11 7 days of 17 α E2 administration downregulates markers for excitatory presynaptic terminals

To examine how prolonged 17 α E2 treatment, with and without visual stimulus, impacts the presynaptic innervation of deprived cMD V1b, I examined the size and number of VGlut1 and VGlut2 immunoreactive puncta. Prolonged 17 α E2 treatment induced a significant decrease in the size of VGlut1 and VGlut2 immunoreactive puncta in V1b contralateral and ipsilateral to the occluded eye, similar to a single dose of 17 α E2 (Table 12, Fig 19B; Table 13, Fig 19C, respectively). VGlut2 number was reduced in both hemispheres following 7 days 17 α E2 +/- visual stimulation (Table 13, Fig.19C), and VGlut1 number was reduced in both hemispheres only in response to 7 day 17 α E2 with visual stimulus (Table 12, Fig.19B). Again, the increase in postsynaptic size (PSD95 puncta size) induced by 7 days of 17 α E2 in the aged V1 is not matched by an increase in the size of the presynaptic component of the synapse.

Table 12: VGlut1 size / number following 7d 17αE2			
VGlut1 Puncta Size	Average+/- SEM	n	P value
Contra cMD	0.17±0.02μm ² vs.	6	KS test
Contra 7d 17αE2	0.138±0.02μm ²	4	*=p<0.001 v. Contra MD
Contra 7d 17αE2 Stim	0.096±0.04μm ²	4	*=p<0.001 v. Contra MD
Ipsi cMD	0.17±0.02μm ²	6	KS test
Ipsi 7d 17αE2	0.13±0.02μm ²	4	*p<0.001 v. Ipsi MD
Ipsi 7d 17αE2 Stim	0.10±0.006μm ²	4	*p<0.001 v. Ipsi MD
VGlut1 Puncta #	Average+/- SEM	n	P value
Contra cMD	348.00±31.03	6	one-way ANOVA, F(df,13)=6.49, p=0.01
Contra 7d 17αE2	256.92±63.72	4	NS, p>0.05
Contra 7d 17αE2 Stim	176.17±8.23	4	*=p<0.05 TK post hoc
Ipsi cMD	376.89±28.74	6	one-way ANOVA, F(df,13)=5.62, p=0.02
Ipsi 7d 17αE2	271.33±74.77	4	NS, p>0.05
Ipsi 7d 17αE2 Stim	206.25±12.18	4	*=p<0.05 TK post hoc

Table 13: VGlut2 size / number following 7d 17αE2			
VGlut2 Puncta Size	Average+/- SEM	n	P value
Contra cMD	0.18±0.01 μm ²	6	KS test
Contra 7d 17αE2	0.136±0.01μm ² ,	8	*=p<0.001 v. Contra MD
Contra 7d 17αE2 Stim	0.135±0.02μm ²	8	*=p<0.001 v. Contra MD
Ipsi cMD	0.17±0.02 μm ²	6	KS test
Ipsi 7d 17αE2	0.145±0.01μm ²	8	*p<0.001 v. Ipsi MD
Ipsi 7d 17αE2 Stim	0.15±0.01μm ²	8	*p<0.001 v. Ipsi MD
VGlut2 Puncta #	Average+/- SEM	n	P value
Contra cMD	373.69±26.56	6	one-way ANOVA, F(df,20)=5.07, p=0.02
Contra 7d 17αE2	161.77±13.55	8	*=p<0.05 TK post hoc
Contra 7d 17αE2 Stim	129.26±10.03	8	*=p<0.05 TK post hoc
Ipsi cMD	287.69±49.28	6	one-way ANOVA, F(df,20)=8.27, p=0.002
Ipsi 7d 17αE2	174.06±14.15	8	*=p<0.01 TK post hoc
Ipsi 7d 17αE2 Stim	140.48±18.25	8	*=p<0.01 TK post hoc

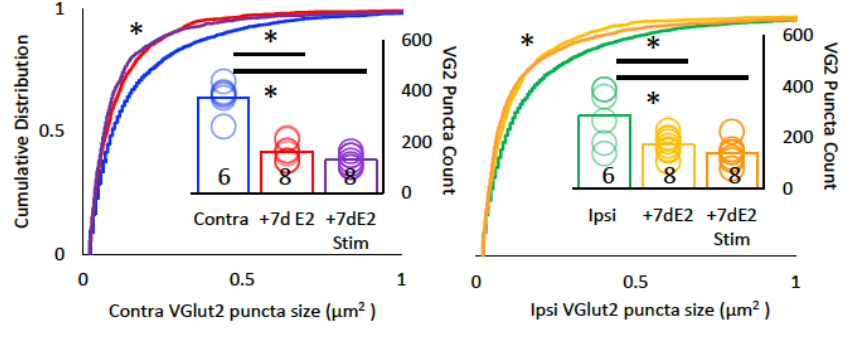
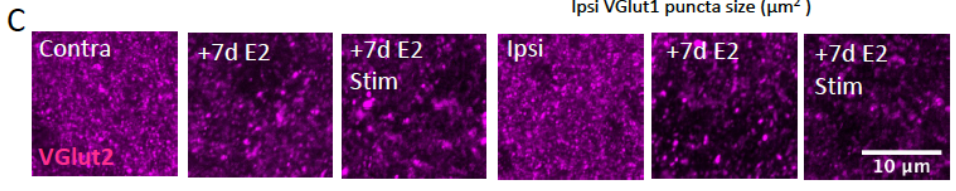
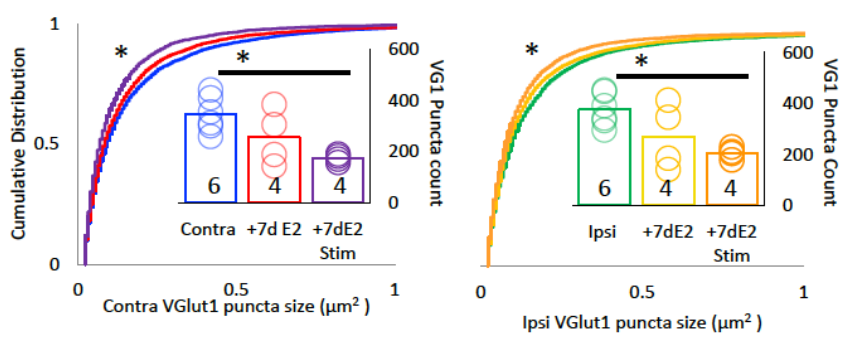
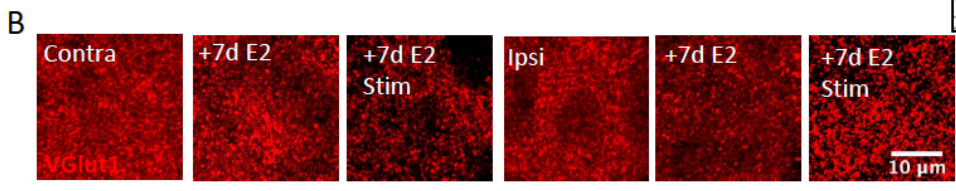


Figure 19. 7 days of 17 α E2 decreases markers for cortico-cortical and thalamocortical synapses

A. Left: Experimental timeline. Subjects receive cMD and 17 α E2 (15 μ g/kg, s.c., 1x/day for 7 days) +/- visual stimulus (200 phase reversal of high contrast grating at a single orientation) following last day of 17 α E2 treatment. Right: Fluorescent micrograph ROI in Layer 4 of V1b (red box). **B.** Top: Fluorescent micrographs of VGlut1 immunoreactivity (red) in V1b contralateral (left) and ipsilateral (right) to cMD and following 7 days of 17 α E2 and 7 days of 17 α E2 followed by visual stimulation, (ML: 4mm AP: -6.72 mm DV: 1.5mm; ~500 μ m from surface; ROI: 28.34 μ m x 28.34 μ m x 40 μ m, 100x mag with 3x digital zoom; MIP). Bottom: Cumulative distribution of VGlut1 immunoreactive puncta size (red) reveals significant increase in V1b contralateral (left) and ipsilateral (right) to the occluded eye following both 7 days of 17 α E2 +/- visual stimulation, $*=p<0.01$, K-S Test. VGlut1 puncta count is significantly reduced following 7 days 17 α E2 and visual stimulus in V1b contralateral (left) and ipsilateral (right) to the occluded eye. Contralateral V1b: one-way ANOVA, $F(df,13)=6.49$, $p=0.01$, $*=p<0.05$, T-K post hoc; Ipsilateral V1b: one-way ANOVA, $F(df,13)=5.62$, $p=0.02$, $*=p<0.05$, T-K post hoc, $n=6, 4, 4$, respectively. **C.** Top: Fluorescent micrographs of VGlut2 immunoreactivity (magenta) in V1b contralateral (left) and ipsilateral (right) to cMD and after 7 days of 17 α E2 +/- visual stimulation, (V1; ML: 4mm AP: -6.72 mm DV: 1.5mm; ~500 μ m from surface; ROI: 28.34 μ m x 28.34 μ m x 40 μ m, 100x mag with 3x digital zoom; MIP). Bottom: Cumulative distribution of VGlut2 immunoreactive puncta reveals significant decrease in V1b contralateral (left) and ipsilateral (right) to cMD eye following both 7 days of 17 α E2 +/- visual stimulation, $*=p<0.001$, K-S Test. VGlut2 puncta count is significantly reduced following both 7 days 17 α E2 paradigms in V1b contralateral (left) and ipsilateral (right) to the occluded eye. Contralateral V1b: one-way ANOVA, $F(df,20)=5.07$, $p=0.02$, $*=p<0.05$, T-K post hoc; Ipsilateral V1b: $F(df,20)=8.27$, $p=0.002$, $*=p<0.01$, T-K post hoc, $n=6, 8, 8$, respectively.

3.4.12 7 days of 17 α E2 increases colocalization of synaptic markers

To ask if prolonged 17 α E2 treatment impacted the co-localization of the markers employed to track per- and postsynaptic specializations, I performed PCC analysis for marker pairs. The PCC analysis revealed an increase in PSD95 colocalization with VGlut1 (cortico-cortical marker) in V1b contralateral and ipsilateral to the deprived eye after 7 days of 17 α E2 with and without visual stimulus (Table 14, Fig.20A). Interestingly, the colocalization of pS831 with VGlut1 and VGlut2 also increased in V1b contralateral and ipsilateral to deprived eye after 7 days of 17 α E2 with and without visual stimulus (Table 14, Fig.20B, Fig.21B, respectively). However, PSD95 colocalization with VGlut2 and pS831 colocalization was unchanged in both hemispheres of V1b (Table 13, Fig 21A).

This analysis makes the important point that the smaller VGlut puncta continue to co-localize with post-synaptic markers, suggesting that the markers are tracking competent synapses.

Table 14: Colocalization of synaptic markers following 7d 17αE2			
PSD95-VGlut1 Coloc.	Average+/- SEM	n	P value
Contra cMD	0.57 \pm 0.04	6	one-way ANOVA, F(df,17)=18.67, p<0.001
Contra 7d 17 α E2	0.77 \pm 0.01	6	*=p<0.01 TK post hoc
Contra 7d 17 α E2 Stim	0.79 \pm 0.02	6	*=p<0.01 TK post hoc
Ipsi cMD	0.58 \pm 0.03	6	one-way ANOVA, F(df,17)=16.85, p<0.001
Ipsi 7d 17 α E2	0.73 \pm 0.02	6	*=p<0.01 TK post hoc
Ipsi 7d 17 α E2 Stim	0.77 \pm 0.02	6	*=p<0.01 TK post hoc
pS831-VGlut1 Coloc.	Average+/- SEM	n	P value
Contra cMD	0.42 \pm 0.05	6	one-way ANOVA, F(df,17)=9.86, p=0.002
Contra 7d 17 α E2	0.65 \pm 0.05	6	*=p<0.01 TK post hoc
Contra 7d 17 α E2 Stim	0.70 \pm 0.04	6	*=p<0.01 TK post hoc

Ipsi cMD	0.45±0.03	6	one-way ANOVA, F(df,17)=7.30, p=0.006
Ipsi 7d 17αE2	0.58±0.07	6	*=p<0.01 TK post hoc
Ipsi 7d 17αE2 Stim	0.70±0.04	6	*=p<0.01 TK post hoc
PSD95-VGlut2 Coloc.	Average+/- SEM	n	P value
Contra cMD	0.45±0.03	4	one-way ANOVA, F(df,13)=0.64, p=0.54
Contra 7d 17αE2	0.41±0.01	4	NS, p>0.05
Contra 7d 17αE2 Stim	0.47±0.05	4	NS, p>0.05
Ipsi cMD	0.45±0.02	6	one-way ANOVA, F(df,13)=0.59, p=0.57
Ipsi 7d 17αE2	0.46±0.02	4	NS, p>0.05
Ipsi 7d 17αE2 Stim	0.48±0.03	4	NS, p>0.05
pS831-VGlut2 Coloc.	Average+/- SEM	n	P value
Contra cMD	0.37±0.03	6	one-way ANOVA, F(df,17)=23.86, p<0.001
Contra 7d 17αE2	0.56±0.01	4	*=p<0.01 TK post hoc
Contra 7d 17αE2 Stim	0.60±0.02	4	*=p<0.01 TK post hoc
Ipsi cMD	0.38±0.03	6	one-way ANOVA, F(df,17)=26.51, p<0.0001
Ipsi 7d 17αE2	0.59±0.01	4	*=p<0.01 TK post hoc

Ipsi 7d 17 α E2 Stim	0.60 \pm 0.03	4	*=p<0.01 TK post hoc
pS831-PSD95 Coloc.	Average\pm SEM	n	P value
Contra cMD	0.48 \pm 0.02	6	one-way ANOVA, F(df,13)=0.28, p=0.76
Contra 7d 17 α E2	0.45 \pm 0.01	4	NS, p>0.05
Contra 7d 17 α E2 Stim	0.46 \pm 0.05	4	NS, p>0.05
Ipsi cMD	0.50 \pm 0.02	6	one-way ANOVA, F(df,13)=0.38, p=0.69
Ipsi 7d 17 α E2	0.49 \pm 0.03	4	NS, p>0.05
Ipsi 7d 17 α E2 Stim	0.47 \pm 0.05	4	NS, p>0.05

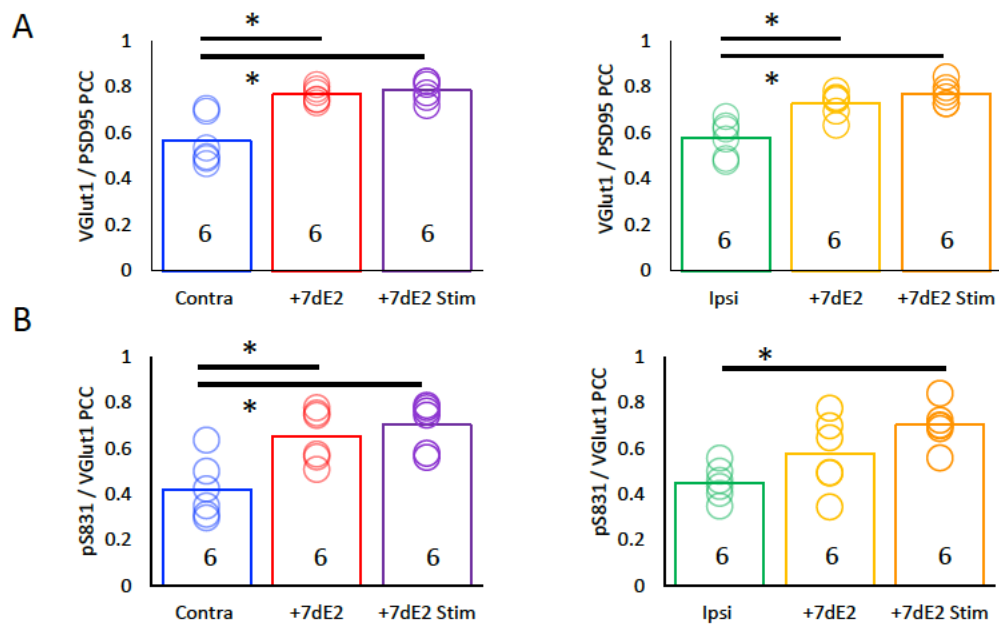


Figure 20. Colocalization of cortico-cortical marker increased following 7 days of 17 α E2

A. VGlut1-PSD95 Pearson's Correlation Coefficient (PCC) in cMD V1b is significantly increased following both 7 days 17 α E2 paradigms in V1b contralateral (left) and ipsilateral (right) to the occluded eye. Contralateral V1b: one-way ANOVA, $F(df,17)=18.67$, $p<0.001$, $*=p<0.01$ Tukey-Kramer post hoc; Ipsilateral V1b: one-way ANOVA, $F(df,17)=16.85$, $p<0.001$, $*=p<0.01$ Tukey-Kramer post hoc, $n=6$. **B.** VGlut1-pS831 PCC in contralateral cMD V1b is significantly increased following 7 days 17 α E2 +/- visual, but only increased significantly after 7 days 17 α E2 followed by visual stimulation in ipsilateral cMD V1b. Contralateral V1b: one-way ANOVA, $F(df,17)=9.86$, $p=0.002$, $*=p<0.01$ Tukey-Kramer post hoc ; Ipsilateral V1b: one-way ANOVA, $F(df,17)=7.30$, $p=0.006$, $*=p<0.01$ Tukey-Kramer post hoc, $n=6$.

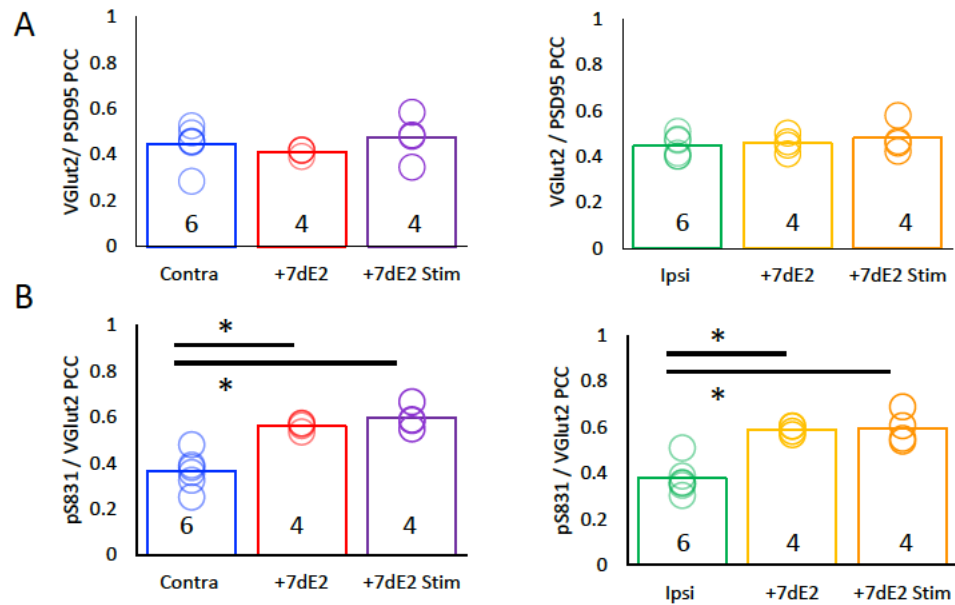


Figure 21. Colocalization of thalamocortical marker with pS831 increased following 7 days of 17 α E2

A. No change in VGlut2-PSD95 Pearson's Correlation Coefficient (PCC) in cMD V1b following either paradigm in contralateral and ipsilateral hemispheres, n= 6, 4, 4, respectively. **B.** VGlut2-pS831 PCC is significantly increased in both hemispheres of cMD V1b following both paradigms. Contralateral V1b: one-way ANOVA, F(df,17)=23.86, p<0.001, *=p<0.01 Tukey-Kramer post hoc; Ipsilateral V1b: one-way ANOVA, F(df,17)=26.51, p<0.0001, *=p<0.01 Tukey-Kramer post hoc , n= 6, 4, 4, respectively.

3.4.13 Assessing the effect of 17 α E2 administration on Stimulus-Selective Response Potentiation

One way to assess the functional impact of the 17 α E2-induced changes in V1 of cMD subjects is to probe the response to repetitive visual stimulation (Sam F Cooke & Bear, 2010; Furmanski et al., 2004; Teyler et al., 2005). Repeated presentation of a visual stimuli has been shown in humans and other species to induce a potentiation of the amplitude of the physiologically recorded visual response. In fact, so called "photic LTP" induced by repetitive flash stimulation to rats was sufficient to induce rapid (15 minutes after onset of stimulus)

potentiation of visually-evoked potentials (VEPs) that was comparable to theta burst stimulation applied directly to the LGN (Heynen & Bear, 2001). Repetitive visual stimulation (400 cycles / day of 0.05 cycles per degree (cpd), 100% contrast, full field gratings at 0.5 Hz) has also been shown to induce a slowly emerging, long-lasting, stimulus-specific response potentiation (SRP) of the V1 VEP (Sam F Cooke & Bear, 2010; Frenkel et al., 2006). Importantly, SRP induction requires hundreds of repetitions of the visual stimulus, and the response potentiation is highly stimulus-selective, therefore observed in response to the familiar stimulus. Importantly, fewer presentations of the visual stimulus (100-200 cycles) do not induce this form of VEP potentiation, but manipulations that enhance plasticity in adult V1, such as dark exposure, promote SRP in response to this subthreshold induction protocol (Montey et al., 2013).

Therefore, to ask if 17 α E2 promotes SRP in V1, I presented the subthreshold visual stimulus binocularly (200 x 1 second trials of square-wave gratings (0.05 cpd, 100% contrast, full-field 45 degree gratings reversing at 1 Hz)). 24 hours later we measured the amplitude of visually-evoked potentials recorded from Layer 4 (~ 500 microns from the dura surface) of anesthetized (2.5% isoflurane in 100% O₂) subjects in response to the familiar and a novel visual stimulus. As expected, in control subjects, the visual stimulation protocol did not induce SRP, as the VEP amplitude was similar in response to the familiar and novel stimuli presented to either the previously deprived or previously non-

deprived eye (μV , $\text{AVG}\pm\text{SEM}$; non-deprived eye; familiar: 22.37 ± 1.28 , novel: 22.71 ± 2.55 , $n=4$; deprived; familiar: 21.65 ± 3.59 , novel: 19.99 ± 3.359 , $n=4$, Fig. 22B&C). However, $17\alpha\text{E}2$ treatment prior to visual stimulation resulted in a significant SRP in the VEP evoked from the non-deprived eye, as VEP amplitudes were significantly increased in response to the familiar but not novel stimulus (μV , $\text{AVG}\pm\text{SEM}$; familiar: 36.10 ± 6.38 , novel: 27.11 ± 4.93 , $n=6$ subjects, two-tailed paired t-test, $p = 0.024$, $t=2.570$, Fig. 22C). No SRP was observed in the amplitude of the VEP evoked from the previously deprived eye (μV , $\text{AVG}\pm\text{SEM}$; familiar: 25.56 ± 4.49 , novel: 29.154 ± 3.80 , $n=6$ subjects, Fig. 22C). Together this demonstrates that experience-dependent plasticity can be enhanced by $17\alpha\text{E}2$ in amblyopic V1, but the enhancement is specific to the intact / non-deprived pathway.

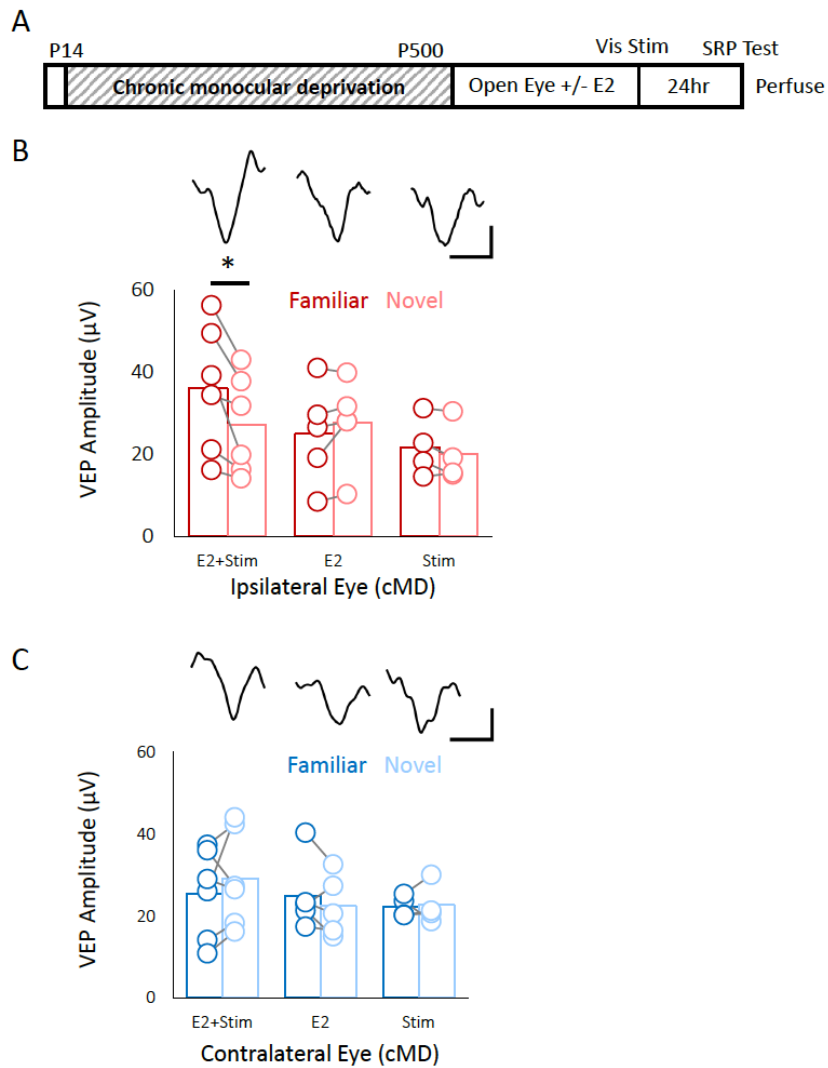


Figure 22. 17 α E2 promotes SRP specifically in non-deprived eye responses
A. Experimental timeline. Subjects receive monocular deprivation from eye opening (~P14) to adulthood (>P180) and receive 17 α E2 (15 μ g/kg, s.c.) 30 minutes prior to eye opening and binocular visual stimulation (200 phase reversal of high contrast grating at a single orientation). VEPs in response to flash, and familiar and novel stimulus orientations are assessed after 24 hours. **B.** Increase in average VEP amplitude in response to familiar (dark red) versus novel (light red) stimuli presented to ipsilateral eye following 17 α E2 treatment. Inset: representative VEP waveforms in response to the familiar stimulus, scale 0.1s, 10 μ V. * p <0.05, two-way paired t-test, 17 α E2+Stim n =6, 17 α E2 n =5, Stim n =4. **C.** No increase in average VEP amplitude in response to familiar (dark blue) stimulus presented to contralateral eye following 17 α E2 treatment. Inset: Representative VEP waveforms in response to the familiar stimuli (above), scale 0.1s, 10 μ V, 17 α E2+Stim n =6, 17 α E2 n =5, Stim n =4.

3.4.14. Markers for constrained plasticity are differentially regulated following 17 α E2 administration and SRP stimulation protocol

Unfortunately, the SRP experiment does not provide an additional timepoint (24 hours post 17 α E2 delivery) to my investigation of the regulation of plasticity by 17 α E2, as all of the subjects in this cohort received visual stimulation to record visually evoked potentials. However, this allows me to ask how the SRP-inducing visual stimulation impacts cortical markers for plasticity and synapses. 24 hours after 17 α E2 and visual stimulus, I observed a significant increase in the expression of PV and a significant decrease in WFA in both hemispheres (AVG \pm SEM; PV: Contra cMD 26.18 \pm 2.67 vs. Contra 17 α E2 24hr 42.23 \pm 4.38, p <0.001; vs. Contra 17 α E2 24hr Stim 42.70 \pm 3.00, p <0.001; Ipsi cMD 25.59 \pm 1.42 vs. Ipsi 17 α E2 24hr 48.38 \pm 6.32, p <0.001; vs. Ipsi 17 α E2 24hr Stim 37.90 \pm 2.07; WFA: Contra cMD 16.63 \pm 2.08 vs. Contra 17 α E2 24hr 10.70 \pm 1.77, p <0.001; vs. Contra 17 α E2 24hr Stim 12.13 \pm 1.51, p <0.001; Ipsi cMD 18.23 \pm 2.79 vs. Ipsi 17 α E2 24hr 11.83 \pm 2.15; \ast = p <0.001, vs. Ipsi 17 α E2 24hr Stim 10.38 \pm 1.03; p <0.001, K-S Test, n =6, 5, 6, respectively, Fig.23C). This is an interesting result, consistent with the observation that PV activity is necessary for the induction of SRP (Kaplan et al., 2016), as 17 α E2 followed by visual stimulus induces an early decrease in both PV expression and WFA staining (Figure 16).

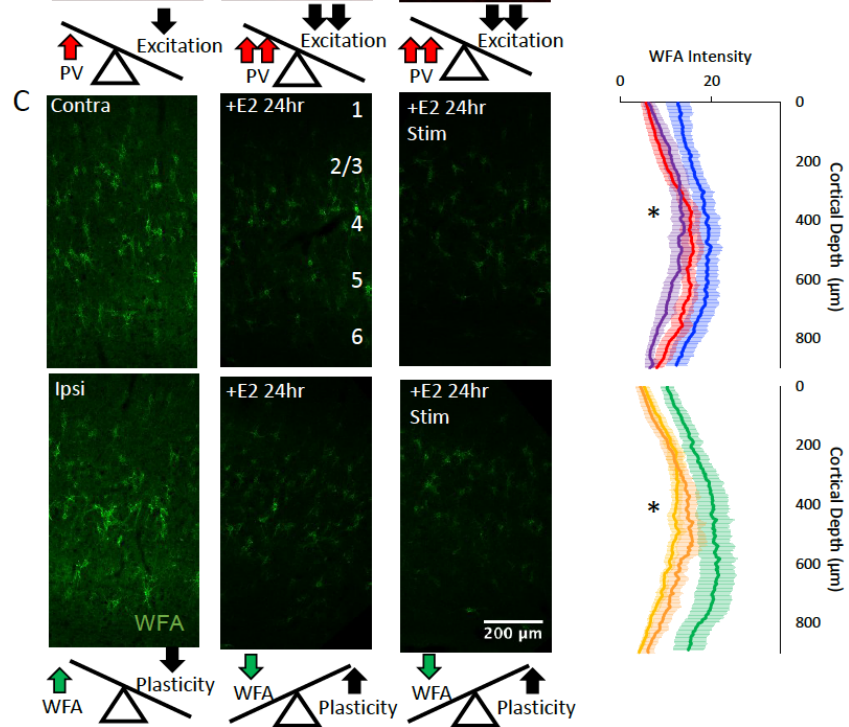
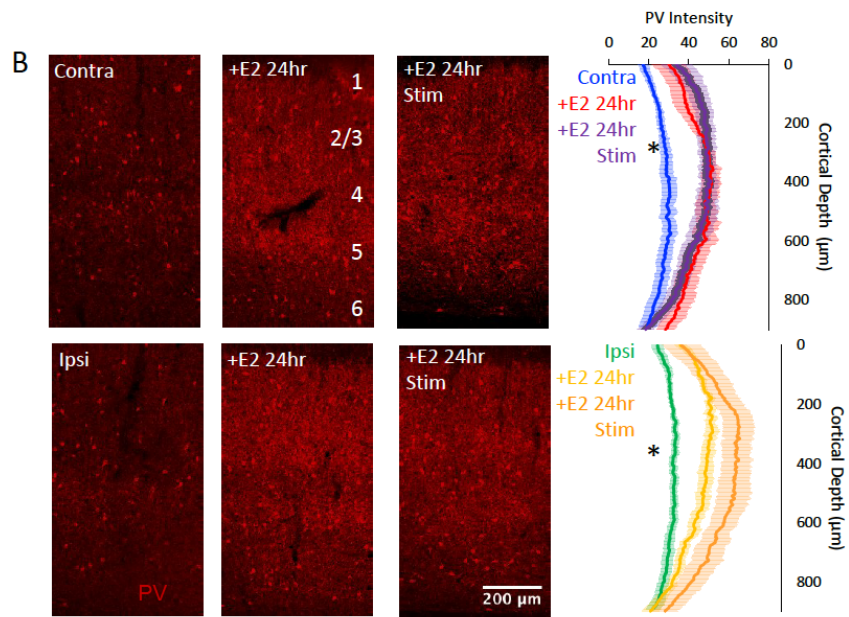


Figure 23: 17 α E2 before SRP protocol reduces PV and WFA staining in cMD V1b

A. Experimental timeline. Subjects receive cMD and 17 α E2 (15 μ g/kg, s.c.) 30 minutes prior to eye opening, a subset received binocular visual stimulation (200 phase reversal of high contrast grating at a single orientation). VEPs in response to flash, and familiar and novel stimulus orientations are assessed after 24 hours. **B.** Top Left: Fluorescent micrographs of PV distribution in V1b (red, V1; ML: 4 mm AP: -6.72 mm DV: 1.5mm; ROI: 900 μ m x 500 μ m; 10x mag; MIP). Bottom Left: Graphic representations of impact of PV expression on pyramidal neuron excitability. Right: 17 α E2 with or without visual stimulus and followed by the SRP protocol 24 hours later significantly increases PV intensity in V1b contralateral and ipsilateral to cMD, $*=p<0.001$, K-S Test, $n=6, 5, 6$, respectively. **C.** Top Left: Fluorescent micrographs of WFA distribution in V1b (green, V1; ML: 4mm AP: -6.72 mm DV: 1.5mm; ROI: 900 μ m x 500 μ m; 10x mag; MIP). Bottom Left: Graphic representation of impact of WFA expression on plasticity. Right: : 17 α E2 with or without visual stimulus and followed by the SRP protocol 24 hours later significantly decreases WFA intensity in V1b contralateral and ipsilateral to cMD, $*=p<0.001$, K-S Test, $n=6, 5, 6$.

3.4.15. 17 α E2 administration followed by SRP stimulation protocol increases markers for excitatory synapses

As expected, 24 hours after 17 α E2 plus visual stimulation, I observed a significant increase in the size and number of PSD95 and pS831 immunoreactive puncta (Table 15-16, Fig.24) in V1b contralateral and ipsilateral to the occluded eye (Table 15-16, Fig.24) as well as an increase in the size, but not number, of VGlut2 puncta (Table 17, Fig.25B). It is tempting to speculate that the increase in PSD95, pS831, and VGlut2 represent the stimulus-selective response potentiation of synapses serving the non-deprived eye.

Table 15: PSD95 size / number following 17αE2 24hrs			
PSD95 Puncta Size	Average+/- SEM	n	P value
Contra cMD	0.080±0.01 μm ²	6	KS test
Contra 17αE2 24hr	0.111±0.009 μm ²	5	*=p<0.001 v. Contra MD
Contra 17αE2 24hr Stim	0.136±0.008 μm ²	6	*=p<0.001 v. Contra MD
Ipsi cMD	0.078±0.01 μm ²	6	KS test
Ipsi 17αE2 24h	0.0121±0.008 μm ²	5	*p<0.001 v. Ipsi MD
Ipsi 17αE2 24hr Stim	0.133±0.008 μm ²	6	*p<0.001 v. Ipsi MD
PSD95 Puncta #	Average+/- SEM	n	P value
Contra cMD	250.97±29.30	6	one-way ANOVA, F(df,16) =8.05, p=0.005,
Contra 17αE2 24hr	381.58±48.68	5	*=p<0.01 TK post hoc
Contra 17αE2 24hr Stim	473.85±53.43	6	*=p<0.01 TK post hoc
Ipsi cMD	235.60±35.44	6	one-way ANOVA, F(df,16) =1.81 p=0.199
Ipsi 17αE2 24h	341.43±51.72	5	NS, p>0.05
Ipsi 17αE2 24hr Stim	313.49±47.76	6	NS, p>0.05

Table 16: pS831 size / number following 17αE2 24hrs			
pS831 Puncta Size	Average+/- SEM	n	P value
Contra cMD	0.073±0.002 μm ²	6	KS test
Contra 17αE2 24hr	0.109±0.004μm ²	5	*=p<0.001 v. Contra MD
Contra 17αE2 24hr Stim	0.145±0.04μm ²	6	*=p<0.001 v. Contra MD
Ipsi cMD	0.069±0.005 μm ²	6	KS test
Ipsi 17αE2 24h	0.070±0.003 μm ²	5	*p<0.001 v. Ipsi MD
Ipsi 17αE2 24hr Stim	0.101±0.004 μm ²	6	*p<0.001 v. Ipsi MD
pS831 Puncta #	Average+/- SEM	n	P value
Contra cMD	234.74±49.94	6	one-way ANOVA, F(df,16) =19.66, p<0.0001
Contra 17αE2 24hr	725.62±71.32	5	*=p<0.01 TK post hoc
Contra 17αE2 24hr Stim	650.92±75.28	6	*=p<0.01 TK post hoc
Ipsi cMD	240.40±64.77	6	one-way ANOVA, F(df,16) =17.75, p=0.0001
Ipsi 17αE2 24h	494.73±75.72	5	*=p<0.01 TK post hoc
Ipsi 17αE2 24hr Stim	719.61±54.91	6	*=p<0.01 TK post hoc

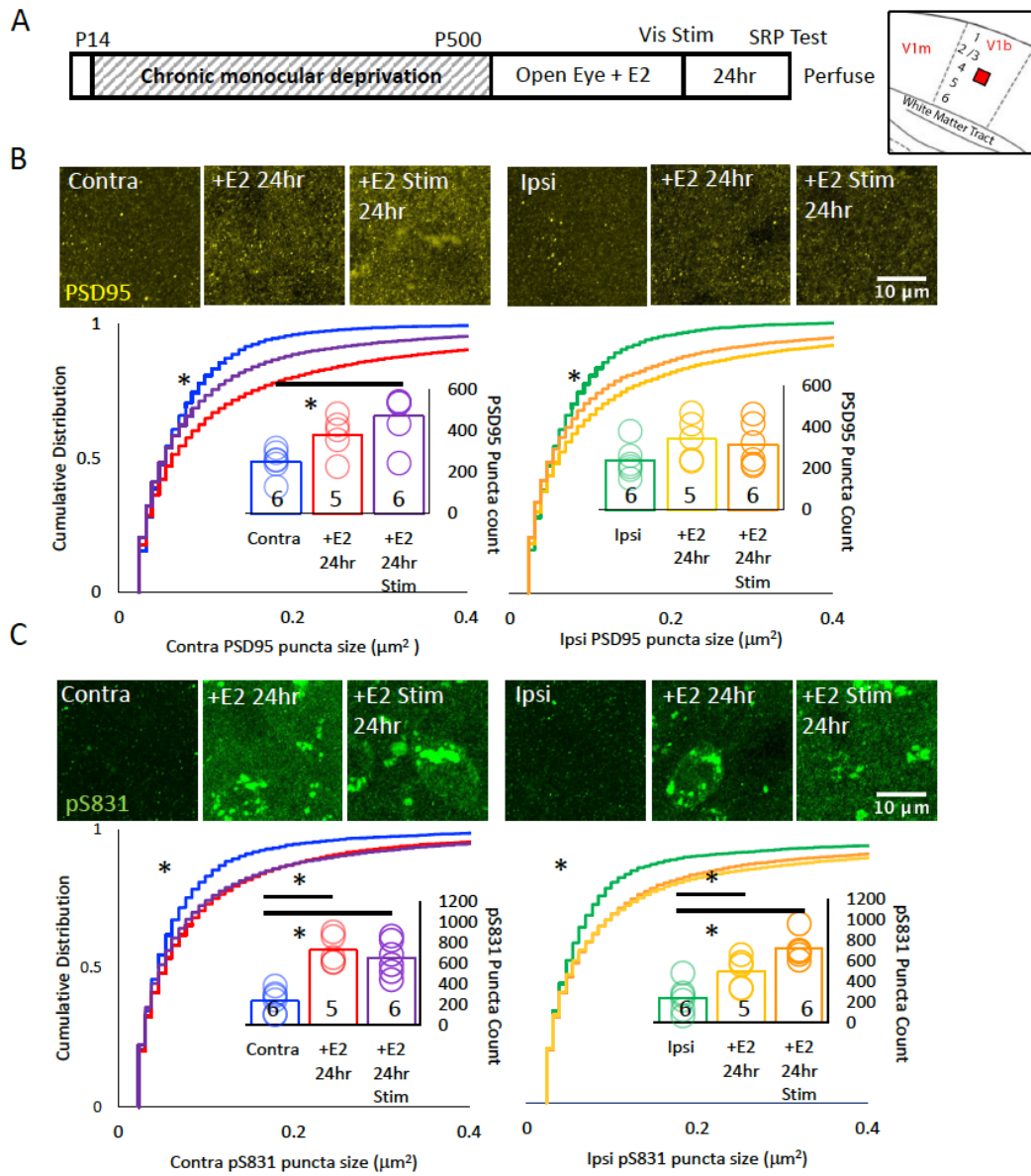


Figure 24. 17 α E2 prior to SRP protocol increases markers for excitatory synapses and activity

A. Left: Experimental timeline. Subjects receive cMD and then 17 α E2 (15 μ g/kg, s.c.) 30 minutes prior to eye opening, a subset received binocular visual stimulation (200 phase reversal of high contrast grating at a single orientation). VEPs in response to flash, and familiar and novel stimulus orientations are assessed after 24 hours. Right: Fluorescent micrograph ROI location in Layer 4 of V1b (red box). **B.** Top: Fluorescent micrographs of PSD95 immunoreactivity (yellow) in V1b contralateral (left) and ipsilateral (right) to the cMD eye and after 17 α E2 +/- visual stimulation and followed by the SRP protocol, (ML: 4mm AP: -6.72 mm DV: 1.5mm; ~500 μ m from surface; ROI: 28.34 μ m x 28.34 μ m x 40 μ m, 100x mag with 3x digital zoom; MIP). Bottom: Cumulative distribution of PSD95 immunoreactive puncta size (yellow) reveals significant increase in V1b contralateral (left) and ipsilateral (right) to the occluded eye with 17 α E2 +/- visual stimulation prior to the SRP protocol, \ast = p <0.001, K-S Test. PSD95 puncta number was significantly increased in V1b contralateral to the occluded eye in subjects that received 17 α E2 and visual stimulus prior to SRP assessment; one-way ANOVA, F (df,16)=8.05, p =0.005, \ast = p <0.01 T-K post hoc, n =6, 5, 6, respectively. **C.** Top: Fluorescent micrographs of pS831 immunoreactivity (green) in V1b contralateral (left) and ipsilateral (right) to the cMD eye and after 17 α E2 +/- visual stimulation and followed by the SRP protocol, (V1; ML: 4mm AP: -6.72 mm DV: 1.5mm; ~500 μ m from surface; ROI: 28.34 μ m x 28.34 μ m x 40 μ m, 100x mag with 3x digital zoom; MIP). Bottom: Cumulative distribution of pS831 immunoreactive puncta reveals significant increase in size V1b contralateral (left) and ipsilateral (right) to the cMD eye following both 17 α E2 +/- visual stimulation prior to the SRP protocol, \ast = p <0.001, K-S Test. pS831 puncta count is significantly increased following both paradigms in V1b contralateral (left) and ipsilateral (right) to the occluded eye. Contralateral V1b: one-way ANOVA, F (df,16)=19.66, p <0.0001, \ast = p <0.01 T-K post hoc; Ipsilateral V1b: one-way ANOVA, F (df,16)=17.75, p =0.0001, \ast = p <0.05 T-K post hoc, n =6, 5, 6, respectively.

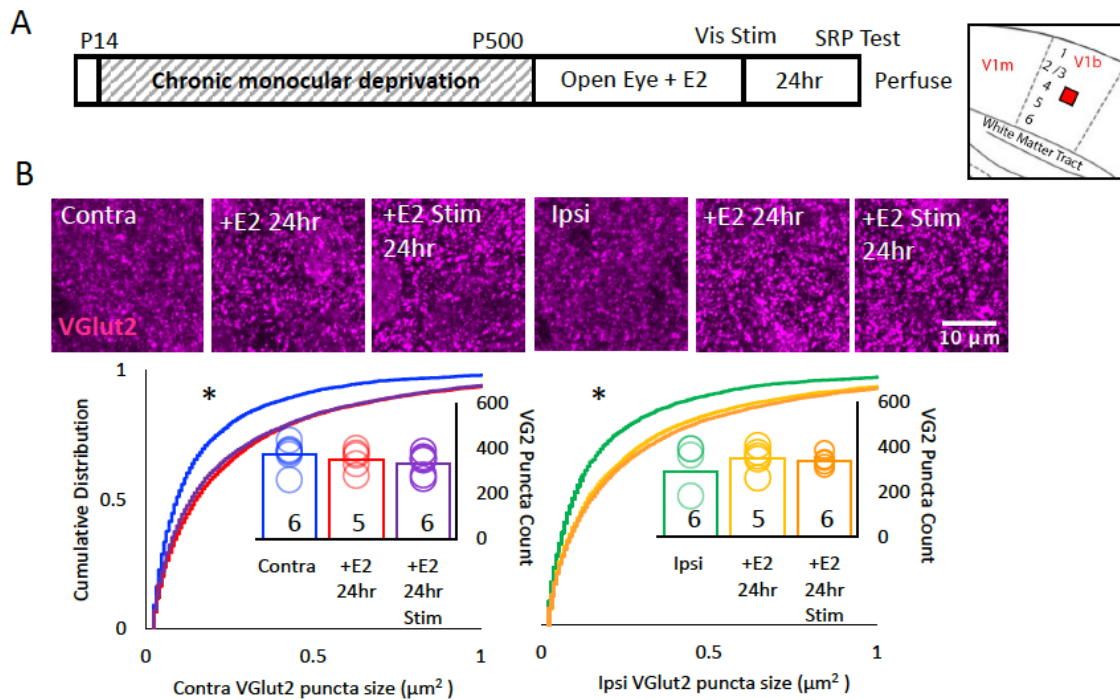


Figure 25. 17 α E2 before SRP protocol increases size of thalamocortical afferent markers

A. Left: Experimental timeline. Subjects receive monocular deprivation from eye opening (~P14) to adulthood (>P180) and 7 days receive 17 α E2 (15 μ g/kg, s.c., 1x/day for 7 days) and visual stimulus (200 phase reversal of high contrast grating at a single orientation) following last day of 17 α E2 treatment. Right: Fluorescent micrograph ROI location in Layer 4 of V1b (red box). **B.** Top: Fluorescent micrographs of VGlut2 immunoreactivity (magenta) in V1b contralateral (left) and ipsilateral (right) to the cMD eye and after 17 α E2 with or without visual stimulus and followed by the SRP protocol 24 hours later, (V1; ML: 4mm AP: -6.72 mm DV: 1.5mm; ~500 μ m from surface; ROI: 28.34 μ m x 28.34 μ m x 40 μ m, 100x mag with 3x digital zoom; MIP). Bottom: Cumulative distribution of VGlut2 immunoreactive puncta reveals significant increase in V1b contralateral (left) and ipsilateral (right) to the cMD eye following both 17 α E2 and 17 α E2 and visual stimulus prior to the SRP assessment protocol, $*=p<0.001$, K-S Test. VGlut2 puncta count is unchanged in V1b contralateral (left) and ipsilateral (right) to the occluded eye, $n=6, 5, 6$, respectively.

Table 17: VGlut2 size / number following 17αE2 24hrs			
VGlut2 Puncta Size	Average+/- SEM	n	P value
Contra cMD	18±0.01 μm ²	6	KS test
Contra 17αE2 24hr	0.13±0.01 μm ²	5	*=p<0.001 v. Contra MD
Contra 17αE2 24hr Stim	0.304±0.03μm ²	6	*=p<0.001 v. Contra MD
Ipsi cMD	0.17±0.02 μm ²	6	KS test
Ipsi 17αE2 24h	0.300±0.009μm ²	5	*p<0.001 v. Ipsi MD
Ipsi 17αE2 24hr Stim	0.300±0.009μm ²	6	*p<0.001 v. Ipsi MD
VGlut2 Puncta #	Average+/- SEM	n	P value
Contra cMD	373.69±26.56	6	one-way ANOVA, F(df,16) =0.86, p=0.44
Contra 17αE2 24hr	352.82±23.67	5	NS, p>0.05
Contra 17αE2 24hr Stim	334.24±21.33	6	NS, p>0.05
Ipsi cMD	287.69±49.28	6	one-way ANOVA, F(df,16) =1.11, p=0.35
Ipsi 17αE2 24h	348.17±27.00	5	NS, p>0.05
Ipsi 17αE2 24hr Stim	338.25±11.42	6	NS, p>0.05

Finally, 17 α E2 administration and subsequent SRP induction paradigm did not affect the colocalization between pre- and post-synaptic markers (Table 18).

Table 18: Colocalization of synaptic markers following size / number following 17αE2 24hrs			
PSD95-VGlut2 Coloc.	Average+/- SEM	n	P value
Contra cMD	0.45 \pm 0.03	6	one-way ANOVA, F(df,16) =0.85, p=0.44
Contra 17 α E2 24hrs	0.41 \pm 0.02	5	NS, p>0.05
Contra 17 α E2 24hrs Stim	0.47 \pm 0.04	6	NS, p>0.05
Ipsi cMD	0.45 \pm 0.02	6	one-way ANOVA, F(df,16) =3.04, p=0.08
Ipsi 17 α E2 24hrs	0.38 \pm 0.02	5	NS, p>0.05
Ipsi 17 α E2 24hrs Stim	0.47 \pm 0.03	6	NS, p>0.05
pS831-VGlut2 Coloc.	Average+/- SEM	n	P value
Contra cMD	0.37 \pm 0.03	6	one-way ANOVA, F(df,16) =1.08, p=0.36
Contra 17 α E2 24hrs	0.37 \pm 0.02	5	NS, p>0.05

Contra 17αE2 24hrs Stim	0.43±0.04	6	NS, p>0.05
Ipsi cMD	0.38±0.03	6	one-way ANOVA, F(df,16) =0.57, p=0.58
Ipsi 17αE2 24hrs	0.36±0.01	5	NS, p>0.05
Ipsi 17αE2 24hrs Stim	0.40±0.03	6	NS, p>0.05
pS831-PSD95 Coloc.	Average+/- SEM	n	P value
Contra cMD	0.48±0.02	6	one-way ANOVA, F(df,16) =0.29, p=0.75
Contra 17αE2 24hrs	0.44±0.02	5	NS, p>0.05
Contra 17αE2 24hrs Stim	0.47±0.05	6	NS, p>0.05
Ipsi cMD	0.50±0.02	6	one-way ANOVA, F(df,16) =1.49, p=0.25
Ipsi 17αE2 24hrs	0.43±0.02	5	NS, p>0.05
Ipsi 17αE2 24hrs Stim	0.40±0.03	6	NS, p>0.05

3.5 Discussion

ERs persist in the visual cortex of aged males and females, and therefore offer a potential opportunity for the use of estrogen to promote plasticity. Using fixed-tissue immunohistochemistry and electrophysiology I asked if estrogen, employed in either in a single, physiologically-relevant dose or a week-long course, can reverse the anatomical and functional deficits of cMD. I found that 17 α E2 treatment induces changes in the cortex that are indicative of enhanced plasticity in deprived and non-deprived V1, and these changes are amplified when 17 α E2 is followed by visual stimulation. Importantly, 17 α E2 treatment promoted plasticity in the amblyopic visual cortex, but stimulus-selective response potentiation was observed only in the pathway served by the deprived eye. This suggests that the selectivity of estrogen may be used to enhance receptive field plasticity at intact, non-injured synapses, such as those that surround a cortical infract or scotoma. Although the current experiments cannot distinguish between individual synapses that are dominated by input from the deprived versus non-deprived eye, one possibility is that increase in the excitatory synaptic markers that increase in size serve the non-deprived eye.

The presence of ERs in adult rodent V1 has been controversial (Jeong et al., 2011; Mitra et al., 2003; Shughrue & Merchenthaler, 2001), it was therefore important to first demonstrate the expression of ERs in rodent V1, identify the subtypes expressed and to ask if there are differences in the expression between intact males and females. I confirmed a heretofore uncorroborated report of

expression of both classical estrogen receptor subtypes in rodent visual cortex (Jeong et al., 2011), and demonstrated that these receptors do not co-localize with a nuclear marker. This is consistent with previous reports of extranuclear ERs in hippocampus (Milner et al., 2001; Milner et al., 2005), prefrontal cortex, and dorsal striatum (Almey et al., 2016), regions of the brain shown to express rapid, estrogen-dependent synaptic plasticity. $17\alpha\text{E}2$ enhancement of synaptic plasticity includes potentiation of synaptic responses, increases in spine density, or improvement of behavioral performance. Importantly, these effects of estrogen are observed rapidly, between 30 minutes to 2 hours (Kramár et al., 2013; Kramár et al., 2009; Luine et al., 2003; MacLusky et al., 2005), and locally activate kinase pathways at the synapse. Although synaptic signaling is distinct from transcriptional effects (Dominguez & Micevych, 2010; Lai et al., 2017; Srivastava et al., 2010), the two pathways may act cooperatively to express plasticity (Titolo et al., 2008). Most experiments detailed in this dissertation are performed on a similar timescale (~2.5 hours). However, I cannot rule out a transcriptional response, as transcriptional mechanisms can be engaged by 2 hours to engage after steroid hormone treatment (Marino et al., 2006).

Although the majority of estrogen replacement work examines the effect of 17β treatment, I chose to use the 17α isomer of estradiol. Previous electron microscopic examination of rat hippocampal CA1 revealed a significant increase in pyramidal neuron spiny synapses 30 minutes after peripheral administration of 17α $17\alpha\text{E}2$ treatment (MacLusky et al., 2005). 17α $17\alpha\text{E}2$ also increased

performance in novel object recognition tasks when $17\alpha\text{E}2$ was given during sample acquisition trials (Luine et al., 2003). In addition, 17α $17\alpha\text{E}2$ has been shown to induce less off-target effects, an observation that I confirmed by demonstrating no change in gonadal wet weight after a 7 day course of $17\alpha\text{E}2$. Since certain dosages and types of estrogens used in hormone therapy in humans have been shown to be oncogenic, I chose to use the isoform that had potentially lower risk (Dietel et al., 2005).

Many changes in synaptic, neuronal and circuit structure occur with age and contribute to reduced plasticity. A dense ECM and strong inhibition from PV+ and other interneurons subtypes has been repeatedly associated with aging and an environment that is not permissive for synaptic plasticity (Hensch et al., 1998; Lensjø et al., 2017). Indeed, the maturation of GABA-ergic inhibition has been shown to terminate the critical period for ocular dominance plasticity (Fagiolini & Hensch, 2000; Kuhlman et al., 2013). Furthermore, PNNs, robust ECM specializations which surround mature PV+ interneurons and are associated with enhanced excitability (Balmer, 2016), further restrict structural and functional plasticity (Ye & Miao, 2013). Accordingly, reduction of inhibition, either through pharmacological or genetic methods (Bochner et al., 2014; Gu et al., 2016; Morishita et al., 2010), can reactivate plasticity in adults. Similarly, proteolytic digestion of the ECM reactivates juvenile-like plasticity in the adult visual cortex (Pizzorusso et al., 2002, 2006). Furthermore, dark exposure (DE), a non-invasive method to reactivates ocular dominance plasticity in adults, reduces GABA-ergic

inhibition (He et al., 2006; S. Huang et al., 2015). DE followed by light re-exposure (LRx) induces a significant reduction in the density of the extracellular matrix (Murase et al., 2017). 17 α E2 administration to cMD subjects induced a reduction in markers for both PV and ECM contralateral and ipsilateral to the occluded eye, which was enhanced in the contralateral hemisphere when 17 α E2 was followed by visual stimulation. This suggests a permissive environment synaptic activity may further promote synaptic plasticity. Interestingly, when 17 α E2 was followed by the SRP protocol, WFA levels remained low but PV expression increased, consistent with the idea that repetitive visual stimulation increases excitation onto PV neurons. The SRP-induced increase in PV expression may contribute to the stability of SRP, and has previously been shown to be important in SRP induction (Kaplan et al., 2016).

I found that 17 α E2 treatment alone increases the size, but not number of PSD95 in V1b contralateral to the occluded eye, and increases colocalization of pS831 and VGlut2, suggesting the 17 α E2 may increase activity at thalamocortical synapses. This is consistent with reports that PSD95 number does not change with 17 α E2 in hippocampal slices from intact male or female rodents (W. Wang et al., 2016). 17 α E2 alone can also enhance synaptic strength, which contributes to the promotion of LTP (Córdoba Montoya & Carrer, 1997; Kramár et al., 2009; Oberlander & Woolley, 2016). Consistent with a 'two-step wiring plasticity' hypothesis (Srivastava, 2012), transient synapses induced by hormone administration are silent (NMDAR-only) and require activity-

dependent AMPAR incorporation to stabilize newly-formed synapses (Srivastava et al., 2008). In support of this hypothesis, I showed that the effects of $17\alpha\text{E}2$ on PSD95 and pS831 are augmented by visual stimulation. 7 days of $17\alpha\text{E}2$ did not appear to confer any additional benefit to synaptic size or activity over a single dose. The $17\alpha\text{E}2$ -induced decrease in VGlut1 and VGlut2 was counter-intuitive, as activity-dependent changes in postsynaptic size are often accompanied by a similar increase in size of the pre-synaptic specialization (Futai et al., 2007). However, these reductions could be indicative of decreased glutamate re-uptake in response to the administration of the hormone, which can also be regulated by membrane ER α (Sato et al., 2003).

Finally, the SRP results revealed an unexpected specificity to the effects of $17\alpha\text{E}2$ on plasticity in cMD V1. Brief MD has been shown to increase the probability of release at synapses innervated by the deprived eye (Krahe & Guido, 2011; Yashiro et al., 2005). Similarly, we demonstrated a more rapid depression of the response to repetitive flash stimuli to the deprived eye than non-deprived eye, suggesting that cMD regulates the probability of neurotransmitter release. Importantly, estrogen administration can increase probability of release at excitatory synapses which have low initial probability release (Smejkalova & Woolley, 2010). $17\alpha\text{E}2$ promoted plasticity in the adult amblyopic cortex, but the stimulus-dependent increase in VEP amplitude was observed only in the VEP evoked in the non-deprived eye. I propose that a MD-induced increase in release probability in synapses serving the deprived eye,

suggested by the more rapid depression to repetitive visual stimulation, limited SRP to the synapses serving the non-deprived eye which have an initially low release probability. It would be interesting to see if visual stimulation could be used to drive down release probability in the deprived eye pathway to increase the sensitivity to estrogen-induced modulation.

The expression of SRP after $17\alpha E2$ at 24 hours in cMD subjects may be reflected in the increase in markers of excitatory synapses relative to the 2 hour time point. As an increase in synaptic size is also indicative of an increase in synaptic strength (Ehrlich et al., 2007; Zhang & Lisman, 2012), a larger PSD95 following $17\alpha E2$ would also support the potentiation of the VEP. Additional controls must be performed to distinguish between these two possibilities, including 24 hours after $17\alpha E2$ alone and 24 hours after SRP induction protocol alone. Nonetheless, these results demonstrate that the aged V1 retains sensitivity to enhancement plasticity by estrogen, which may be therapeutically beneficial in promoting plasticity of spared inputs around a scotoma to recover a 'blind spot', or a cortical infarct where there is ischemic damage.

Chapter 4 : Implications of Results & Future Directions for research

4.1 Discussion of Results

4.1.1 Novel observations regarding the anatomical consequences of cMD in aged V1

Although the amblyopia induced by cMD is resistant to recovery in adults, manipulations that increase plasticity in amblyopic V1b promote the recovery of visual function (Bochner et al., 2014; Pizzorusso et al., 2002; Sale et al., 2007; Vetencourt et al., 2008). Indeed, we have previously shown that deprived eye acuity fully recovers when the enhancement of cortical plasticity by dark exposure is followed by visual training (Eaton et al., 2016). One contribution of this work is the extension of the characterization of the impact of cMD on V1b in adult rodents to excitability of PV expressing interneurons, extracellular matrix density, excitatory synapse size and number, and regulation of presynaptic release probability. PV interneuron maturation is developmentally regulated, with a large body of evidence supporting an essential role in the onset and closure of critical period plasticity (Beurdeley et al., 2012; Hensch, 2005; Kuhlman et al., 2013; Levelt & Hübener, 2012). Brief MD during the critical period induces a rapid decrease in the excitability of PV INs, which is reflected in decreased parvalbumin expression (Cellerino et al., 1992). In contrast, when MD is prolonged, PV expression returns to control levels (Mainardi et al., 2009). My work utilizing cMD revealed an increase in overall PV intensity in both ipsilateral and contralateral V1b of cMD subjects, suggesting a homeostatic response to

prolonged MD. Suppression of PV IN output can re-engage the critical period for ocular dominance plasticity (Kuhlman et al., 2013), but suppression of PV interneurons after MD does not (Kaplan et al., 2016). PV-expressing interneurons are preferentially surrounded by dense extracellular matrix, that is increased by cMD. The increase in PV expression and ECM density following cMD V1b is expected to contribute to the constraint in reversing the effects of cMD in adults, and identifies potential targets for therapies to reintroduce plasticity and recovery of visual function.

We have previously reported that cMD induces a significant reduction in dendritic spine density in all cortical layers of V1b, including those that receive thalamic innervation (Montey & Quinlan, 2011). My own data utilizing viral transneuronal tracers demonstrates a reduction in innervation from the deprived eye to V1b. However, the number of PSD95 puncta and VGlut1/VGlut2 puncta were unchanged by cMD. One possibility is that cMD induces a collapse of dendritic spines onto the dendritic shaft, with no change in the number of excitatory synapses. Accordingly, during hibernation of some rodent species, dendritic spines collapse onto the shaft, yet they maintain synaptive connectivity and can later re-emerge as spiny synapses (Kirov et al., 2004; Roelandse, 2004). Additionally, in pyramidal neuron culture, retraction of dendritic spines is independent of a loss of PSD95, and in some cases, spine retraction is associated with an increase in PSD95 fluorescence on the dendritic shaft (Woods et al., 2011). This interpretation is consistent with the observation that

despite cMD, visual stimulation of the chronically deprived eye continues to evoke weak responses in deprived V1 (Montey & Quinlan, 2011), as shaft synapses produce synaptic potentials that are many orders of magnitude smaller than those elicited from a spiny synapse (Gulledge et al., 2012; Kawato & Tsukahara, 1984). Another possibility is that following cMD, a loss of deprived eye synapses is masked by an increase in non-deprived eye synapses, or that excitatory synapses onto excitatory neurons are reduced, while excitatory synapses onto inhibitory neurons are increased. Indeed, my data also indicates that PV expression is increased following cMD, supporting the latter possibility.

In addition, *in vivo* recordings revealed that the visual response evoked from the deprived eye depresses more quickly than the visual response evoked from the non-deprived eye, which is indicative of an increase probability of release. The increase in release probability likely reflects homeostatic plasticity employed to maintain synaptic activity in the face of prolonged sensory deprivation (Krahe & Guido, 2011; Maffei et al., 2004; Yashiro et al., 2005). This observation suggests that therapies to enhance synaptic function via regulation of presynaptic release probability, such as estrogen, will not be effective at synapses serving the deprived eye.

4.1.2 Assessing the effects of estrogen and visual stimulation on V1 of cMD adult rats

The primary focus of my thesis work was to determine the potential for the

enhancement of structural and functional plasticity by $17\alpha\text{E}2$ to promote recovery of visual function lost by cMD. The persistence of robust, non-genomic ER expression after menopause/estropause has been well documented in primates and rodents, especially in the hippocampus, hypothalamus, and frontal cortex (Sharma & Thakur, 2006; Waters et al., 2011; Wilson et al., 2002). Although the presence of ERs in primary sensory cortices has been controversial (Jeong et al., 2011; Mitra et al., 2003; Shughrue & Merchenthaler, 2001), I demonstrate robust ER α and ER β expression in V1b of aged rats. Importantly, these appear to be largely extranuclear, similar to previous reports of extranuclear receptors in hippocampus (Milner et al., 2005, 2001), which have been implicated in engaging rapid anatomical and physiological synaptic plasticity (Srivastava et al., 2011).

I showed that a single dose of E2 induces robust changes in the molecular composition of cMD V1b. $17\alpha\text{E}2$ reduces the density of the ECM after cMD, similar to other interventions that enhance plasticity in adult V1 (Murase et al., 2017; Sale et al., 2007). Indeed, proteolytic digestion of ECM enhances synaptic plasticity in rodent V1, amygdala, perirhinal cortex, and hippocampus (Carstens et al., 2016; Pizzorusso et al., 2002, 2006; Romberg et al., 2013). A single dose of $17\alpha\text{E}2$ to cMD subjects also reduces the expression of PV, a proxy for the excitability of FS INs which is inversely correlated with the excitability of pyramidal neurons (Donato et al., 2013; Murase et al., 2017). Estrogen treatment of rat organotypic slice cultures has also been shown to reduce PV expression (Ross & Porter, 2002). This reduction in WFA and PV is even greater

if $17\alpha\text{E}2$ treatment is paired with visual stimulation. Interestingly, WFA expression was further reduced after SRP induction in $17\alpha\text{E}2$ -treated subjects, similar to previous findings that visual experience after dark exposure increases digestion of the ECM (Murase et al., 2017). The increase in PV expression following SRP is consistent with previous reports that sustained visual stimulation increases the activity of PV INs (Atallah et al., 2012) and the observation that PV activity is essential for the expression of SRP (Kaplan et al., 2016).

The hypothesis that estrogen would promote the recovery from cMD was based on previous reports that estrogen administration increases the number of dendritic spines and/or spiny excitatory synapses (Kramár et al., 2013; Woolley & McEwen, 1993). However, in the aged V1b, I found an increase in the size, rather than the number, of PSD95 puncta, which suggests an enlargement of pre-existing excitatory synapses. I obtained similar results with multiple $17\alpha\text{E}2$ treatments, $17\alpha\text{E}2$ followed by visual stimulation, or 7 days of $17\alpha\text{E}2$ followed by visual stimulus. An increase in F-actin, without a change in PSD95 puncta number, is observed following brief estrogen exposure in hippocampal slices from young male and middle-aged OVX female rats (Kramár et al., 2009; Wang et al., 2016). Golgi stains of mouse hippocampal tissue also reveal an increase in the number of large, mushroom-type spines following estrogen treatment in OVX females (Li et al., 2004). Interestingly, I observed a significant increase in pS831 size when a single dose of $17\alpha\text{E}2$ was followed by visual stimulus and after 7 days of $17\alpha\text{E}2$, but not in response to a single acute dose of $17\alpha\text{E}2$ alone. This

suggests that the 17 α E2-induced increase in size of pre-existing excitatory synapses is independent of AMPAR trafficking through CaMKII/PKC phosphorylation of AMPAR-GluA1 with 17 α E2 alone, consistent with previous work that GluA1-containing AMPARs are not upregulated after estrogen administration (Ferri et al., 2014). However, 17 α E2 with visual stimulation or prolonged 17 α E2 treatment activates CaMKII / PKC signaling, or promotes the incorporation of new synapses into functional circuits which can respond to changes in synaptic CaMKII / PKC (Srivastava, 2012). Although longer duration estrogen treatment regulates the expression of ER α /ER β (Gréco et al., 2001), *in vivo* two-photon imaging of young adult OVX thy1-GFP mouse sensory cortex reveals more estrogen-induced spine formation following acute than chronic estrogen (Wang et al., 2018).

Curiously, the expression of the presynaptic glutamate transporters is reduced in response to estrogen treatment, despite previous reports that estrogen increases the expression of VGlut1 in cultured cortical neurons (Khan et al., 2013). However, estrogen has been shown to decrease glutamate re-uptake through an ER α - dependent mechanism, which may be mediated by a decrease in the expression of VGlut1 and VGlut2 (Sato et al., 2003). My results demonstrate an exception to the observation that pre- and post-synaptic size are typically co-regulated (Futai et al., 2007).

How do these 17 α E2-induced changes in synaptic composition compare

to known effects of $17\alpha\text{E}2$ on synaptic function? Estrogen administration has been demonstrated to have wide-ranging effects on synaptic strength and plasticity, which can vary by brain region. $17\alpha\text{E}2$ fluctuations correlate with changes in the expression of LTP at excitatory synapses (Warren et al., 1995), increases in the amplitude and frequency of mEPSCs in rat hippocampal CA1 pyramidal neurons in both sexes, and increases in glutamate uncaging-evoked EPSCs and calcium transients at a subset of dendritic spines (Oberlander & Woolley, 2016). Additionally, it has been reported that acute estrogen lowers the threshold and increases the magnitude of LTP induced by theta burst stimulation of excitatory synapses in the hippocampus of OVX rats (Córdoba Montoya & Carrer, 1997) and may induce a modest LTP-like strengthening of synapses alone (Kramár et al., 2013; Mukai et al., 2007). However, hormone replacement in OVX young mice increases mIPSC frequency and paired pulse depression at inhibitory synapses in frontal cortex, but not somatosensory cortex (Piekarski et al., 2017), indicating a difference in estrogen-induced action across brain regions.

My experiments cannot determine if $17\alpha\text{E}2$ in cMD V1 is facilitating plasticity via $\text{ER}\alpha$ or $\text{ER}\beta$, or the if receptors localized in the presynaptic or postsynaptic compartment mediate the observed effects. determination is complicated by the presence of both receptor subtypes in V1 of adult rodents, the presence of membrane-bound $\text{ER}\alpha$ and $\text{ER}\beta$ in excitatory and inhibitory neurons, and their localization in both the post- or presynaptic specializations of these

cells. However, my results are best explained by estrogen acting upon ERs at the presynaptic terminals of both inhibitory and excitatory neurons. Activation of presynaptic ER α reduces the strength of inhibitory synapses. In hippocampal neurons in culture, 24 hours of estrogen administration decreases mIPSCs, increases mEPSCs, and increases dendritic spine density (Murphy et al., 1998). Acute estrogen rapidly reduces mIPSC frequency in pyramidal neurons of layer 2/3 V1 in older mice, and an ER α antagonist occludes the decrease in mIPSC amplitude observed following dark exposure (Gao et al., 2017). These results are consistent with estrogen reducing the strength of inhibitory transmission via presynaptic ER α and support my findings that 17 α E2 administration decreases PV+ interneuron activity and reduces WFA staining for ECM, which may disinhibit excitatory pyramidal neurons. While 17 α estradiol shows preferential activation of ER α over ER β (Toran-Allerand et al., 2005), other findings of my work indicate involvement of presynaptic ER β activation in excitatory neurons. Estrogen administration has been shown to potentiate glutamatergic synaptic transmission, via an ER β -dependent mechanism, by increasing release probability specifically at synapses with initially low probability of release (Smejkalova & Woolley, 2010). This supports the specific enhancement of the non-deprived eye VEP in response to a familiar orientation (SRP), which was occluded in synapses with an increased probability of release due to cMD. Furthermore, post-synaptic activation of ERs on excitatory neurons is associated with formation of new spine synapses (Hojo et al., 2008; Kramár et al., 2009; Srivastava & Woolfrey, 2010), which I did not observe following any 17 α E2 administration paradigms. To test

these predictions, further experiments can utilize ER α or ER β selective agonists; propyl pyrazole triol (PPT) for ER α and diarylpropionitrile (DPN) and WAY2700 for ER β , (Harrington et al., 2003). These compounds could be used in conjunction with receptor-specific antagonists, methyl-piperidinopyrazole (MPP) against ER α and R,R-tetrahydrochrysenes (R,R-THC) against ER β (Harrington et al., 2003), in rodent V1 to specifically activate the different receptor types and their downstream effectors.

As stated previously, 17 α E2 treatment of adult amblyopes enabled the induction of SRP of the visual responses evoked by non-deprived eye stimulation. Estrogen potentiation of EPSCs in hippocampus has been shown to occur selectively at synapses with an initially low probability of glutamate release (Smejkalova & Woolley, 2010). As VEPs acquired from the previously deprived eye depress more rapidly than the non-deprived eye in response to repetitive stimulation, a cMD-induced increase in release probability may occlude the enhancement of plasticity by estrogen at synapses serving the deprived eye. Deprived eye responses are also significantly weaker and less stimulus selective than non-deprived eye responses following cMD (Montey et al., 2013). However, these changes are not likely to explain the absence of SRP in the deprived eye pathway, as high contrast, low spatial frequency stimuli elicit visual responses through the deprived eye and can be enhanced by dark exposure (Montey et al., 2013; Montey & Quinlan, 2011). Interestingly, the strengthening of non-deprived

eye synapses which is part of the normal response to cMD does not occlude the induction of SRP or the enhancement of plasticity by $17\alpha\text{E}2$, suggesting that the mechanisms engaged by these pathways are not saturated in amblyopic cortex. Moreover, these results suggest that the specificity of $17\alpha\text{E}2$ is defined by synaptic characteristics that reflect the history of synaptic activity. Importantly, the persistence of ERs in aged V1 and the enhancement of plasticity of synapses in the intact, non-deprived eye pathway opens up the possibility that $17\alpha\text{E}2$ could be combined with perceptual training to abate the loss of visual acuity with age. Therefore, selective enhancement of plasticity by $17\alpha\text{E}2$ at synapses with initially low release probability may also promote plasticity of spared inputs around a scotoma or a cortical infarct.

4.2 Limitations of Experimental Approach

As with any experiment, there are limitations to the interpretations of the presented work. Methodologically, the use of markers for excitatory synapses in fixed tissue prevents the assessment of changes in spine density within a single neuron or individual over time, which could be revealed with a method like in vivo two photon imaging of GFP-filled dendrites. Additionally, the cohort sizes used in my studies did not allow me to analyze males and females separately. Increasing the number of subjects would permit the exploration of any sex-specific differences in the effects $17\alpha\text{E}2$ administration to cMD V1, as estrogen-induced

plasticity may act through distinct mechanisms in males and females (Oberlander & Woolley, 2016).

Furthermore, we employed acute rather than chronic electrophysiology to examine the effects of cMD and 17 α E2 administration to deprived visual cortex. This allowed for the assessment of the effects of cMD and 17 α E2 on visual responses evoked by deprived and non-deprived eye stimulation, with minimal damage to V1b to allow for post mortem immunohistochemistry. However, repeated physiological recordings following chronic electrode implantation would have allowed for a more detailed time course of the effects of 17 α E2, including the timing of the initial response, response longevity, and confirmation of the homeostatic changes predicted in Chapter 3.

4.3 Recommendations for Future Research

Our work revealed that estrogen enhancement of synaptic function may be limited to a subset of synapses with an initial low probability of release, and support previous reports in hippocampus (Smejkalova & Woolley, 2010). The cMD-induced increase in response probability may preclude the effects of estrogen at deprived eye synapses. This synapse specific targeting could be harnessed for therapeutically-relevant treatment of deficits other than amblyopia. Pathological scotoma, or visual blind spots, can be initiated by a retinal lesion (Baseler et al., 2009), optic nerve injury (Knight & Hoyt, 1972) or cortical damage due to lesion or infarct (Pula & Yuen, 2017; Rizzo & Robin, 1996). These deficits

sometimes spontaneously improve (Rizzo & Robin, 1996), and successful treatment paradigms using repetitive visual stimulation indicate that the locus of recovery from these deficits may occur in V1 (Zihl & Von Cramon, 1985). This mechanism may be ideal for enhancing plasticity at preserved inputs around injuries. Additionally, it has been demonstrated that reduction in presynaptic release probability suppresses low, but not high frequency synaptic transmission (Seeburg, 2004). Therefore, it may be useful to test the effect of 17 α E2 on SRP induced in cMDs with visual stimuli of higher temporal frequencies. In addition, release probability could be experimentally manipulated to enhance sensitivity to estrogen. One interesting possibility would be to present experimental subjects with repetitive visual stimulation to the deprived eye, to drive down the initial probability of release, to ask if this enhances the sensitivity to subsequent 17 α E2 administration (Saviane et al., 2002).

Ideally, I would have combined cytoplasmic fills of neurons to assess dendritic spines with immunohistochemical assessment of excitatory synapse components. This approach would have also allowed be to resolve the effect of the acute administration of 17 α E2 in V1 on the diverse morphologies of dendritic spines (filopodial, thin, mushroom, stubby), as well as synaptic composition. However Golgi impregnation makes co-staining with other synaptic markers difficult (Gould et al., 1990; Li et al., 2004; Woolley & McEwen, 1993). In pilot experiments, I delivered an AAV2-GFP regulated by a CaMKII promoter intracortically to V1 of cMD subjects to induce sparse, whole neuron fluorescence

in pyramidal cells (Watakabe et al., 2015) . However, expression was too sparse in the aged cortex and did not provide any of the intended whole neuron, cytoplasmic fill, possibly due to increased extracellular matrix expression in these cMD subjects, as dense extracellular matrix around cancer cells prevents their infection by therapeutic AAV (Yata et al., 2015), so I abandoned this technique. Therefore, another possibility would be to repeat these experiments in transgenic mice expressing Thy1-GFP, which have been have been used successfully in recent estrogen plasticity studies to examine the changes in cortical spine morphology *in vivo* over the course of naturally-occurring estrogen fluctuations (Alexander et al., 2018) or following estrogen administration (S. Wang et al., 2018). The addition of more time points and controls would strengthen the interpretation of some of these experiments. For example, PV and WFA staining are different 2 versus 24 hours after 17 α E2 administration, but the 24 hour measurement was after SRP stimulation. Additional controls would include 24 hours after 17 α E2 alone 24 hours after SRP induction protocol alone. Furthermore, additional time course experiments could be used to determine the optimal delivery schedule for 17 α E2, as well as determine the advantage of a continuous or discontinuous delivery of hormone, as there is ongoing investigation of the benefits and risks of each regimen type (Grant et al., 2015). Interestingly, non-continuous estrogen administration to rodents (1x/3 days) was more effective than daily administration(1x/3-4 days) in protecting against neurodegeneration in the dentate gyrus following OVX (Shoukry & Soliman, 2014).

In another set of pilot experiments, I investigated the impact of the steroid corticosterone on synaptic plasticity on the cMD V1, which has been shown in hippocampal slice culture to induce spinogenesis within an hour of administration (Murakami et al., 2018). However, my results indicated that acute administration of corticosterone had an overall negative impact on synaptic density and size in V1 contralateral and ipsilateral to the occlusion. Future experiments could combine 17 α E2 with another steroid hormone, as 17 α E2 plus progesterone has been demonstrated to enhance hippocampal spine density (J.-R. Chen et al., 2009; Gould et al., 1990) and object memory consolidation in rodents (Harburger et al., 2009), and improve executive function in non-human primates compared to placebo-administered controls (Voytko et al., 2009). I also examined the possibility of directing 17 α E2 to the visual cortex using magnetic beads and an external magnetic field, but this method was abandoned as it causing inflammation and damage. Alternatively, infusion of 17 α E2 directly into cortex would circumvent off-target effects, and has been employed successfully in other studies (Fan et al., 2010; Fernandez et al., 2008; Xiao et al., 2013). Direct infusion of estrogen into either hippocampal structures or striatum demonstrated region-specific, independent effects on place and response learning (Zurkovsky et al., 2007).

Finally, the prediction that 17 α E2 treatment may be useful to promote receptor field plasticity of spared inputs is exciting and testable. Hormone therapy

has demonstrated great potential for the improvement of brain function, and this body of research provides a foundation for advancement of relatively low-risk, high compliance acute hormone therapy for the reversal of previously intractable sensory deficits in the adult, aged brain.

Bibliography

- Akama, K. T., & McEwen, B. S. (2003). Estrogen Stimulates Postsynaptic Density-95 Rapid Protein Synthesis via the Akt/Protein Kinase B Pathway. *The Journal of Neuroscience*, 23(6), 2333–2339. Retrieved from <http://www.jneurosci.org/content/23/6/2333.abstract>
- Alexander, B. H., Barnes, H. M., Trimmer, E., Davidson, A. M., Ogola, B. O., Lindsey, S. H., & Mostany, R. (2018). Stable Density and Dynamics of Dendritic Spines of Cortical Neurons Across the Estrous Cycle While Expressing Differential Levels of Sensory-Evoked Plasticity. *Frontiers in Molecular Neuroscience*, 11(March), 1–13. <https://doi.org/10.3389/fnmol.2018.00083>
- Almey, A., Milner, T. A., & Brake, W. G. (2016). Implication for Dopamine-Dependent Cognition in Females, (514), 125–138. <https://doi.org/10.1016/j.yhbeh.2015.06.010>. Estrogen
- Anggono, V., & Huganir, R. L. (2012). Regulation of AMPA receptor trafficking and synaptic plasticity. *Current Opinion in Neurobiology*, 22(3), 461–469. <https://doi.org/10.1016/J.CONB.2011.12.006>
- Atallah, B. V., Bruns, W., Carandini, M., & Scanziani, M. (2012). Parvalbumin-Expressing Interneurons Linearly Transform Cortical Responses to Visual Stimuli. *Neuron*, 73(1), 159–170. <https://doi.org/10.1016/j.neuron.2011.12.013>
- Avila, J. A., Alliger, A. A., Carvajal, B., Zanca, R. M., Serrano, P. A., & Luine, V. N. (2017). Estradiol rapidly increases GluA2-mushroom spines and decreases GluA2-filopodia spines in hippocampus CA1. *Hippocampus*, 27(12). <https://doi.org/10.1002/hipo.22768>
- Bagger, Y. Z., Tanko, L. B., Alexandersen, P., Qin, G. R., Christiansen, C., & Grp, P. S. (2005). Early postmenopausal hormone therapy may prevent cognitive impairment later in life. *Menopause-the Journal of the North American Menopause Society*. <https://doi.org/10.1097/01.GME.0000127660.81276.2B>
- Bailey, M. E. E., Wang, A. C. J. C. J., Hao, J., Janssen, W. G. M. G. M., Hara, Y., Dumitriu, D., ... Morrison, J. H. (2011). Interactive effects of age and estrogen on cortical neurons: implications for cognitive aging. *Neuroscience*, 191(0), 148–158. <https://doi.org/10.1016/j.neuroscience.2011.05.045>
- Balmer, T. S. (2016). Perineuronal Nets Enhance the Excitability of Fast-Spiking Neurons. *ENeuro*, 3(4). <https://doi.org/10.1523/ENEURO.0112-16.2016>
- Barria, A., Derkach, V., & Soderling, T. (1997). Identification of the Ca²⁺/Calmodulin-dependent Protein Kinase II Regulatory Phosphorylation Site in the α -Amino-3-hydroxyl-5-methyl-4-isoxazole-propionate-type Glutamate Receptor. *Journal of Biological Chemistry*, 272(52), 32727–32730. <https://doi.org/10.1074/jbc.272.52.32727>
- Bartoletti, A., Medini, P., Berardi, N., & Maffei, L. (2004). Environmental enrichment prevents effects of dark-rearing in the rat visual cortex. *Nature Neuroscience*. <https://doi.org/10.1038/nn1201>
- Baseler, H. A., Gouws, A., & Morland, A. B. (2009). The organization of the visual cortex in patients with scotomata resulting from lesions of the central retina. *Neuro-Ophthalmology*, 33(3), 149–157. <https://doi.org/10.1080/01658100903050053>
- Beurdeley, M., Spatazza, J., Lee, H. H. C., Sugiyama, S., Bernard, C., Di Nardo, A. A., ... Prochiantz, A. (2012). Otx2 Binding to Perineuronal Nets Persistently Regulates Plasticity in the Mature Visual Cortex. *Journal of Neuroscience*, 32(27), 9429–9437. <https://doi.org/10.1523/JNEUROSCI.0394-12.2012>
- Bliss, T. V. P., & Cooke, S. F. (2011). Long-term potentiation and long-term depression: a clinical perspective. *Clinics*, 66, 3–17.
- Bloss, E. B., Janssen, W. G., Ohm, D. T., Yuk, F. J., Wadsworth, S., Saardi, K. M., ... Morrison, J. H. (2011). Evidence for Reduced Experience-Dependent Dendritic Spine Plasticity in the Aging Prefrontal Cortex. *Journal of Neuroscience*, 31(21), 7831–7839.

- <https://doi.org/10.1523/JNEUROSCI.0839-11.2011>
- Bochner, D. N., Sapp, R. W., Adelson, J. D., Zhang, S., Lee, H., Djurasic, M., ... Shatz, C. J. (2014). Blocking PirB up-regulates spines and functional synapses to unlock visual cortical plasticity and facilitate recovery from amblyopia. *Science Translational Medicine*, 6(258), 258ra140. <https://doi.org/10.1126/scitranslmed.3010157>
- Bourne, J. N., & Harris, K. M. (2008). Balancing Structure and Function at Hippocampal Dendritic Spines. *Annual Review of Neuroscience*, 31, 47–67. <https://doi.org/10.1146/annurev.neuro.31.060407.125646>
- Bove, R., Secor, E., Chibnik, L. B., Barnes, L. L., Schneider, J. A., Bennett, D. A., & De Jager, P. L. (2014). Age at surgical menopause influences cognitive decline and Alzheimer pathology in older women. *Neurology*, 82(3), 222–229. <https://doi.org/10.1212/WNL.0000000000000033>
- Bridi, M. C. D., De Pasquale, R., Lantz, C. L., Gu, Y., Borrell, A., Choi, S. Y., ... Kirkwood, A. (2018). Two distinct mechanisms for experience-dependent homeostasis. *Nature Neuroscience*. <https://doi.org/10.1038/s41593-018-0150-0>
- Bullitt, E. (1990). Expression of C-fos-like protein as a marker for neuronal activity following noxious stimulation in the rat. *The Journal of Comparative Neurology*, 296(4), 517–530. <https://doi.org/10.1002/cne.902960402>
- Cane, M., Maco, B., Knott, G., & Holtmaat, A. (2014). The Relationship between PSD-95 Clustering and Spine Stability In Vivo. *Journal of Neuroscience*, 34(6), 2075–2086. <https://doi.org/10.1523/JNEUROSCI.3353-13.2014>
- Carreau, S., Lambard, S., Delalande, C., Denis-Galeraud, I., Bilinska, B., & Bourguiba, S. (2003). Aromatase expression and role of estrogens in male gonad: A review. *Reproductive Biology and Endocrinology*. <https://doi.org/10.1186/1477-7827-1-35>
- Carstens, K. E., Phillips, M. L., Pozzo-Miller, L., Weinberg, R. J., & Dudek, S. M. (2016). Perineuronal Nets Suppress Plasticity of Excitatory Synapses on CA2 Pyramidal Neurons. *Journal of Neuroscience*, 36(23), 6312–6320. <https://doi.org/10.1523/JNEUROSCI.0245-16.2016>
- Carulli, D., Pizzorusso, T., Kwok, J. C. F., Putignano, E., Poli, A., Forostyak, S., ... Fawcett, J. W. (2010). Animals lacking link protein have attenuated perineuronal nets and persistent plasticity. *Brain*, 133(8), 2331–2347. <https://doi.org/10.1093/brain/awq145>
- Cellerino, A., Siciliano, R., Domenici, L., & Maffei, L. (1992). Parvalbumin immunoreactivity: A reliable marker for the effects of monocular deprivation in the rat visual cortex. *Neuroscience*, 51(4), 749–753. [https://doi.org/https://doi.org/10.1016/0306-4522\(92\)90514-3](https://doi.org/https://doi.org/10.1016/0306-4522(92)90514-3)
- Chen, J.-R., Yan, Y.-T., Wang, T.-J., Chen, L.-J., Wang, Y.-J., & Tseng, G.-F. (2009). Gonadal hormones modulate the dendritic spine densities of primary cortical pyramidal neurons in adult female rat. *Cerebral Cortex (New York, N.Y. : 1991)*. <https://doi.org/10.1093/cercor/bhp048>
- Chen, Q., Cichon, J., Wang, W., Qiu, L., Lee, S.-J. R., Campbell, N. R., ... Feng, G. (2012). Imaging Neural Activity Using Thy1-GCaMP Transgenic Mice. *Neuron*, 76(2), 297–308. <https://doi.org/http://dx.doi.org/10.1016/j.neuron.2012.07.011>
- Chen, X., Nelson, C. D., Li, X., Winters, C. A., Azzam, R., Sousa, A. A., ... Reese, T. S. (2011). PSD-95 Is Required to Sustain the Molecular Organization of the Postsynaptic Density. *The Journal of Neuroscience*, 31(17), 6329–6338. <https://doi.org/10.1523/JNEUROSCI.5968-10.2011>
- Cooke, S. F., & Bear, M. F. (2010). Visual experience induces long-term potentiation in the primary visual cortex. *Journal of Neuroscience*, 30(48), 16304–16313. <https://doi.org/10.1523/JNEUROSCI.4333-10.2010>
- Cooke, S. F., & Bliss, T. V. P. (2006). Plasticity in the human central nervous system. *Brain : A Journal of Neurology*, 129(Pt 7), 1659–1673. <https://doi.org/10.1093/brain/awl082>
- Córdoba Montoya, D. A., & Carrer, H. F. (1997). Estrogen facilitates induction of long term

- potentiation in the hippocampus of awake rats. *Brain Research*, 778(2), 430–438.
[https://doi.org/10.1016/S0006-8993\(97\)01206-7](https://doi.org/10.1016/S0006-8993(97)01206-7)
- Cui, J., Shen, Y., & Li, R. (2013). Estrogen synthesis and signaling pathways during aging: From periphery to brain. *Trends in Molecular Medicine*, 19(3), 197–209.
<https://doi.org/10.1016/j.molmed.2012.12.007>
- Dietel, M., Lewis, M. A., & Shapiro, S. (2005). Hormone replacement therapy: Pathobiological aspects of hormone-sensitive cancers in women relevant to epidemiological studies on HRT: A mini-review. *Human Reproduction*, 20(8), 2052–2060. <https://doi.org/10.1093/humrep/dei043>
- Dominguez, R., & Micevych, P. (2010). Estradiol Rapidly Regulates Membrane Estrogen Receptor α Levels in Hypothalamic Neurons. *The Journal of Neuroscience*, 30(38), 12589–12596.
<https://doi.org/10.1523/JNEUROSCI.1038-10.2010>
- Donato, F., Rompani, S. B., & Caroni, P. (2013). Parvalbumin-expressing basket-cell network plasticity induced by experience regulates adult learning. *Nature*, 504, 272. Retrieved from <http://dx.doi.org/10.1038/nature12866>
- Du, A.-T., Schuff, N., Kramer, J. H., Rosen, H. J., Gorno-Tempini, M. L., Rankin, K., ... Weiner, M. W. (2007). Different regional patterns of cortical thinning in Alzheimer's disease and frontotemporal dementia. *Brain: A Journal of Neurology*. <https://doi.org/10.1093/brain/awm016>
- Duan, H., Wearne, S. L., Rocher, A. B., Macedo, A., Morrison, J. H., & Hof, P. R. (2003). Age-related Dendritic and Spine Changes in Corticocortically Projecting Neurons in Macaque Monkeys. *Cerebral Cortex*, 13(9), 950–961. <https://doi.org/10.1093/cercor/13.9.950>
- Dumitriu, D., Hao, J., Hara, Y., Kaufmann, J., Janssen, W. G. M., Lou, W., ... Morrison, J. H. (2010). Selective Changes in Thin Spine Density and Morphology in Monkey Prefrontal Cortex Correlate with Aging-Related Cognitive Impairment. *Journal of Neuroscience*, 30(22), 7507–7515.
<https://doi.org/10.1523/JNEUROSCI.6410-09.2010>
- Dumitriu, D., Rapp, P. R., McEwen, B. S., & Morrison, J. H. (2010). Estrogen and the aging brain: an elixir for the weary cortical network. *Annals of the New York Academy of Sciences*, 1204(1), 104–112. <https://doi.org/10.1111/j.1749-6632.2010.05529.x>
- Dunn, K. W., Kamocka, M. M., & McDonald, J. H. (2011). A practical guide to evaluating colocalization in biological microscopy. *American Journal of Physiology - Cell Physiology*, 300(4), C723–C742. <https://doi.org/10.1152/ajpcell.00462.2010>
- Eaton, N. C., Sheehan, H. M., & Quinlan, E. M. (2016). Optimization of visual training for full recovery from severe amblyopia in adults. *Learning and Memory*. <https://doi.org/10.1101/lm.040295.115>
- Ehrlich, I., Klein, M., Rumpel, S., & Malinow, R. (2007). PSD-95 is required for activity-driven synapse stabilization. *Proceedings of the National Academy of Sciences*, 104(10), 4176–4181.
<https://doi.org/10.1073/pnas.0609307104>
- El-Husseini, A. E.-D., Schnell, E., Chetkovich, D. M., Nicoll, R. A., & Bredt, D. S. (2000). PSD-95 Involvement in Maturation of Excitatory Synapses. *Science*, 290(5495), 1364–1368. Retrieved from <http://science.sciencemag.org/content/290/5495/1364.abstract>
- Fagiolini, M., & Hensch, T. K. (2000). Inhibitory threshold for critical-period activation in primary visual cortex. *Nature*, 404(6774), 183–186. <https://doi.org/10.1038/35004582>
- Fagiolini, M., Pizzorusso, T., Berardi, N., Domenici, L., & Maffei, L. (1994). Functional postnatal development of the rat primary visual cortex and the role of visual experience: dark rearing and monocular deprivation. *Vision Research*. [https://doi.org/10.1016/0042-6989\(94\)90210-0](https://doi.org/10.1016/0042-6989(94)90210-0)
- Fan, L., Zhao, Z., Orr, P. T., Chambers, C. H., Lewis, M. C., & Frick, K. M. (2010). Estradiol-Induced Object Memory Consolidation in Middle-Aged Female Mice Requires Dorsal Hippocampal Extracellular Signal-Regulated Kinase and Phosphatidylinositol 3-Kinase Activation. *Journal of Neuroscience*, 30(12), 4390–4400. <https://doi.org/10.1523/JNEUROSCI.4333-09.2010>

- Fernandez, S. M., Lewis, M. C., Pechenino, A. S., Harburger, L. L., Orr, P. T., Gresack, J. E., ... Frick, K. M. (2008). Estradiol-Induced Enhancement of Object Memory Consolidation Involves Hippocampal Extracellular Signal-Regulated Kinase Activation and Membrane-Bound Estrogen Receptors. *Journal of Neuroscience*. <https://doi.org/10.1523/JNEUROSCI.1968-08.2008>
- Ferrario, C. R., Loweth, J. A., Milovanovic, M., Wang, X., & Wolf, M. E. (2011). Distribution of AMPA receptor subunits and TARPs in synaptic and extrasynaptic membranes of the adult rat nucleus accumbens. *Neuroscience Letters*, *490*(3), 180–184. <https://doi.org/http://dx.doi.org/10.1016/j.neulet.2010.12.036>
- Ferri, S. L., Hildebrand, P. F., Way, S. E., & Flanagan-Cato, L. M. (2014). Estradiol regulates markers of synaptic plasticity in the hypothalamic ventromedial nucleus and amygdala of female rats. *Hormones and Behavior*. <https://doi.org/10.1016/j.yhbeh.2014.06.016>
- Frenkel, M. Y., Sawtell, N. B., Diogo, A. C. M., Yoon, B., Neve, R. L., & Bear, M. F. (2006). Instructive Effect of Visual Experience in Mouse Visual Cortex. *Neuron*, *51*(3), 339–349. <https://doi.org/10.1016/j.neuron.2006.06.026>
- Freund, T. F., & Katona, I. (2007). Perisomatic Inhibition. *Neuron*, *56*(1), 33–42. <https://doi.org/10.1016/j.neuron.2007.09.012>
- Furmanski, C. S., Schluppeck, D., & Engel, S. A. (2004). Learning Strengthens the Response of Primary Visual Cortex to Simple Patterns. *Current Biology*, *14*(7), 573–578. <https://doi.org/10.1016/j.cub.2004.03.032>
- Futai, K., Kim, M. J., Hashikawa, T., Scheiffele, P., Sheng, M., & Hayashi, Y. (2007). Retrograde modulation of presynaptic release probability through signaling mediated by PSD-95-neuroigin. *Nature Neuroscience*, *10*(2), 186–195. <https://doi.org/10.1038/nn1837>
- Gauthier, S., Reisberg, B., Zaudig, M., Petersen, R. C., Ritchie, K., Broich, K., ... Winblad, B. (2006). Mild cognitive impairment. *The Lancet*, *367*(9518), 1262–1270. [https://doi.org/10.1016/S0140-6736\(06\)68542-5](https://doi.org/10.1016/S0140-6736(06)68542-5)
- Gibbs, R. B. (1999). Estrogen replacement enhances acquisition of a spatial memory task and reduces deficits associated with hippocampal muscarinic receptor inhibition. *Hormones and Behavior*. <https://doi.org/10.1006/hbeh.1999.1541>
- Gogolla, N., Caroni, P., A, L., & C, H. (2009). Perineuronal nets protect fear memories from erasure: *Science (New York, N.Y.)*, *325*(5945), 1258–1261. Retrieved from <papers2://publication/uuid/F3595F8C-4671-4CDB-883D-F9526608A315>
- Gordon, J. a, & Stryker, M. P. (1996). Experience-dependent plasticity of binocular responses in the primary visual cortex of the mouse. *The Journal of Neuroscience : The Official Journal of the Society for Neuroscience*. [https://doi.org/0270-6474/96/163274-13\\$05.00/0](https://doi.org/0270-6474/96/163274-13$05.00/0)
- Gould, E., Woolley, C. S., Frankfurt, M., & McEwen, B. S. (1990). Gonadal steroids regulate dendritic spine density in hippocampal pyramidal cells in adulthood. *The Journal of ...*, *10*(4), 1286–1291. Retrieved from <http://www.jneurosci.org/content/10/4/1286.abstract>
- Grant, M. D., Marbella, A., Wang, A. T., Pines, E., Hoag, J., Bonnell, C., ... Aronson, N. (2015). Menopausal Symptoms: Comparative Effectiveness of Therapies. *Menopausal Symptoms: Comparative Effectiveness of Therapies*.
- Gréco, B., Allegretto, E. a, Tetel, M. J., & Blaustein, J. D. (2001). Coexpression of ER beta with ER alpha and progesterin receptor proteins in the female rat forebrain: effects of estradiol treatment. *Endocrinology*, *142*(12), 5172–5181. <https://doi.org/10.1210/en.142.12.5172>
- Greifzu, F., Pielecka-Fortuna, J., Kalogeraki, E., Krempler, K., Favaro, P. D., Schluter, O. M., & Lowel, S. (2014). Environmental enrichment extends ocular dominance plasticity into adulthood and protects from stroke-induced impairments of plasticity. *Proceedings of the National Academy of Sciences*. <https://doi.org/10.1073/pnas.1313385111>
- Gresack, J. E., & Frick, K. M. (2006). Post-training estrogen enhances spatial and object memory

- consolidation in female mice. *Pharmacology Biochemistry and Behavior*.
<https://doi.org/10.1016/j.pbb.2006.04.013>
- Gu, Y., Huang, S., Chang, M., Worley, P., Kirkwood, A., & Quinlan, E. (2013). Obligatory role for the immediate early gene NARP in critical period plasticity. *Neuron*, *79*, 335–346.
<https://doi.org/10.1016/j.neuron.2013.05.016>
- Gu, Y., Tran, T., Murase, S., Borrell, A., Kirkwood, A., & Quinlan, E. M. (2016). Neuregulin-Dependent Regulation of Fast-Spiking Interneuron Excitability Controls the Timing of the Critical Period. *The Journal of Neuroscience*, *36*(40), 10285–10295.
<https://doi.org/10.1523/JNEUROSCI.4242-15.2016>
- Gulledge, A. T., Carnevale, N. T., & Stuart, G. J. (2012). Electrical advantages of dendritic spines. *PLoS ONE*, *7*(4). <https://doi.org/10.1371/journal.pone.0036007>
- Gunning-Dixon, F. M., & Raz, N. (2003). Neuroanatomical correlates of selected executive functions in middle-aged and older adults: A prospective MRI study. *Neuropsychologia*, *41*(14), 1929–1941. [https://doi.org/10.1016/S0028-3932\(03\)00129-5](https://doi.org/10.1016/S0028-3932(03)00129-5)
- Guo, Y., Huang, S., de Pasquale, R., McGehrin, K., Lee, H.-K., Zhao, K., & Kirkwood, A. (2012). Dark exposure extends the integration window for spike-timing-dependent plasticity. *The Journal of Neuroscience : The Official Journal of the Society for Neuroscience*, *32*(43), 15027–15035.
<https://doi.org/10.1523/JNEUROSCI.2545-12.2012>
- Hao, J., Rapp, P. R., Leffler, A. E., Leffler, S. R., Janssen, W. G. M., Lou, W., ... Morrison, J. H. (2006). Estrogen Alters Spine Number and Morphology in Prefrontal Cortex of Aged Female Rhesus Monkeys. *The Journal of Neuroscience*, *26*(9), 2571–2578.
<https://doi.org/10.1523/JNEUROSCI.3440-05.2006>
- Hara, Y., Waters, E. M., McEwen, B. S., & Morrison, J. H. (2015). Estrogen Effects on Cognitive and Synaptic Health Over the Lifecourse. *Physiological Reviews*, *95*(3), 785–807.
<https://doi.org/10.1152/physrev.00036.2014>
- Hara, Y., Yuk, F., Puri, R., Janssen, W. G. M., Rapp, P. R., & Morrison, J. H. (2016). Estrogen Restores Multisynaptic Boutons in the Dorsolateral Prefrontal Cortex while Promoting Working Memory in Aged Rhesus Monkeys. *The Journal of Neuroscience*, *36*(3), 901–910.
<https://doi.org/10.1523/JNEUROSCI.3480-13.2016>
- Harauzov, A., Spolidoro, M., DiCristo, G., De Pasquale, R., Cancedda, L., Pizzorusso, T., ... Maffei, L. (2010). Reducing Intracortical Inhibition in the Adult Visual Cortex Promotes Ocular Dominance Plasticity. *Journal of Neuroscience*, *30*(1), 361–371.
<https://doi.org/10.1523/JNEUROSCI.2233-09.2010>
- Harburger, L. L., Saadi, A., & Frick, K. M. (2009). Dose-dependent effects of post-training estradiol plus progesterone treatment on object memory consolidation and hippocampal extracellular signal-regulated kinase activation in young ovariectomized mice. *Neuroscience*, *160*(1), 6–12.
<https://doi.org/10.1016/j.neuroscience.2009.02.024>
- Harrington, W. R., Sheng, S., Barnett, D. H., Petz, L. N., Katzenellenbogen, J. A., & Katzenellenbogen, B. S. (2003). Activities of estrogen receptor alpha- and beta-selective ligands at diverse estrogen responsive gene sites mediating transactivation or transrepression. *Molecular and Cellular Endocrinology*, *206*(1–2), 13–22. [https://doi.org/10.1016/S0303-7207\(03\)00255-7](https://doi.org/10.1016/S0303-7207(03)00255-7)
- Harris, K. M., Jensen, F. E., & Tsao, B. (1992). Three-dimensional structure of dendritic spines and synapses in rat hippocampus (CA1) at postnatal day 15 and adult ages: implications for the maturation of synaptic physiology and long-term potentiation. *The Journal of Neuroscience : The Official Journal of the Society for Neuroscience*. <https://doi.org/10.1016/j.tcb.2009.06.001>
- He, H.-Y., Hodos, W., & Quinlan, E. M. (2006). Visual Deprivation Reactivates Rapid Ocular Dominance Plasticity in Adult Visual Cortex. *The Journal of Neuroscience*, *26*(11), 2951–2955.

- <https://doi.org/10.1523/JNEUROSCI.5554-05.2006>
- He, H. H.-Y., Hodos, W., & Quinlan, E. E. M. (2006). Visual deprivation reactivates rapid ocular dominance plasticity in adult visual cortex. *The Journal of Neuroscience*, *26*(11), 2951–2955. <https://doi.org/10.1523/JNEUROSCI.5554-05.2006>
- He, H. H.-Y., Ray, B., Dennis, K., & Quinlan, E. E. M. (2007). Experience-dependent recovery of vision following chronic deprivation amblyopia. *Nature Neuroscience*, *10*(9), 1134–1136. <https://doi.org/10.1038/nn1965>
- He, W., Goodkind, D., & Kowal, P. (2016). An Aging World : 2015 International Population Reports. *Aging*. <https://doi.org/P95/09-1>
- Head, D., Rodrigue, K. M., Kennedy, K. M., & Raz, N. (2008). Neuroanatomical and cognitive mediators of age-related differences in episodic memory. *Neuropsychology*. Head, Denise: Department of Psychology, Washington University, 1 Brooking Drive-Box 1125, Saint Louis, MO, US, 63130, dhead@wustl.edu: American Psychological Association. <https://doi.org/10.1037/0894-4105.22.4.491>
- Hensch, T. K. (2005). Critical period plasticity in local cortical circuits. *Nature Reviews Neuroscience*, *6*(11), 877–888. <https://doi.org/10.1038/nrn1787>
- Hensch, T. K., Fagiolini, M., Mataga, N., Stryker, M. P., Baekkeskov, S., & Kash, S. F. (1998). 49Local GABA circuit control of experience-dependent plasticity in developing visual cortex. *Science (New York, N.Y.)*, *282*(5393), 1504–1508. <https://doi.org/10.1016/j.biotechadv.2011.08.021.Secreted>
- Heynen, A. J., & Bear, M. F. (2001). Long-Term Potentiation of Thalamocortical Transmission in the Adult Visual Cortex In Vivo. *The Journal of Neuroscience*, *21*(24), 9801–9813. <https://doi.org/10.1523/JNEUROSCI.21-24-09801.2001>
- Hojo, Y., Murakami, G., Mukai, H., Higo, S., Hatanaka, Y., Ogiue-Ikeda, M., ... Kawato, S. (2008). Estrogen synthesis in the brain--role in synaptic plasticity and memory. *Molecular and Cellular Endocrinology*, *290*(1–2), 31–43. <https://doi.org/10.1016/j.mce.2008.04.017>
- Hotulainen, P., & Hoogenraad, C. C. (2010). Actin in dendritic spines: connecting dynamics to function. *The Journal of Cell Biology*, *189*(4), 619–629. <https://doi.org/10.1083/jcb.201003008>
- Huang, G. Z., & Woolley, C. S. (2012). Estradiol Acutely Suppresses Inhibition in the Hippocampus through a Sex-Specific Endocannabinoid and mGluR-Dependent Mechanism. *Neuron*, *74*(5), 801–808. <https://doi.org/10.1016/j.neuron.2012.03.035>
- Huang, S., Gu, Y., Quinlan, E. M., & Kirkwood, A. (2010). A Refractory Period for Rejuvenating GABAergic Synaptic Transmission and Ocular Dominance Plasticity with Dark Exposure. *Journal of Neuroscience*. <https://doi.org/10.1523/JNEUROSCI.4384-10.2010>
- Huang, S., Hokenson, K., Bandyopadhyay, S., Russek, S. J., & Kirkwood, A. (2015). Brief Dark Exposure Reduces Tonic Inhibition in Visual Cortex. *Journal of Neuroscience*. <https://doi.org/10.1523/JNEUROSCI.1813-15.2015>
- Iwai, Y., Fagiolini, M., Obata, K., & Hensch, T. K. (2003). Rapid critical period induction by tonic inhibition in visual cortex. *The Journal of Neuroscience : The Official Journal of the Society for Neuroscience*. <https://doi.org/10.1523/JNEUROSCI.23-17-6695> [pii]
- Jeong, J. J.-K., Tremere, L. A., Burrows, K., Majewska, A. K., & Pinaud, R. (2011). The mouse primary visual cortex is a site of production and sensitivity to estrogens. *PloS One*, *6*(5), 1–12. <https://doi.org/10.1371/journal.pone.0020400>
- Kalogeraki, E., Pielecka-Fortuna, J., & Löwel, S. (2017). Environmental enrichment accelerates ocular dominance plasticity in mouse visual cortex whereas transfer to standard cages resulted in a rapid loss of increased plasticity. *PLoS ONE*. <https://doi.org/10.1371/journal.pone.0186999>
- Kaplan, E. S., Cooke, S. F., Komorowski, R. W., Chubykin, A. A., Thomazeau, A., Khibnik, L. A., ...

- Bear, M. F. (2016). Contrasting roles for parvalbumin-expressing inhibitory neurons in two forms of adult visual cortical plasticity. *ELife*, 5(MARCH2016), 1–27. <https://doi.org/10.7554/eLife.11450>
- Kasai, H., Fukuda, M., Watanabe, S., Hayashi-takagi, A., & Noguchi, J. (2010). Structural dynamics of dendritic spines in memory and cognition. *Trends in Neurosciences*, 33(3), 121–129. <https://doi.org/10.1016/j.tins.2010.01.001>
- Kawato, M., & Tsukahara, N. (1984). Electrical properties of dendritic spines with bulbous end terminals. *Biophysical Journal*, 46(2), 155–166. [https://doi.org/10.1016/S0006-3495\(84\)84008-4](https://doi.org/10.1016/S0006-3495(84)84008-4)
- Khan, M. M., Dhandapani, K. M., Zhang, Q.-G., & Brann, D. W. (2013). Estrogen regulation of spine density and excitatory synapses in rat prefrontal and somatosensory cerebral cortex. *Steroids*. <https://doi.org/10.1016/j.steroids.2012.12.005>
- Kim, M. J., Futai, K., Jo, J., Hayashi, Y., Cho, K., & Sheng, M. (2007). Synaptic Accumulation of PSD-95 and Synaptic Function Regulated by Phosphorylation of Serine-295 of PSD-95. *Neuron*, 56(3), 488–502. <https://doi.org/10.1016/j.neuron.2007.09.007>
- Kirkwood, A., Lee, H., & Bear, M. (1995). Co-regulation of long-term potentiation and experience-dependent synaptic plasticity in visual cortex by age and experience. *Nature*, 375(6529), 328–331. Retrieved from <http://www.nature.com/nature/journal/v375/n6529/abs/375328a0.html>
- Kirov, S. A., Petrak, L. J., Fiala, J. C., & Harris, K. M. (2004). Dendritic spines disappear with chilling but proliferate excessively upon rewarming of mature hippocampus. *Neuroscience*, 127(1), 69–80. <https://doi.org/https://doi.org/10.1016/j.neuroscience.2004.04.053>
- Knight, C. L., & Hoyt, W. F. (1972). Monocular blindness from drusen of the optic disk. *American Journal of Ophthalmology*, 73(6), 890–892. [https://doi.org/10.1016/0002-9394\(72\)90458-8](https://doi.org/10.1016/0002-9394(72)90458-8)
- Krahe, T. E., & Guido, W. (2011). Homeostatic plasticity in the visual thalamus by monocular deprivation, 31(18), 6842–6849. <https://doi.org/10.1523/JNEUROSCI.1173-11.2011.Homeostatic>
- Kramár, E. A., Babayan, A. H., Gall, C. M., & Lynch, G. (2013). Estrogen promotes learning-related plasticity by modifying the synaptic cytoskeleton. *Neuroscience*, 239(0), 3–16. <https://doi.org/10.1016/j.neuroscience.2012.10.038>
- Kramár, E. E. A., Chen, L. Y. L., Brandon, N. J., Rex, C. S., Liu, F., Gall, C. M., & Lynch, G. (2009). Cytoskeletal changes underlie estrogen's acute effects on synaptic transmission and plasticity. *The Journal of ...*, 29(41), 12982–12993. <https://doi.org/10.1523/JNEUROSCI.3059-09.2009>
- Kuhlman, S. J., Olivas, N. D., Tring, E., Ikrar, T., Xu, X., & Trachtenberg, J. T. (2013). A disinhibitory microcircuit initiates critical-period plasticity in the visual cortex. *Nature*, 501(7468), 543–546. <https://doi.org/10.1038/nature12485>
- Kuiper, G. G. J. M., Carlsson, B., Grandien, K., Enmark, E., Häggblad, J., Nilsson, S., & Gustafsson, J. Å. (1997). Comparison of the ligand binding specificity and transcript tissue distribution of estrogen receptors and α and β . *Endocrinology*, 138(3), 863–870. <https://doi.org/10.1210/en.138.3.863>
- Kumar, R., Zakharov, M. N., Khan, S. H., Miki, R., Jang, H., Toraldo, G., ... Jasuja, R. (2011). The Dynamic Structure of the Estrogen Receptor. *Journal of Amino Acids*. <https://doi.org/10.4061/2011/812540>
- Lai, Y. J., Yu, D., Zhang, J. H., & Chen, G. J. (2017). Cooperation of Genomic and Rapid Nongenomic Actions of Estrogens in Synaptic Plasticity. *Molecular Neurobiology*, 54(6), 4113–4126. <https://doi.org/10.1007/s12035-016-9979-y>
- Lei, W., Deng, Y., Liu, B., Mu, S., Guley, N. M., Wong, T., & Reiner, A. (2013). Confocal laser scanning microscopy and ultrastructural study of VGLUT2 thalamic input to striatal projection neurons in rats. *Journal of Comparative Neurology*, 521(6), 1354–1377. <https://doi.org/10.1002/cne.23235>
- Lenšj, K. K., Lepperød, M. E., Dick, G., Hafting, T., & Fyhn, M. (2017). Removal of Perineuronal

- Nets Unlocks Juvenile Plasticity Through Network Mechanisms of Decreased Inhibition and Increased Gamma Activity. *The Journal of Neuroscience*, 37(5), 1269–1283. <https://doi.org/10.1523/JNEUROSCI.2504-16.2016>
- Levelt, C. N., & Hübener, M. (2012). Critical-Period Plasticity in the Visual Cortex. *Annual Review of Neuroscience*, 35(1), 309–330. <https://doi.org/10.1146/annurev-neuro-061010-113813>
- Levin, E. R. (2005). Integration of the Extranuclear and Nuclear Actions of Estrogen. *Molecular Endocrinology*. <https://doi.org/10.1210/me.2004-0390>
- Li, C., Brake, W. G., Romeo, R. D., Dunlop, J. C., Gordon, M., Buzescu, R., ... McEwen, B. S. (2004). Estrogen alters hippocampal dendritic spine shape and enhances synaptic protein immunoreactivity and spatial memory in female mice. *Proceedings of the National Academy of Sciences*, 101(7), 2185–2190. <https://doi.org/10.1073/pnas.0307313101>
- Liguz-Leczna, M., & Skangiel-Kramska, J. (2007a). Vesicular glutamate transporters (VGLUTs): the three musketeers of glutamatergic system. *Acta Neurobiologiae Experimentalis*, 67(3), 207–218. Retrieved from <http://www.ncbi.nlm.nih.gov/pubmed/17957901>
- Liguz-Leczna, M., & Skangiel-Kramska, J. (2007b). Vesicular glutamate transporters VGLUT1 and VGLUT2 in the developing mouse barrel cortex. *International Journal of Developmental Neuroscience*, 25(2), 107–114. <https://doi.org/10.1016/j.ijdevneu.2006.12.005>
- Lombardi, G., Zarrilli, S., Colao, A., Paesano, L., Di Somma, C., Rossi, F., & De Rosa, M. (2001). Estrogens and health in males. In *Molecular and Cellular Endocrinology*. [https://doi.org/10.1016/S0303-7207\(01\)00420-8](https://doi.org/10.1016/S0303-7207(01)00420-8)
- Luine, V. N., Jacome, L. F., & Maclusky, N. J. (2003). Rapid enhancement of visual and place memory by estrogens in rats. *Endocrinology*, 144(7), 2836–2844. <https://doi.org/10.1210/en.2003-0004>
- MacLennan, A. H., Henderson, V. W., Paine, B. J., Mathias, J., Ramsay, E. N., Ryan, P., ... Grp, P. S. (2006). Hormone therapy, timing of initiation, and cognition in women aged older than 60 years: the REMEMBER pilot study. *Menopause*, 13(1). <https://doi.org/10.1097/01.GME.0000127660.81276.2B>
- MacLusky, N. J., Luine, V. N., Hajszan, T., & Leranth, C. (2005). The 17 α and 17 β Isomers of Estradiol Both Induce Rapid Spine Synapse Formation in the CA1 Hippocampal Subfield of Ovariectomized Female Rats. *Endocrinology*, 146(1), 287–293. <https://doi.org/10.1210/en.2004-0730>
- Maffei, A., Nelson, S. B., & Turrigiano, G. G. (2004). Selective reconfiguration of layer 4 visual cortical circuitry by visual deprivation. *Nature Neuroscience*. <https://doi.org/10.1038/nn1351>
- Mainardi, M., Landi, S., Berardi, N., Maffei, L., & Pizzorusso, T. (2009). Reduced Responsiveness to Long-Term Monocular Deprivation of Parvalbumin Neurons Assessed by c-Fos Staining in Rat Visual Cortex. *PLoS ONE*, 4(2), e4342. <https://doi.org/10.1371/journal.pone.0004342>
- Malenka, R. C., & Bear, M. F. (2004). LTP and LTD: An embarrassment of riches. *Neuron*. <https://doi.org/10.1016/j.neuron.2004.09.012>
- Mammen, a. L., Kameyama, K., Roche, K. W., & Huganir, R. L. (1997). Phosphorylation of the alpha-Amino-3-hydroxy-5-methylisoxazole4-propionic Acid Receptor GluR1 Subunit by Calcium/Calmodulin-dependent Kinase II. *Journal of Biological Chemistry*, 272(51), 32528–32533. <https://doi.org/10.1074/jbc.272.51.32528>
- Manson, J. A. E., Chlebowski, R. T., Stefanick, M. L., Aragaki, A. K., Rossouw, J. E., Prentice, R. L., ... Wallace, R. B. (2014). Menopausal hormone therapy and health outcomes during the intervention and extended poststopping phases of the women's health initiative randomized trials. *Obstetrical and Gynecological Survey*. <https://doi.org/10.1097/01.ogx.0000444679.66386.38>
- Marino, M., Galluzzo, P., & Ascenzi, P. (2006). Estrogen signaling multiple pathways to impact gene

- transcription. *Curr Genomics*, 7(8), 497–508. <https://doi.org/10.2174/138920206779315737>
- Matsuzaki, M., Honkura, N., Ellis-Davies, G. C. R., & Kasai, H. (2004). Structural basis of long-term potentiation in single dendritic spines. *Nature*, 429(6993), 761–766. <https://doi.org/10.1038/nature02617>
- McAllister, A. K. (2007). Dynamic aspects of CNS synapse formation. *Annual Review of Neuroscience*, 30(530), 425–450. <https://doi.org/10.1146/annurev.neuro.29.051605.112830>
- Mechoulam, R., Brueggemeier, R. W., & Denlinger, D. L. (1984). Estrogens in insects. *Experientia*. <https://doi.org/10.1007/BF01946450>
- Melmed, S. (2016). *Williams textbook of endocrinology*. Elsevier Health Sciences. <https://doi.org/10.1016/C2013-0-15980-6>
- Micevych, P., & Christensen, A. (2012). Membrane-initiated estradiol actions mediate structural plasticity and reproduction. *Frontiers in Neuroendocrinology*, 33(4), 331–341. <https://doi.org/10.1016/j.yfrne.2012.07.003>
- Milner, T. A., Ayoola, K., Drake, C. T., Herrick, S. P., Tabori, N. E., McEwen, B. S., ... Alves, S. E. (2005). Ultrastructural localization of estrogen receptor β immunoreactivity in the rat hippocampal formation. *The Journal of Comparative Neurology*, 491(2), 81–95. <https://doi.org/10.1002/cne.20724>
- Milner, T. A., McEwen, B. S., Hayashi, S., Li, C. J., Reagan, L. P., & Alves, S. E. (2001). Ultrastructural evidence that hippocampal alpha estrogen receptors are located at extranuclear sites. *The Journal of Comparative Neurology*, 429(3), 355–371. [https://doi.org/10.1002/1096-9861\(20010115\)429:3<355::AID-CNE1>3.0.CO;2-#](https://doi.org/10.1002/1096-9861(20010115)429:3<355::AID-CNE1>3.0.CO;2-#)
- Milner, T. a, Ayoola, K., Drake, C. T., Herrick, S. P., Tabori, N. E., McEwen, B. S., ... Alves, S. E. (2005). Ultrastructural localization of estrogen receptor beta immunoreactivity in the rat hippocampal formation. *The Journal of Comparative Neurology*. <https://doi.org/10.1002/cne.20724>
- Mitra, S. W., Hoskin, E., Yudkovitz, J., Pear, L., Wilkinson, H. A., Hayashi, S., ... Alves, S. E. (2003). Immunolocalization of estrogen receptor ?? in the mouse brain: Comparison with estrogen receptor ?? *Endocrinology*, 144(5), 2055–2067. <https://doi.org/10.1210/en.2002-221069>
- Miyata, S., & Kitagawa, H. (2016). Chondroitin 6-Sulfation Regulates Perineuronal Net Formation by Controlling the Stability of Aggrecan. *Neural Plasticity*, 2016, 7–9. <https://doi.org/10.1155/2016/1305801>
- Montey, K. L. K., Eaton, N. C. N., & Quinlan, E. E. M. (2013). Repetitive visual stimulation enhances recovery from severe amblyopia. *Learning & Memory*, 20(6), 311–317. <https://doi.org/10.1101/lm.030361.113>
- Montey, K. L. K., & Quinlan, E. E. M. (2011). Recovery from chronic monocular deprivation following reactivation of thalamocortical plasticity by dark exposure. *Nature Communications*, 2(May), 317–318. <https://doi.org/10.1038/ncomms1312>
- Monyer, H., Burnashev, N., Laurie, D. J., Sakmann, B., & Seeburg, P. H. (1994). Developmental and regional expression in the rat brain and functional properties of four NMDA receptors. *Neuron*, 12(3), 529–540. [https://doi.org/10.1016/0896-6273\(94\)90210-0](https://doi.org/10.1016/0896-6273(94)90210-0)
- Morales, B., Choi, S.-Y., & Kirkwood, A. (2002). Dark rearing alters the development of GABAergic transmission in visual cortex. *The Journal of Neuroscience*. <https://doi.org/10.1523/JNEUROSCI.2218-02.2002>
- Morishita, H., Miwa, J. M., Heintz, N., & Hensch, T. K. (2010). Lynx1, a Cholinergic Brake, Limits Plasticity in Adult Visual Cortex. *Science*, 330(6008), 1238–1240. <https://doi.org/10.1126/science.1195320>
- Morrison, J. H., & Hof, P. R. (1997). Life and death of neurons in the aging brain 3985. *Science*, 278(October), 412–419.

- Morrison, J. H. J., & Baxter, M. G. M. (2012). The ageing cortical synapse: hallmarks and implications for cognitive decline. *Nature Reviews Neuroscience*, *13*(April), 240–250. <https://doi.org/10.1038/nrn3200>
- Mower, G. D. (1991). The effect of dark rearing on the time course of the critical period in cat visual cortex. *Developmental Brain Research*. [https://doi.org/10.1016/0165-3806\(91\)90001-Y](https://doi.org/10.1016/0165-3806(91)90001-Y)
- Mower, G. D., Berry, D., Burchfiel, J. L., & Duffy, F. H. (1981). Comparison of the effects of dark rearing and binocular suture on development and plasticity of cat visual cortex. *Brain Research*. [https://doi.org/10.1016/0006-8993\(81\)91216-6](https://doi.org/10.1016/0006-8993(81)91216-6)
- Mukherjee, J., Cardarelli, R. A., Cantaut-Belarif, Y., Deeb, T. Z., Srivastava, D. P., Tyagarajan, S. K., ... Moss, S. J. (2017). Estradiol modulates the efficacy of synaptic inhibition by decreasing the dwell time of GABA_A receptors at inhibitory synapses. *Proceedings of the National Academy of Sciences*, *114*(44), 11763–11768. <https://doi.org/10.1073/pnas.1705075114>
- Murakami, G., Hojo, Y., Kato, A., Komatsuzaki, Y., Horie, S., Soma, M., ... Kawato, S. (2018). Rapid nongenomic modulation by neurosteroids of dendritic spines in the hippocampus: Androgen, oestrogen and corticosteroid. *Journal of Neuroendocrinology*, *30*(2), 1–13. <https://doi.org/10.1111/jne.12561>
- Murase, S., Lantz, C. L., & Quinlan, E. M. (2017). Light reintroduction after dark exposure reactivates plasticity in adults via perisynaptic activation of MMP-9. *ELife*, *6*, 1–23. <https://doi.org/10.7554/eLife.27345>
- Murphy, D. D., Cole, N. B., Greenberger, V., & Segal, M. (1998). Estradiol increases dendritic spine density by reducing GABA neurotransmission in hippocampal neurons. *Journal of Neuroscience*, *18*(7), 2550–2559. <https://doi.org/10.1523/JNEUROSCI.18-07-02550.1998>
- Nunzi, M. G., Milan, F., Guidolin, D., & Toffano, G. (1987). Dendritic spine loss in hippocampus of aged rats. Effect of brain phosphatidylserine administration. *Neurobiology of Aging*, *8*(6), 501–510. [https://doi.org/https://doi.org/10.1016/0197-4580\(87\)90124-2](https://doi.org/https://doi.org/10.1016/0197-4580(87)90124-2)
- Nusser, Z., Lujan, R., Laube, G., Roberts, J. D. B., Molnar, E., & Somogyi, P. (1998). Cell type and pathway dependence of synaptic AMPA receptor number and variability in the hippocampus. *Neuron*, *21*(3), 545–559. [https://doi.org/10.1016/S0896-6273\(00\)80565-6](https://doi.org/10.1016/S0896-6273(00)80565-6)
- Oberlander, J. G., & Woolley, C. S. (2016). 17 α -Estradiol Acutely Potentiates Glutamatergic Synaptic Transmission in the Hippocampus through Distinct Mechanisms in Males and Females. *Journal of Neuroscience*, *36*(9), 2677–2690. <https://doi.org/10.1523/JNEUROSCI.4437-15.2016>
- Oray, S., Majewska, A., & Sur, M. (2004). Dendritic spine dynamics are regulated by monocular deprivation and extracellular matrix degradation. *Neuron*, *44*(6), 1021–1030. <https://doi.org/10.1016/j.neuron.2004.12.001>
- Ozon, R. (1972). *Steroids in Nonmammalian Vertebrates*. *Steroids in Nonmammalian Vertebrates*. <https://doi.org/10.1016/B978-0-12-370350-7.50010-8>
- Pacheco, J., Goh, J. O., Kraut, M. A., Ferrucci, L., & Resnick, S. M. (2015). Greater cortical thinning in normal older adults predicts later cognitive impairment. *Neurobiology of Aging*. <https://doi.org/10.1016/j.neurobiolaging.2014.08.031>
- Paoletti, P., Bellone, C., & Zhou, Q. (2013). NMDA receptor subunit diversity: Impact on receptor properties, synaptic plasticity and disease. *Nature Reviews Neuroscience*, *14*(6), 383–400. <https://doi.org/10.1038/nrn3504>
- Perusquía, M., & Navarrete, E. (2005). Evidence that 17 α -estradiol is biologically active in the uterine tissue: Antiuterotonic and antiuterotrophic action. *Reproductive Biology and Endocrinology*, *3*(1), 1–11. <https://doi.org/10.1186/1477-7827-3-30>
- Pfeffer, C. K., Xue, M., He, M., Huang, Z. J., & Scanziani, M. (2013). Inhibition of inhibition in visual cortex: the logic of connections between molecularly distinct interneurons. *Nature Neuroscience*, *16*, 1068. Retrieved from <http://dx.doi.org/10.1038/nn.3446>

- Phan, A., Gabor, C. S., Favaro, K. J., Kaschack, S., Armstrong, J. N., MacLusky, N. J., & Choleris, E. (2012). Low doses of 17 β -estradiol rapidly improve learning and increase hippocampal dendritic spines. *Neuropsychopharmacology*. <https://doi.org/10.1038/npp.2012.82>
- Phan, A., Suschkov, S., Molinaro, L., Reynolds, K., Lymer, J. M., Bailey, C. D. C., ... Choleris, E. (2015). Rapid increases in immature synapses parallel estrogen-induced hippocampal learning enhancements. *Proceedings of the National Academy of Sciences*, *112*(52), 16018–16023. <https://doi.org/10.1073/pnas.1522150112>
- Picq, J.-L., Aujard, F., Volk, A., & Dhenain, M. (2012). Age-related cerebral atrophy in nonhuman primates predicts cognitive impairments. *Neurobiology of Aging*, *33*(6), 1096–1109. <https://doi.org/10.1016/j.neurobiolaging.2010.09.009>
- Pizzorusso, T., Medini, P., Berardi, N., Chierzi, S., Fawcett, J. W., & Maffei, L. (2002). Reactivation of ocular dominance plasticity in the adult visual cortex. *Science (New York, N.Y.)*, *298*(5596), 1248–1251. <https://doi.org/10.1126/science.1072699>
- Pizzorusso, T., Medini, P., Landi, S., Baldini, S., Berardi, N., & Maffei, L. (2006). Structural and functional recovery from early monocular deprivation in adult rats. *Proceedings of the National Academy of Sciences*, *103*(22), 8517–8522. <https://doi.org/10.1073/pnas.0602657103>
- Pula, J. H., & Yuen, C. A. (2017). Eyes and stroke: The visual aspects of cerebrovascular disease. *Stroke and Vascular Neurology*, *2*(4), 210–220. <https://doi.org/10.1136/svn-2017-000079>
- Quinlan, E. M., Olstein, D. H., & Bear, M. F. (1999). Bidirectional, experience-dependent regulation of N-methyl-D-aspartate receptor subunit composition in the rat visual cortex during postnatal development. *Proceedings of the National Academy of Sciences of the United States of America*, *96*(22), 12876–12880. <https://doi.org/10.1073/PNAS.96.22.12876>
- Rapp, P. R., Morrison, J. H., & Roberts, J. a. (2003). Cyclic estrogen replacement improves cognitive function in aged ovariectomized rhesus monkeys. *The Journal of Neuroscience : The Official Journal of the Society for Neuroscience*, *23*(13), 5708–5714. <https://doi.org/23/13/5708> [pii]
- Rapp, S. R., Espeland, M. A., Shumaker, S. A., Henderson, V. W., Brunner, R. L., Manson, J. E., ... for the WHIMS Investigators. (2003). Effect of Estrogen Plus Progestin on Global Cognitive Function in Postmenopausal Women. *Jama*, *289*(20), 2663. <https://doi.org/10.1001/jama.289.20.2663>
- Raz, N., Gunning-Dixon, F. M., Head, D., Dupuis, J. H., & Acker, J. D. (1998). Neuroanatomical correlates of cognitive aging: evidence from structural magnetic resonance imaging. *Neuropsychology*. <https://doi.org/10.1126/science.1067020>
- Regal, D. M., Boothe, R., Teller, D. Y., & Sackett, G. P. (1976). Visual acuity and visual responsiveness in dark-reared monkeys (*Macaca nemestrina*). *Vision Research*. [https://doi.org/10.1016/0042-6989\(76\)90034-1](https://doi.org/10.1016/0042-6989(76)90034-1)
- Regehr, W. G. (2012). Short-term presynaptic plasticity. *Cold Spring Harbor Perspectives in Biology*, *4*(7), a005702. <https://doi.org/10.1101/cshperspect.a005702>
- Rizzo, M., & Robin, D. A. (1996). Bilateral effects of unilateral visual cortex lesions in human. *Brain*. <https://doi.org/10.1093/brain/119.3.951>
- Roche, K. W., O'Brien, R. J., Mammen, A. L., Bernhardt, J., & Huganir, R. L. (1996). Characterization of multiple phosphorylation sites on the AMPA receptor GluR1 subunit. *Neuron*, *16*(6), 1179–1188. [https://doi.org/10.1016/S0896-6273\(00\)80144-0](https://doi.org/10.1016/S0896-6273(00)80144-0)
- Roelandse, M. (2004). Hypothermia-Associated Loss of Dendritic Spines. *Journal of Neuroscience*, *24*(36), 7843–7847. <https://doi.org/10.1523/JNEUROSCI.2872-04.2004>
- Romberg, C., Yang, S., Melani, R., Andrews, M. R., Horner, A. E., Spillantini, M. G., ... Saksida, L. M. (2013). Depletion of perineuronal nets enhances recognition memory and long-term depression in the perirhinal cortex. *The Journal of Neuroscience*, *33*(16), 7057–7065. <https://doi.org/10.1523/JNEUROSCI.6267-11.2013>

- Ross, N. R., & Porter, L. L. (2002). Effects of dopamine and estrogen upon cortical neurons that express parvalbumin in vitro. *Developmental Brain Research*. [https://doi.org/10.1016/S0165-3806\(02\)00364-4](https://doi.org/10.1016/S0165-3806(02)00364-4)
- Salat, D. H., Buckner, R. L., Snyder, A. Z., Greve, D. N., Desikan, R. S. R., Busa, E., ... Fischl, B. (2004). Thinning of the cerebral cortex in aging. *Cerebral Cortex*, *14*(7), 721–730. <https://doi.org/10.1093/cercor/bhh032>
- Saldanha, C. J., Remage-Healey, L., & Schlinger, B. A. (2011). Synaptocrine signaling: Steroid synthesis and action at the synapse. *Endocrine Reviews*, *32*(4), 532–549. <https://doi.org/10.1210/er.2011-0004>
- Sale, A., Maya Vetencourt, J. F., Medini, P., Cenni, M. C., Baroncelli, L., De Pasquale, R., & Maffei, L. (2007). Environmental enrichment in adulthood promotes amblyopia recovery through a reduction of intracortical inhibition. *Nature Neuroscience*, *10*(6), 679–681. <https://doi.org/10.1038/nn1899>
- Sato, K., Matsuki, N., Ohno, Y., & Nakazawa, K. (2003). Estrogens inhibit l-glutamate uptake activity of astrocytes via membrane estrogen receptor alpha. *Journal of Neurochemistry*, *86*(6), 1498–1505. <https://doi.org/10.1046/j.1471-4159.2003.01953.x>
- Saviane, C., Savtchenko, L. P., Raffaelli, G., Voronin, L. L., & Cherubini, E. (2002). Frequency-dependent shift from paired-pulse facilitation to paired-pulse depression at unitary CA3-CA3 synapses in the rat hippocampus. *Journal of Physiology*, *544*(2), 469–476. <https://doi.org/10.1113/jphysiol.2002.026609>
- Savonenko, A. V., & Markowska, A. L. (2003). The cognitive effects of ovariectomy and estrogen replacement are modulated by aging. *Neuroscience*, *119*(3), 821–830. [https://doi.org/10.1016/S0306-4522\(03\)00213-6](https://doi.org/10.1016/S0306-4522(03)00213-6)
- Schulster, M., Bernie, A., & Ramasamy, R. (2016). The role of estradiol in male reproductive function. *Asian Journal of Andrology*. <https://doi.org/10.4103/1008-682X.173932>
- Seeburg, D. P. (2004). Frequency-Dependent Modulation of Retinogeniculate Transmission by Serotonin. *Journal of Neuroscience*, *24*(48), 10950–10962. <https://doi.org/10.1523/JNEUROSCI.3749-04.2004>
- Sharma, P. K., & Thakur, M. K. (2006). Expression of estrogen receptor (ER) α and β in mouse cerebral cortex: Effect of age, sex and gonadal steroids. *Neurobiology of Aging*. <https://doi.org/10.1016/j.neurobiolaging.2005.04.003>
- Sheng, M., & Kim, E. (2011). The Postsynaptic Organization of Synapses. *Cold Spring Harbor Perspectives in Biology*, *3*(12), a005678–a005678. <https://doi.org/10.1101/cshperspect.a005678>
- Shoukry, Y., & Soliman, N. B. (2014). Effect of cyclic versus continuous hormonal replacement therapy on the structure of dentate gyrus of ovariectomized adult albino rats: A histological and immunohistochemical study. *Egyptian Journal of Histology*. <https://doi.org/10.1097/01.EHX.0000446581.96572.dc>
- Shughrue, P. J., & Merchenthaler, I. (2001). Distribution of estrogen receptor beta immunoreactivity in the rat central nervous system. *The Journal of Comparative Neurology*. <https://doi.org/10.1002/cne.1054>
- Singh, V., Chertkow, H., Lerch, J. P., Evans, A. C., Dorr, A. E., & Kabani, N. J. (2006). Spatial patterns of cortical thinning in mild cognitive impairment and Alzheimer's disease. *Brain*. <https://doi.org/10.1093/brain/awl256>
- Smejkalova, T., & Woolley, C. S. (2010). Estradiol acutely potentiates hippocampal excitatory synaptic transmission through a presynaptic mechanism. *The Journal of Neuroscience: The Official Journal of the Society for Neuroscience*, *30*(48), 16137–16148. <https://doi.org/10.1523/JNEUROSCI.4161-10.2010>
- Smith, C. C., Smith, L. A., Bredemann, T. M., & McMahon, L. L. (2016). 17 β estradiol recruits

- GluN2B-containing NMDARs and ERK during induction of long-term potentiation at temporoammonic-CA1 synapses. *Hippocampus*, 26(1), 110–117. <https://doi.org/10.1002/hipo.22495>
- Song, I., & Huganir, R. L. (2002). Regulation of AMPA receptors during synaptic plasticity. *Trends in Neurosciences*, 25(11), 578–588. [https://doi.org/10.1016/S0166-2236\(02\)02270-1](https://doi.org/10.1016/S0166-2236(02)02270-1)
- Srivastava, D. P. (2012). Two-Step Wiring Plasticity - A mechanism for estrogen-induced rewiring of cortical circuits. *Journal of Steroid Biochemistry and Molecular Biology*, 131(1–2), 17–23. <https://doi.org/10.1016/j.jsbmb.2012.01.006>
- Srivastava, D. P. D., Waters, E. M., Mermelstein, P. G., Kramár, E. A., Shors, T. J., & Liu, F. (2011). Rapid estrogen signaling in the brain: implications for the fine-tuning of neuronal circuitry. *The Journal of ...*, 31(45), 16056–16063. <https://doi.org/10.1523/JNEUROSCI.4097-11.2011>
- Srivastava, D. P., Woolfrey, K., Jones, K. A., Shum, Y., Lash, L. L., Swanson, G. T., ... Gilbert, P. U. P. A. (2008). Rapid enhancement of two-step wiring plasticity, 105(38).
- Srivastava, D. P., Woolfrey, K. M., Liu, F., Brandon, N. J., & Penzes, P. (2010). Estrogen Receptor β Activity Modulates Synaptic Signaling and Structure. *The Journal of Neuroscience*, 30(40), 13454–13460. <https://doi.org/10.1523/JNEUROSCI.3264-10.2010>
- Srivastava, D., & Woolfrey, K. (2010). Estrogen receptor β activity modulates synaptic signaling and structure. *The Journal of ...*, 30(40), 13454–13460. <https://doi.org/10.1523/JNEUROSCI.3264-10.2010>. Estrogen
- Sun, N., Cassell, M. D., & Perlman, S. (1996). Anterograde, transneuronal transport of herpes simplex virus type 1 strain H129 in the murine visual system. *Journal of Virology*, 70(8), 5405–5413.
- Sun, Q., & Turrigiano, G. (2011). PSD-95 and PSD-93 play critical but distinct roles in synaptic scaling up and down. *The Journal of Neuroscience*, 31(18), 6800–6808. <https://doi.org/10.1523/JNEUROSCI.5616-10.2011>
- Syken, J., Grandpre, T., Kanold, P. O., & Shatz, C. J. (2006). PirB restricts ocular-dominance plasticity in visual cortex. *Science (New York, N. Y.)*, 313(5794), 1795–1800. <https://doi.org/10.1126/science.1128232>
- Tagawa, Y., Kanold, P. O., Majdan, M., & Shatz, C. J. (2005). Multiple periods of functional ocular dominance plasticity in mouse visual cortex. *Nature Neuroscience*. <https://doi.org/10.1038/nn1410>
- Tang, Y., Janssen, W. G. M., Hao, J., Roberts, J. A., McKay, H., Lasley, B., ... Morrison, J. H. (2004). Estrogen Replacement Increases Spinophilin-immunoreactive Spine Number in the Prefrontal Cortex of Female Rhesus Monkeys. *Cerebral Cortex*, 14(2), 215–223. <https://doi.org/10.1093/cercor/bhg121>
- Teyler, T. J., Hamm, J. P., Clapp, W. C., Johnson, B. W., Corballis, M. C., & Kirk, I. J. (2005). Long-term potentiation of human visual evoked responses. *The European Journal of Neuroscience*, 21(7), 2045–2050. <https://doi.org/10.1111/j.1460-9568.2005.04007.x>
- Thornton, J. W. (2001). Evolution of vertebrate steroid receptors from an ancestral estrogen receptor by ligand exploitation and serial genome expansions. *Proceedings of the National Academy of Sciences*, 98(10), 5671–5676. <https://doi.org/10.1073/pnas.091553298>
- Tian, L., Hires, S. A., Mao, T., Huber, D., Chiappe, M. E., Chalasani, S. H., ... Looger, L. L. (2009). Imaging neural activity in worms, flies and mice with improved GCaMP calcium indicators. *Nat Meth*, 6(12), 875–881. Retrieved from <http://dx.doi.org/10.1038/nmeth.1398>
- Titolo, D., Mayer, C. M., Dhillon, S. S., Cai, F., & Belsham, D. D. (2008). Estrogen Facilitates both Phosphatidylinositol 3-Kinase/Akt and ERK1/2 Mitogen-Activated Protein Kinase Membrane Signaling Required for Long-Term Neuropeptide Y Transcriptional Regulation in Clonal, Immortalized Neurons. *Journal of Neuroscience*. <https://doi.org/10.1523/JNEUROSCI.0514->

08.2008

- Toran-Allerand, C. D., Tinnikov, A. A., Singh, R. J., & Nethrapalli, I. S. (2005). 17α -Estradiol: A brain active estrogen? *Endocrinology*, *146*(9), 3843–3850. <https://doi.org/10.1210/en.2004-1616>
- Vetencourt, J. F. M., Sale, A., Viegi, A., Baroncelli, L., De Pasquale, R., F. O'Leary, O., ... Maffei, L. (2008). The Antidepressant Fluoxetine Restores Plasticity in the Adult Visual Cortex. *Science*, *320*(5874), 385–388. <https://doi.org/10.1126/science.1150516>
- Vicini, S., Wang, J. F., Li, J. H., Zhu, W. J., Wang, Y. H., Luo, J. H., ... Grayson, D. R. (1998). Functional and Pharmacological Differences Between Recombinant *N*-Methyl- D -Aspartate Receptors. *Journal of Neurophysiology*. <https://doi.org/10.1152/jn.1998.79.2.555>
- Voytko, M. L., Murray, R., & Higgs, C. J. (2009). Executive Function and Attention Are Preserved in Older Surgically Menopausal Monkeys Receiving Estrogen or Estrogen Plus Progesterone. *Journal of Neuroscience*, *29*(33), 10362–10370. <https://doi.org/10.1523/JNEUROSCI.1591-09.2009>
- Wang, S., Zhu, J., & Xu, T. (2018). 17β -estradiol (17α E2) promotes growth and stability of new dendritic spines via estrogen receptor β pathway in intact mouse cortex. *Brain Research Bulletin*, *137*(December 2017), 241–248. <https://doi.org/10.1016/j.brainresbull.2017.12.011>
- Wang, W., Kantorovich, S., Babayan, A. H., Hou, B., Gall, C. M., & Lynch, G. (2016). Estrogen's Effects on Excitatory Synaptic Transmission Entail Integrin and TrkB Transactivation and Depend Upon β 1-integrin function. *Neuropsychopharmacology*, *41*(11), 2723–2732. <https://doi.org/10.1038/npp.2016.83>
- Watakabe, A., Ohtsuka, M., Kinoshita, M., Takaji, M., Isa, K., Mizukami, H., ... Yamamori, T. (2015). Comparative analyses of adeno-associated viral vector serotypes 1, 2, 5, 8 and 9 in marmoset, mouse and macaque cerebral cortex. *Neuroscience Research*, *93*, 144–157. <https://doi.org/10.1016/j.neures.2014.09.002>
- Waters, E. M., Yildirim, M., Janssen, W. G. M., Lou, W. Y. W., McEwen, B. S., Morrison, J. H., & Milner, T. A. (2011). Estrogen and aging affect the synaptic distribution of estrogen receptor beta-immunoreactivity in the CA1 region of female rat hippocampus. *Brain Research*, *1379*, 86–97. <https://doi.org/10.1016/j.brainres.2010.09.069>
- Webber, A. L., & Wood, J. (2005). Amblyopia: prevalence, natural history, functional effects and treatment. *Clinical and Experimental Optometry*, *88*(6), 365–375. <https://doi.org/10.1111/j.1444-0938.2005.tb05102.x>
- Weiser, M. J., Foradori, C. D., & Handa, R. J. (2008). Estrogen receptor beta in the brain: From form to function. *Brain Research Reviews*, *57*(2), 309–320. <https://doi.org/10.1016/j.brainresrev.2007.05.013>
- Whissell, P. D., Cajanding, J. D., Fogel, N., & Kim, J. C. (2015). Comparative density of CCK- and PV-GABA cells within the cortex and hippocampus. *Frontiers in Neuroanatomy*, *9*(September), 1–16. <https://doi.org/10.3389/fnana.2015.00124>
- Whitlock, J. R. J., Heynen, A. J. A., Shuler, M. M. G., & Bear, M. M. F. (2006). Learning induces long-term potentiation in the hippocampus. *Science*, *313*(August), 1093–1097. <https://doi.org/10.1126/science.1128134>
- Wiesel, T. N., & Hubel, D. H. (1963). Responses in Striate Deprived of Vision Cortex of One Eye. *Journal of Neurophysiology*. <https://doi.org/10.1152/jn.1963.26.6.1003>
- Wiesel, T. N., & Hubel, D. H. (1965). Extent of recovery from the effects of visual deprivation in kittens. *Journal of Neurophysiology*. <https://doi.org/10.1152/jn.1965.28.6.1060>
- Wilson, M. E., Rosewell, K. L., Kashon, M. L., Shughrue, P. J., Merchenthaler, I., & Wise, P. M. (2002). Age differentially influences estrogen receptor- α (ER α) and estrogen receptor- β (ER β) gene expression in specific regions of the rat brain. *Mechanisms of Ageing and Development*, *123*(6), 593–601. [https://doi.org/10.1016/S0047-6374\(01\)00406-7](https://doi.org/10.1016/S0047-6374(01)00406-7)

- Woods, G. F., Oh, W. C., Boudewyn, L. C., Mikula, S. K., & Zito, K. (2011). Loss of PSD-95 Enrichment Is Not a Prerequisite for Spine Retraction. *The Journal of Neuroscience*, *31*(34), 12129–12138. <https://doi.org/10.1523/JNEUROSCI.6662-10.2011>
- Woolley, C. S., & McEwen, B. S. (1993). Roles of estradiol and progesterone in regulation of hippocampal dendritic spine density during the estrous cycle in the rat. *The Journal of Comparative Neurology*, *336*(2), 293–306. <https://doi.org/10.1002/cne.903360210>
- Xiao, X., Yang, Y., Zhang, Y., Zhang, X. M., Zhao, Z. Q., & Zhang, Y. Q. (2013). Estrogen in the anterior cingulate cortex contributes to pain-related aversion. *Cerebral Cortex*. <https://doi.org/10.1093/cercor/bhs201>
- Yashiro, K., Corlew, R., & Philpot, B. D. (2005). Visual Deprivation Modifies Both Presynaptic Glutamate Release and the Composition of Perisynaptic/Extrasynaptic NMDA Receptors in Adult Visual Cortex. *The Journal of Neuroscience*, *25*(50), 11684 LP-11692. Retrieved from <http://www.jneurosci.org/content/25/50/11684.abstract>
- Yata, T., Lee, E. L. Q., Suwan, K., Syed, N., Asavarut, P., & Hajitou, A. (2015). Modulation of extracellular matrix in cancer is associated with enhanced tumor cell targeting by bacteriophage vectors. *Molecular Cancer*. <https://doi.org/10.1186/s12943-015-0383-4>
- Ye, Q., & Miao, Q. long. (2013). Experience-dependent development of perineuronal nets and chondroitin sulfate proteoglycan receptors in mouse visual cortex. *Matrix Biology*. <https://doi.org/10.1016/j.matbio.2013.04.001>
- Yoon, B.-K., Chin, J., Kim, J.-W., Shin, M.-H., Ahn, S., Lee, D.-Y., ... Na, D. L. (2018). Menopausal hormone therapy and mild cognitive impairment: a randomized, placebo-controlled trial. *Menopause*, *25*(8). Retrieved from https://journals.lww.com/menopausejournal/Fulltext/2018/08000/Menopausal_hormone_therapy_and_mild_cognitive.5.aspx
- Young, M. E., Ohm, D. T., Dumitriu, D., Rapp, P. R., & Morrison, J. H. (2014). Differential effects of aging on dendritic spines in visual cortex and prefrontal cortex of the rhesus monkey. *Neuroscience*, *274*, 33–43. <https://doi.org/10.1016/j.neuroscience.2014.05.008>
- Zandi, P. P. (2002). Hormone Replacement Therapy and Incidence of Alzheimer Disease in Older Women<SUBTITLE>The Cache County Study</SUBTITLE>. *JAMA*, *288*(17), 2123. <https://doi.org/10.1001/jama.288.17.2123>
- Zhang, P., & Lisman, J. E. (2012). Activity-dependent regulation of synaptic strength by PSD-95 in CA1 neurons. *Journal of Neurophysiology*, *107*(4), 1058–1066. <https://doi.org/10.1152/jn.00526.2011>
- Zihl, J., & Von Cramon, D. (1985). Visual field recovery from scotoma in patients with postgeniculate damage: A REVIEW of 55 cases. *Brain*, *108*(2), 335–365. <https://doi.org/10.1093/brain/108.2.335>
- Zurkovsky, L., Brown, S. L., Boyd, S. E., Fell, J. A., & Korol, D. L. (2007). Estrogen modulates learning in female rats by acting directly at distinct memory systems. *Neuroscience*, *144*(1), 26–37. <https://doi.org/https://doi.org/10.1016/j.neuroscience.2006.09.002>